Report No. 957114-3

FINAL REPORT

UNIFIED CONTROL/STRUCTURE DESIGN AND MODELING RESEARCH

January 8, 1986

D.L. Mingori
J.S. Gibson
P.A. Blelloch
A. Adamian

Mechanical, Aerospace and Nuclear Engineering Department
University of California
Los Angeles, CA 90024

TABLE OF CONTENTS

List of Notation

Chapter 2

Chapter 3

Chapter 4

Abbreviations

General

<u>State</u> <u>Space</u> <u>System</u> <u>Representation</u>

Chapter 5

1.0 INTRODUCTION

The purpose of this research project is to apply control theory for distributed systems to large flexible space structures, and to combine distributed system theory with finite dimensional control theory to produce comprehensive control system design methods for large space structures. The basic idea is to establish the existence and properties of an ideal infinite dimensional compensator for the distributed model of the structure and then approximate the ideal compensator with realizable finite dimensional compensators. For an analysis of the ideal compensator and the resulting performance of the closed-loop system, distributed system theory, which is based on infinite dimensional analysis, is essential. Also, infinite dimensional analysis is necessary for studying convergence of approximations and selecting appropriate approximation schemes. For computing the approximating finite dimensional compensators and determining efficient implementation, finite dimensional control theory is used.

To demonstrate the applicability of the methods to real space structures, the research has focused on a model of a space antenna which consists of a rigid hub, flexible ribs and a mesh reflecting surface. This model was designed to include the most important characteristics of large flexible space structures. In particular, the structure to be controlled has different types of distributed components, as well as rigid-body modes, and, because of the mesh surface, there are many closely packed structural frequencies. This project appears to be the first application of distributed system control theory to a structure of such complexity.

1

It should be emphasized that, although the term "distributed system" usually implies a system involving partial differential equations (as with the model of the flexible components of the antenna here), the methods of this research _do_ _not_ require the solution of partial differential equations. Rather, according to the approximation results, only finite dimensional Riccati and Liapunov matrix equations need be solved.

Chapter 2 describes the space antenna model used in this project and discusses the finite element approximation of the distributed model. A Galerkin component mode approach is used to develop a finite dimensional approximation of the structure. This approach was found to converge rapidly to a model of suitable accuracy.

The basic control problem is to design an optimal or near-optimal compensator to suppress the linear vibrations and rigid-body displacements of the structure, which is modeled as a distributed system because of the flexible components. As is common in finite dimensional optimal control of linear systems, a quadratic performance index is defined to penalize both the disturbance in the structure and the control effort used to eliminate the disturbance. Determining the optimal compensator for this problem and analyzing the response of the system require linear-quadratic-gaussian (LQG) optimal control theory for distributed systems [BA1,CU1,GI1,2]. The application of this infinite dimensional LQG control theory to flexible structure is discussed in Chapter 3.

Distributed system theory yields an infinite dimensional compensator as the optimal, or ideal solution to the control problem. As discussed in Chapter 3 this compensator can be represented in terms of _functional gains_ for

the feedback control and state estimator, and also in terms of an irrational transfer function. Both the functional gains and the Bode plots of the transfer function provide useful graphical representations of the ideal compensator.

Approximation theory is a central topic of this research. Because the ideal compensator is infinite dimensional, it can be neither written down in closed form nor built and implemented exactly. Thus, a finite dimensional approximation of the ideal compensator is required. In this research, there are two stages in the approximation of the ideal compensator. First, increasingly large-order finite dimensional LQG problems are solved until the resulting compensators converge to a finite dimensional compensator that is essentially equal to the ideal compensator. Next, the order of this large compensator is reduced as much as possible using balanced realizations. It is important to note that, in both these stages of approximation, the convergence and truncation criteria are tied to quantitative measures of control system performance.

The approximation theory for constructing the large-order approximation to the ideal compensator is discussed in Ref. [HR1]. At the heart of the infinite dimensional LQG theory, are the infinite dimensional Riccati operator equations whose solutions determine the optimal control and estimator gains for the infinite dimensional compensator. The scheme for computing finite dimensional approximations to the ideal compensator is based on the approximation of the infinite dimensional Riccati equations by finite dimensional Riccati matrix equations of the type found in finite dimensional control theory. These finite dimensional equations are given in [HR1]. Also to be found in

[HR1] are typical functional control gains and the Bode plot for the ideal compensator for the antenna.

While infinite dimensional, or distributed system control theory is the main basis for this research, finite dimensional control theory plays an important role. Indeed, the true richness of the project stems from the combination of a primary infinite dimensional perspective of control theory with finite dimensional control theory and practice. Thus, the project really represents an application of a finite dimensional methods in a infinite dimensional setting.

After the converged approximation to the ideal compensator has been obtained, it must be verified that the lower order approximation to the ideal compensator will still produce a satisfactory closed-loop system. Also, robustness with respect to errors in plant parameters must be studied. Robustness issues were a major focus of the work performed this year. Two basic approaches for robustness enhancement were investigated: Loop Transfer Recovery and Sensitivity Optimization. A third approach synthesized from elements of these two basic approaches is currently under development. The goal of loop recovery is to produce a loop transfer matrix with the same frequency response as full state feedback which is known to have very desirable robustness properties. Sensitivity optimization uses numerical optimization techniques to select regulator and/or estimator gains which reduce sensitivity of the real parts of the closed loop poles to parameter errors. These methods are presented in Sections 4.2 and 4.3 along with numerical examples which illustrate their performance.

In general it was found that the methods worked well on relatively simple problems which were used to test and develop the software. However, results were mixed when the methods were applied to the antenna model. The light damping and complexity of the antenna apparently make this a challenging system for robust controller design. The performance requirements were purposely chosen to ensure that several of the flexible modes were within the controller bandwidth, and this contributed to the difficulty of the problem. The form of the weighting matrix Q in the performance term of the cost function was found to have a strong effect on robustness. For example, Q's which did not penalize velocity terms were found to be less robust than those which did. Also, Q's in which the penalty on rigid body motion was much greater than the penalty on flexible modes were less robust than Q's in which the rigid body mode was not emphasized. These results are reported in Section 4.2.

Sensitivity optimization, a second method for designing robust compensators, is discussed in Section 4.3. This method uses nonlinear programming to find control and estimator gains that minimize the sensitivity of the closed-loop response with respect to uncertain plant parameters. Of the various measures of closed-loop sensitivity that were tried, the sensitivity of the real parts of the closed-loop eigenvalues proved to have the best correlation to robustness. Simulation results are given. As with the loop-recovery methods, the form of state weighting in the control problem affects the robustness significantly.

Chapter 5 discusses control driven finite element approximation of flexible structures. This means choosing the finite element scheme that is most

efficient for approximating the solution to the optimal control problem for the distributed model of the structure. Section 5.1 compares three sets of finite element basis vectors for computing functional control gains and demonstrates that some finite element schemes are much better than others. Section 5.2 discusses the possibility of constructing a finite element scheme to approximate the infinite dimensional Hamiltonian system directly, instead of indirectly as in Chapter 3. The main application of this approach appears to be for structures with history-dependent damping.

2. STRUCTURE MODELS AND FINITE ELEMENT APPROXIMATION

2.1 ANTENNA MODEL

The space antenna model that has served as the primary example of this research is shown in Figure 2.1.1. The flat antenna consists of a rigid hub, eight ribs and a mesh reflecting surface. The ribs are modeled as beams cantilevered to the hub, and the mesh is modeled as circular sectors of membrane tied to the ribs and hub. The center of the hub is fixed but the hub can rotate out of plane, so that there are two rigid-body modes.

This model is based on the Lockheed wrap-rib antenna [LO1]. Since this is the first complex structure to which the methods of this research have been applied, the model has been simplified to a flat antenna with eight instead of the actual 48 ribs, to allow concentration on fundamental issues while maintaining a complex structure with different types of components. Otherwise, the parameters given in Figure 2.1.1 are based on the 48-rib antenna [EL1].

The two actuators apply torques to the hub, and the sensors measure the rotation of the hub and the displacement of the tip of each rib. The compensator is designed to control the out-of- plane motion of the antenna.

For small elastic displacements, the symmetry of the antenna further reduces the complexity of the compensator because the motion of the antenna decouples into two sets of orthogonal modes, with each set controlled independently by one actuator. Each of these sets consists of modes that are asymmetric about one torque axis. Although the actuators can control only the controllable modes, these are the only modes excited by rotating the antenna

7

with the torques on the hub.

The equations of motion for rigid-body rotation and small elastic vibration have the form discussed in Chapter 3. See (3.1.1) – (3.1.10). Here, we will discuss the stiffness and damping operators, which are the primary operators in the equations of motion. The stiffness operator A_o can be separated into rib and mesh components as

$$A_o = A_{or} + A_{om},$$

$$(2.1.1)$$

where

$$A_{or} = EI \, d^4(.)/dr^4,$$

$$(2.1.2)$$

$$A_{om} = T_1[d^2(.)/dr^2 + (1/r)d(.)/dr] - T_2 \, d^2(.)/d\phi^2$$

$$(2.1.3)$$

and T_1 and T_2 are the tensions in the radial and transverse directions, respectively. The term A_{or} operates on the elastic deformation of each rib and A_{om} operates on the elastic deformation of the mesh.

We assume that both the ribs and the mesh have viscoelastic damping, so that the damping operator is

$$D_o = c_r \, A_{or} + c_m \, A_{om}$$

$$(2.1.4)$$

where c_r and c_m are positive scalars. If c_r and c_m are not equal, this structural damping couples the modes -- but not modes that are controllable by one actuator with modes that are uncontrollable by the same actuator.
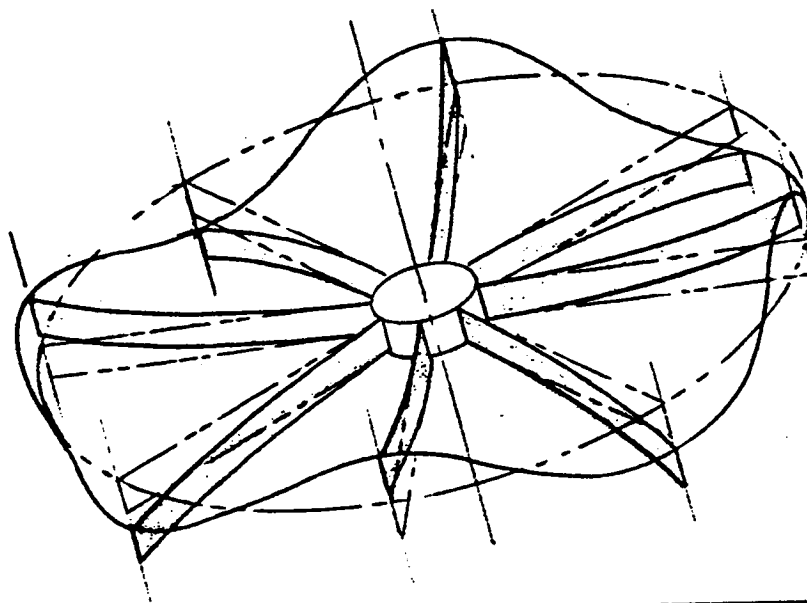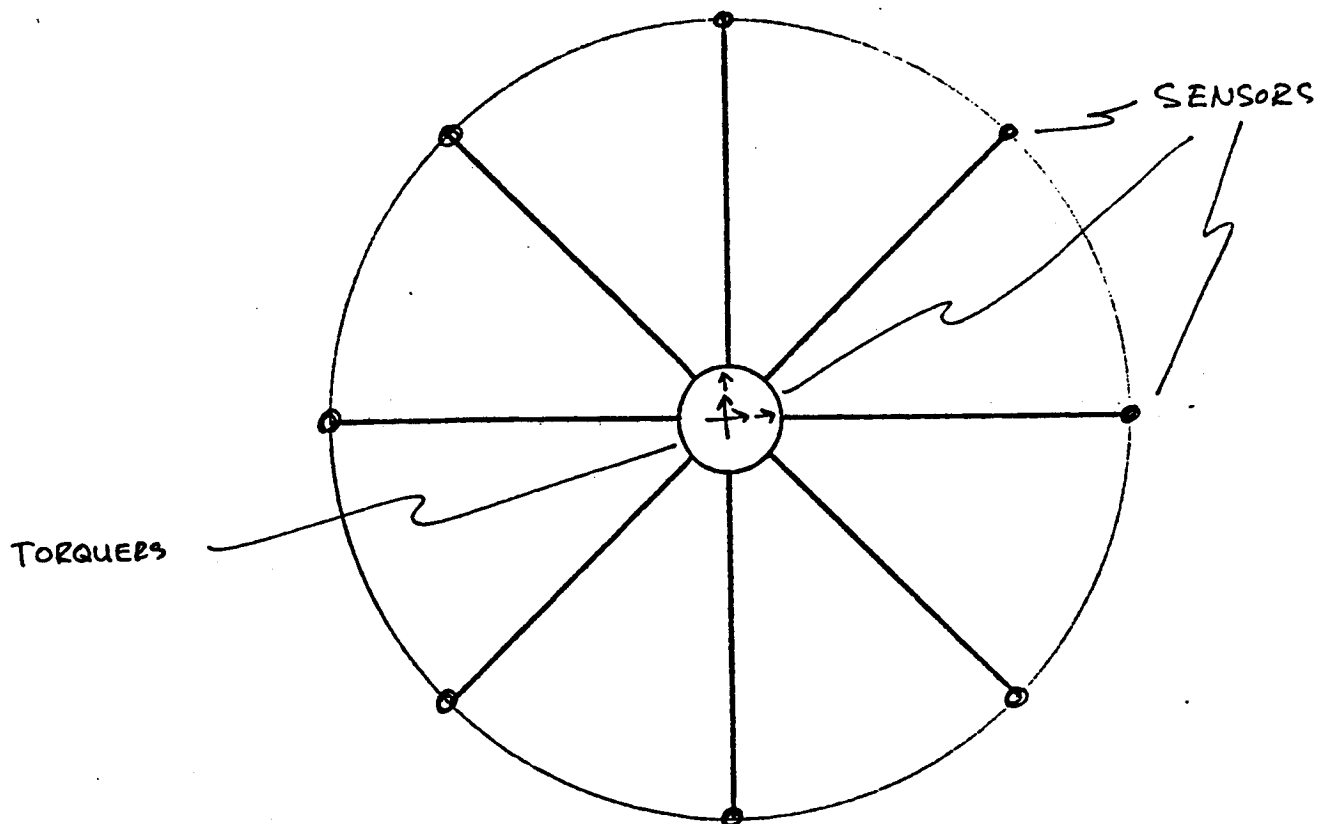
MODEL DATA (based on 48 rib Lockheed wrap rib antenna):

Hub Radius: 46 in.   Hub Weight: 1000 lbs.

Hub Inertias: $I_{xx} = I_{yy} = 342$ lb-in-sec^2
$I_{zz} = 684$ lb-in-sec^2

Rib Length: 86 ft.   Rib Weight: 115 lb. per rib

Rib stiffness: $EI = 4.05 \times 10^7$ lb-in^2

Mesh Weight: 6.94 lb per sector

Figure 2.1.1

2.2 FINITE ELEMENT APPROXIMATION OF THE ANTENNA

The approximation of the antenna is a component modal synthesis for which the component modes of the ribs and mesh were determined by consistent-mass finite element approximations. The ribs were approximated by a standard finite element scheme using Hermite cubic splines, and the mesh sectors were approximated by a Galerkin scheme discussed in Section 2.3.

In an earlier project [HR1], the approximation scheme used in this project was compared to a NASTRAN finite element approximation of the antenna. While both schemes converged to the same mode shapes and frequencies as the order of approximation increased, the component modal synthesis converged faster and was more convenient and cheaper to use. An important advantage of the conponent modal approximation for this project is the fact that the program was written to make the order of approximation easy to vary. In design of controllers for complex structures, it is impossible to determine in advance what order of approximation will be necessary for designing an optimal, or even acceptable compensator. Thus, in a project like this, it is essential to have an approximation scheme of easily variable order.

2.3 GALERKIN APPROXIMATION OF SECTOR

A Galerkin approximation of the antenna was used to compute the optimal control law for the composite sector. The basis vectors have the form

$$(\theta_n, \psi_n^r, \psi_n^m)$$

$$(2.3.1)$$

where (θ_n, ψ_n^r) are the natural modes of the hub and ribs without the mesh, and ψ_n^m are the natural modes of the mesh when the beams and hub are constrained

10

not to move. This Galerkin approximation is then a component modal synthesis of the composite sector.

The mesh modes have the form

$$\psi_n^m(\phi, r) = \sin 8n\phi \, f_{n,k}(r), \quad n = 1, 2, \ldots,$$

$$k = 1, 2, \ldots, \tag{2.3.2}$$

where the functions $f_{n,k}(r)$ are the eigenfunctions of the problem

$$T_1[\beta(64n^2/r^2)f - (f'' + f'/r)] = \omega_{n,k}^2 f \tag{2.3.3}$$

$$f(r_o) = f'(r_o + l_r) = 0 \tag{2.3.4}$$

Here, the eigenvalues $\omega_{n,k}$ are the squares of the natural frequencies of the mesh, T_1 is the radial tension, $T_2/T_1 = \beta = 72$ and l_r is the rib length. This value of β was selected so that the first mesh frequency is approximately half way between the first two controllable beam-hub frequencies.

A standard Ritz-Galerkin approximation with linear splines as basis vectors was used to solve (2.3.3) and (2.3.4) for the mesh modes. As many as 45 splines were used, but convergence of the first 10 frequencies and mode shapes for n = 1 was obtained with 30 splines.

3.0 STATEMENT AND SOLUTION OF CONTROL AND ESTIMATION PROBLEMS

3.1 ABSTRACT CONTROL SYSTEM

The space antenna model used here falls into the large class of flexible structures represented by the abstract control system

$$M_0\ddot{x} + D_0\dot{x} + A_0x = B_0u + \mathcal{U}_1,$$
(3.1.1)

$$y = C_0x + \mathcal{U}_0$$
(3.1.2)

where the generalized displacement $x(t)$ is in a real Hilbert space H, the control $u(t) \in R^m$, the measurement $y(t) \in R^p$. The disturbance $\mathcal{U}_1$ and the noise $\mathcal{U}_0$ are zero-mean Gaussian white noise processes, as in the finite dimensional LQG problem. The mass operator M_0 is bounded, selfadjoint and coercive on H, B_0 is bounded from R^m to H and C_0 is bounded from H to R^p. The unbounded stiffness operator A_0 is selfadjoint and bounded below, with compact resolvent, and the damping operator D_0 is symmetric, nonnegative and A_0 - bounded. A similar abstract description of the LQG control problem has been used by Balas in [BA2] and [BA3] and Gibson in [GI1]. Also, see Balakrishnan [BA1].

As usual, by <u>natural modes</u> we mean the eigenvectors x_j of the problem

$$\omega_j^2 M_0 x_j = A_0x_j, \quad j = 1, 2, \ldots,$$
(3.1.3)

where the ω_j's are the natural frequencies of the structure. In the antenna problem, as in most structure control problems, the only nonpositive eigenvalues of A_0 are zero eigenvalues corresponding to rigid body modes. When these rigid body modes are controllable, they are contained in the positive

eigenspace of $B_O B_O^*$, so that the operator

$$\widetilde{A}_O = A_O + B_O B_O^* \geq m \geq 0,$$

(3.1.4)

for some positive m; i.e., $\widetilde{A}_O$ is coercive.

Next, we define the strain-energy space $V = D(\widetilde{A}_O^{1/2})$ with inner product

$$\langle v_1, v_2 \rangle_V = \langle \widetilde{A}_O^{1/2} v_1, \widetilde{A}_O^{1/2} v_2 \rangle_H.$$

(3.1.5)

This is a natural space for the generalized displacement because usually, as in our example, $\langle x, x \rangle_V$ is just the sum of twice the elastic strain energy and the squares of the rigid body displacements.

To write (3.1.1) in first order form, we define the energy space $E = V \times H_M$ where H_M is H with the equivalent kinetic-energy inner product

$$\langle h_1, h_2 \rangle_M = \langle M h_1, h_2 \rangle_H.$$

(3.1.6)

Thus $\| \dot{x} \|_M^2$ is twice the kinetic energy in the structure. Now we can write (3.1.1) as

$$\dot{z} = Az + Bu + \mathcal{U}_1,$$

(3.1.7)

$$y = Cz + \mathcal{U}_O,$$

(3.1.8)

where

$$z = \begin{pmatrix} x \\ \dot{x} \end{pmatrix} , \quad \mathcal{U}_1 = \begin{bmatrix} 0 \\ M_O^{-1} \mathcal{U}_1 \end{bmatrix} , \quad B = \begin{bmatrix} 0 \\ M_O^{-1} B_O \end{bmatrix}$$

(3.1.9)

and

$$A = \begin{bmatrix} 0 & I \\ -M_o^{-1}A_o & -M_o^{-1}D_o \end{bmatrix} , \quad D(A_o) \times D(A_o) \subset D(A)$$

(3.1.10)

As in [GI1, Sec. 2], D(A) is chosen uniquely so that A generates a C_o-semigroup T(t) on E.

3.2 INFINITE DIMENSIONAL LQG PROBLEM

As in the finite dimensional case, a separation principle [BA1, CU1] allows us to design the optimal compensator by solving the deterministic optimal regulator problem and the stochastic state-estimation problem separately. The infinite dimensional optimal control problem is to choose u to minimize

$$J = \int_0^\infty (\langle Qz, z\rangle_E + \langle Ru, u\rangle_R m)dt,$$

(3.2.1)

where z is the solution to (3.1.7), $Q = Q^*$ is a nonnegative bounded linear operator on E, and $R = R^* > 0$.

To simplify certain technicalities about existence of solutions to the LQG problem, we will assume that $D_o + B_oB_o^*$ is coercive, which means that the flexible components of the structure have coercive damping, and that Q is coercive, which guarantees that the optimal closed-loop system is uniformly exponentially stable.

For this deterministic problem, the optimal control has the feedback form

$$u = - Kz,$$

14

where

$$K = -R^{-1}B^* \Pi$$

and Π is the unique nonnegative selfadjoint element of $L(E)$ which satisfies the infinite dimensional Riccati equation

$$A^* \Pi + \Pi A - \Pi B R^{-1} B^* \Pi + Q = 0$$

See [BA1, CU1, GI1, GI2].

The minimum variance estimator, or infinite dimensional Kalman filter, is [BA1, CU2]

$$\dot{\hat{z}} = A\hat{z} + Bu + G(y - C\hat{z}),$$

where

$$G = \hat{\Pi}C^* \hat{R}^{-1}$$

and $\hat{\Pi}$ satisfies the Riccati equation

$$A\hat{\Pi} + \hat{\Pi}A^* - \hat{\Pi}C^* \hat{R}^{-1} C \hat{\Pi} + \hat{Q} = 0$$

The pxp matrix $\hat{R}$ and the bounded nonnegative operator $\hat{Q} = \hat{Q}^*$ are the covariance operators for $\mathcal{V}_o$ and $\mathcal{V}_1$, respectively. We assume that any undamped modes are observable, so that the closed-loop estimator is uniformly exponentially stable.

We do not require either Q or $\hat{Q}$ to be trace class, as is usually necessary for the infinite dimensional LQG problem [BA1, CU2]. This is not necessary for our definition of the infinite dimensional compensator, and it allows more freedeom in designing the compensator to produce desired closed-loop transient response. See also [GI2].

The optimal compensator consists of the infinite dimensional estimator (3.2.5) and the control law

$$u = - K\hat{z},$$

(3.2.8)

where K is given by (3.2.3) with (3.2.4), and (3.2.5) becomes

$$\dot{\hat{z}} = A_c\hat{z} + Gy,$$

(3.2.9)

where

$$A_c = A - BK - GC .$$

(3.2.10)

Note that the optimal compensator has the irrational transfer function

$$K[sI - A_c]^{-1}G$$

(3.2.11)

Even though this transfer function would require an infinite dimensional state-space realization, the transfer function itself is only a finite dimensional matrix function of the complex variable s. For control of the antenna quadrant, this is just a 1×3 row matrix representing the three control channels from the displacement sensors at the rib tips to the torque actuator on the hub.

3.3 FUNCTIONAL GAINS

When there is a single actuator ($m=1$), the operator B_0 is actually an element of H and $B \varepsilon E$. Hence

$$Kz = R^{-1}B^*\Pi z = \langle \Pi BR^{-1}, z \rangle_E,$$

(3.3.1)

or

$$Kz = \langle f, x \rangle_V + \langle g, \dot{x} \rangle_M$$

(3.3.2)

where

$$\binom{f}{g} = \Pi BR^{-1}$$

(3.3.3)

with $f \varepsilon V$ and $g \varepsilon H_M = H$. We call f and g _functional control gains_.

Similarly, for a single sensor, the measurement y is a scalar and $C^* \varepsilon E$. Then

$$G = \hat{\Pi}C^*R^{-1} = \binom{\hat{f}}{\hat{g}}$$

(3.3.4)

where $\hat{f} \varepsilon V$ and $\hat{g} \varepsilon H$ are _functional estimator gains_.

For the multi-input-multi-output case, there is a pair of functional gains for each actuator and for each sensor.

3.4 APPROXIMATION

To obtain a sequence of approximating finite dimensional LQG problems, we use a Ritz-Galerkin approximation scheme for (3.1.1). We assume a sequence of linearly independent basis vectors e_i, which are complete in V. The nth

approximate solution to (3.1.1) is

$$x_n(t) = \sum_{i=1}^{n} a_i^n(t) e_i,$$

(3.4.1)

which is in V_n = span $(e_1, \ldots, e_n)$. We will need both V_n and H_{Mn}, which are the same set but have the V and H_M inner products, respectively.

Initially, let us consider the case $U_1 = 0$ in (3.1.1). Then the coefficients $a^n(t)$ satisfy

$$M_{on} \ddot{a}^n + D_{on} \dot{a}^n + A_{on} a^n = B_{on} u,$$

(3.4.2)

where $a^n(t)$ is the n-vector containing $a^n(t)$, $i = 1, \ldots, n$. The mass, damping and stiffness matrices are given respectively by

$$M_{on,ij} = \langle e_i, e_j \rangle_M = \langle M_o e_i, e_j \rangle_H,$$

(3.4.3)

$$D_{on,ij} = \langle D_o e_i, e_j \rangle_H,$$

(3.4.4)

$$A_{on,ij} = \langle A_o e_i, e_j \rangle_H$$

(3.4.5)

In general, (3.4.4) and (3.4.5) are valid only if the basis vectors are in $D(A_o)$. Otherwise, we use

$$A_{on,ij} = \langle e_i, e_j \rangle_V - \langle B_o^* e_i, B_o^* e_j \rangle_H$$

(3.4.5)

(Recall (3.1.4) and (3.1.5)) and a similar expression for D_{on} (in our model, D_o is essentially a scalar times A_o.) Also,

$$B_{on,ij} = \langle e_i, B_o e_j \rangle, \quad i = 1, \ldots, n \quad j = 1, \ldots, m \tag{3.4.6}$$

The convergence of such approximations and the corresponding finite dimensional optimal control problems is discussed in [3.5] for $e_i \varepsilon D(A_o)$, which includes the cases where the basis vectors are either natural modes of the structure or component modes. Here, we only outline the formulation of the sequence of n-order LQG problems. The most efficient way to do this is to note that, with (3.4.1), (3.4.2) is equivalent to the following differential equation on H_{Mn} = span $(e_1, \ldots, e_n)$:

$$M_{on} \ddot{x}_n + D_{on} \dot{x}_n + A_{on} x_n = B_{on} u, \tag{3.4.7}$$

where M_{on}, D_{on}, A_{on}, and B_{on} are the operators on H_{Mn} determined by the matrices in (3.4.3) - (3.4.5) and the identification (3.4.1). Of course, we can write (3.4.7) as

$$\dot{z}_n = A_n z_n + B_n u \tag{3.4.8}$$

with $z_n = (x_n, \dot{x}_n)$.

For (3.4.7) and (3.4.8), the optimal regulator problem leads to the finite dimensional Riccati equation

$$A_n^* \Pi_n + \Pi_n A_n - \Pi_n B_n R^{-1} B_n^* \Pi_n + Q_n = 0, \tag{3.4.9}$$

where the operator Q_n is defined as follows. Let $E_n = V_n \times H_{Mn}$ and denote by P_n the projection of E onto E_n. Then

$$Q_n = P_n Q P_n |_{E_n}. \tag{3.4.10}$$

With this Q_n and our preceding hypotheses about damping and the completeness

of the e_i's in V, the Π_n of (3.4.9) is guaranteed to converge strongly to the solution Π of the infinite dimensional Riccati equation (3.2.4).

The functional control gains in (3.3.3) are approximated by

$$\binom{f_n}{g_n} = \Pi_n B_n R^{-1}.$$

(3.4.11)

The strong convergence of Π_n and B_n implies that f_n converges in V to f and g_n converges in H to g.

The functional control gains f_n and g_n are associated with the nth order control law

$$u = - K_n z_n = - \langle f_n, x_n \rangle_V - \langle g_n, \dot{x}_n \rangle_M,$$

(3.4.12)

with

$$K_n = R^{-1} B_n^* \Pi_n$$

(3.4.13)

To approximate the infinite dimensional compensator, we construct a finite dimensional state estimator

$$\dot{\hat{z}}_n = A_n \hat{z}_n + B_n u + G_n (y - C_n \hat{z}_n),$$

(3.4.14)

where

$$G_n = \hat{\Pi}_n \ C_n^* \hat{R}^{-1}$$

(3.4.15)

and $\hat{\Pi}_n$ satisfies the Riccati equation

$$A_n \hat{\Pi}_n + \hat{\Pi}_n A_n^* - \hat{\Pi}_n C_n^* \hat{R}^{-1} C_n \hat{\Pi}_n + \hat{Q}_n = 0.$$

(3.4.16)

The operator $\hat{Q}_n$ is given by

$$\hat{Q}_n = P_n \hat{Q} P_n \qquad (3.4.17)$$

for Q the covariance of the process noise V_1 in (3.1.7). As before, R is the covariance of the measurement noise V_0. The operator P_n is the projection onto $E_n = V_n \times H_{Mn}$.

We now have the components of the nth approximation to the infinite dimensional compensator. The nth finite dimensional compensator consists of (3.4.13) and the control law

$$u = - K_n z_n. \qquad (3.4.18)$$

This compensator has the rational transfer function

$$K_n [sI - A_{cn}]^{-1} G_n \qquad (3.4.19)$$

where

$$A_{cn} = A_n - B_n K_n - G_n C_n. \qquad (3.4.20)$$

For each $s \varepsilon \rho(A_c)$, this transfer function (see Section 9 of [GI2]) the value of the transfer function in (3.2.11) as n increases.

3.5 APPLICATION TO SPACE ANTENNA

The generalized displacement vector x for this system has components representing each of the two out-of-plane rigid body angles, the out-of-plane elastic deformation of each rib and of each mesh. The basic space H is then

21

$$H = R^2 \times L_2(0,1) \times L_2(\Omega) \times \cdots \times L_2(0,1) \times L_2(\Omega),$$ (3.5.1)

for each rib and mesh

where 1 is the length of the ribs and Ω is the area of each mesh sector. The strain-energy space V is like H with $L_2(0,1) \times L_2(\Omega)$ replaced by $H^2(0,1) \times H^1(\Omega)$.

In the numerical studies in [HR1], we used the following data. For the performance index in (3.2.1), the state weighting operator Q and control weighting matrix R are taken as

$$Q = I \quad \text{and } R = .1 \times I.$$ (3.5.2)

Hence $\langle Qz, z \rangle_E$ is twice the total energy in the antenna, plus the sum of the squares of the rigid body angles.

The disturbance V_1 in (3.1.7) and the measurement noise V_0 in (3.1.8) are assumed to have the respective covariances

$$\hat{Q} = \begin{bmatrix} 0 & 0 \\ 0 & I \end{bmatrix} \quad \text{and} \quad \hat{R} = .01 \times I.$$ (3.5.3)

The viscoelastic damping coefficients in (2.1.2) are

$$c_r = .001 \quad \text{and} \quad c_m = .003.$$ (3.5.4)

The functional gains have the form

$$f = (a_1, a_2, \underbrace{\phi_f^r, \phi_f^m}, \ldots, \phi_f^r, \phi_f^m)$$ (3.5.5)

functions for each rib and mesh

4.0 ROBUSTNESS

4.1 OVERVIEW

Robustness refers to the ability of a control system to perform satisfactorily even when the model used for design is an imperfect representation of the actual system. Modeling difficulties are a major concern in designing control systems for LSS. Much of the work on functional gains , described in the Ref. [HR1], is aimed at one particular type of modeling problem: model truncation. Parameter errors are another important source of modeling error. During the current year of research, we have worked on the problem of developing LSS controller designs which are relatively insensitive to parameter errors, but still maintain a satisfactory level of system performance. For antenna structures of the type considered, this is a difficult problem which does not easily yield to standard techniques. Because of its importance, however, it is a problem which cannot be neglected.

Two different techniques for robustness enhancement have been explored during 1985: Loop Transfer Recovery (LTR) and Sensitivity Optimization. Sections 4.2 and 4.3, which follow, describe the basic features of these approaches, and also give examples of their performance. Section 4.4 briefly discusses a controller design approach based on elements of both Loop Transfer Recovery and Sensitivity Optimization. At the present time this synthesized approach is still under development.

As a general rule, an improvement in robustness can only be achieved at the cost of a reduction in some measure of performance. In order to achieve a proper balance between performance and robustness, some constraints must be

imposed. In the loop recovery approach, the open-loop and closed-loop frequency responses are constrained to approximate those of the full state feedback LQR design. Thus, the performance of the system is first determined in the context of the LQR design, and then one tries to obtain an estimated state feedback implementation which has similar performance and also adequate robustness. The sensitivity optimization approach also begins with the solution of an LQR problem and designs an estimated state feedback implementation. In this case, however, there is no constraint to retain the LQR frequency response. Instead, the goal is to minimize the sensitivity of the closed-loop eigenvalues to parameter errors. A constraint must be imposed to keep the closed loop regulator and estimator eigenvalues sufficiently far in the left-half-plane, otherwise the optimization routine would generate a very low performance control system. Designs based on sensitivity optimization tend to be more robust than LTR designs, but their loop gains are also lower.

Both of these approaches rely heavily on the statement of the LQR problem which serves as a starting point for the designs. The state weighting operator in the performance index for the LQR problem discussed in Chapter 3 is Q. Generally, scaling up Q while holding the control weighting matrix R fixed leads to larger control gains and a less robust compensator. The numerical examples presented in Sections 4.2 and 4.3 indicate that in addition to the magnitude of Q, the relative penalization that Q specifies among the different components of the state vector can affect robustness dramatically. For example, Q's which penalize only the RMS[1] surface error of an antenna model were

----

[1] Throughout this report, the term RMS surface error refers to the root mean square displacement of the antenna surface relative to its nominal position in inertial space. Thus RMS surface error includes the effects of rigid

found to lead to designs which were not very robust. However, Q's which penalize the energy or the RMS surface error plus the rate of change of RMS error, were found to be quite robust. While the interpretation of these results is not entirely clear at this point, some observations can be made. Penalizing RMS surface error alone leads to controllers which try to reduce rigid body displacement much faster than elastic deformations. This means that the closed loop eigenvalues for rigid body modes are substantially to the left of those for the lowest flexible modes. In this case, large control torques are produced to control rigid body modes, and the system is not robust because these torques strongly excite the flexible modes, which may be inaccurately known. The other two Q's mentioned above penalize rigid body and flexible modes more equally. The real parts of the closed-loop eigenvalues, and hence the decay rates, for rigid body modes and lowest elastic modes are approximately equal and the compensator is more robust. In our continuing research effort, we plan to pursue further the relationship between the selection of Q and robustness.

----

body rotation as well as elastic deformations of the antenna

4.2 LOOP TRANSFER RECOVERY TECHNIQUES

It is well known that linear quadratic regulator designs have very attractive robustness properties, e.g., one half to infinite gain margin and 60° phase margin. This property is based on the use of full-state feedback. In practice, full-state feedback is virtually never available (certainly not for LSS) and the state must be estimated. The inclusion of an estimator frequently results in loss of the robustness promised by the regulator design. Loop recovery techniques have been proposed as a way to recover a measure of this robustness [DO1,2]. The Loop Transfer Recovery (LTR) approach was originally suggested by Kwakernaak [KW1] and later extended by Doyle and Stein [DO1,2]. Kwakernaak first derived a method to asymptotically recover the loop shape of a given Kalman-Bucy Filter (KBF) at the plant output, by allowing the control weighting in a specific LQR problem to approach zero. This offers the advantage of recovering the minimal sensitivity properties of the Kalman Filter. Doyle and Stein pointed out that the dual to Kwakernaak's approach, allowing the noise covariance in a KBF problem to approach zero, asymptotically recovers the LQR loop shape at the plant input. This offers the advantage of recovering the gain and phase margins of the Full-State Feedback Quadratic Regulator. Both procedures will be referred to as Loop Transfer Recovery (LTR), where Kwakernaak's approach [KW1] recovers a loop shape at the plant output, and is only valid when the plant has at least as many inputs as outputs, while the approach of Doyle and Stein [DO1,2] recovers a loop shape at the plant input, and is only valid when the plant has at least as many outputs as inputs. Both approaches require that the plant be non-minimum phase and it is only in the case of square plants that the designer has a choice of

recovering the loop shape at either the input or output[1]. A recent paper which discusses more fully the various aspects of examining the feedback loop at various points is Ref. [FR1]

The present work examines the application of the LTR approach to designing robust control systems for lightly damped, flexible structures with an unequal number of inputs and outputs. It is relatively common for a flexible structure to have more available measurements than available control inputs. Hence, the case of an excess of outputs over inputs will be emphasized. In particular, the special case of 1-input and m-outputs, which, by reducing the loop gain at the plant input to a scalar function, both simplifies the analysis and clarifies conceptual ideas, will be used extensively. This is motivated by the study of the wrap-rib antenna.

The first implication of the excess of outputs over inputs is that the loop shape can be recovered only at the plant input, while a second implication is that a number of extra degrees of freedom, required to produce a square system, are available. The implication of these degrees of freedom will be carefully considered and two methods for taking advantage of them will be offered. In particular, an algebraic method that will provide Loop Transfer Recovery with arbitrary compensator pole placement and a reduced order compensator, will be presented. An optimization method which chooses the extra degrees of freedom so as to minimize the sensitivity of the closed-loop pole locations with respect to plant frequency errors is discussed in Section 4.4.

----

[1] Margins at both the input and the output can be guaranteed simultaneously only when the inequalities $\underline{\sigma}[I+K(s)G(s)] \geq 1$ and $\underline{\sigma}[I+G(s)K(s)] \geq 1$ both hold [LE1].

It should be noted that at least one paper on an application of LTR to a flexible space antenna has appeared in the literature [SU1]. In this work the design model was reduced to the three rigid body modes of the antenna, while all the flexible modes were treated as uncertainties. Unstructured uncertainties are a good representation of the error due to neglected dynamics so this is a valid application of LTR, but it will clearly result in a very low performance control law[2]. In fact, the resulting control law indicates an open-loop bandwidth below 10^{-3} rad./sec., where the first flexible mode is not encountered until approximately .75 rad./sec. The application studied in the current work involves finding high performance control laws for flexible structures with uncertain frequencies. This means that the control action will actively control the uncertain frequencies, or equivalently, open-loop bandwidths will fall beyond the uncertain frequencies. In this case the uncertainties are best described in terms of parameter errors rather than unmodeled (i.e. truncated) dynamics. As illustrated in Section 4.2.1, unstructured uncertainties are not a good representation of parameter errors in the modeled modes of a lightly damped flexible system and the difficulty in achieving a robust design is greatly increased.

The organization of the next few Sections is as follows. First the question of robustness is discussed, paying particular attention to the modern robustness Theorems of the past 10 years. The most important results relevant to this study are the unstructured representations of plant uncertainty presented by Doyle and Stein [DO1] and by Lehtomaki [LE1,2,3,4]. The unstruc-

----

[2] The reason why this implies a very low performance control law is discussed in Section 4.2.3.

28

tured uncertainty indicates that robustness can be guaranteed by making the minimum singular value of either the return difference or inverse return difference transfer function matrices large enough. This leads to the idea of defining robustness in terms of loop shape, and provides the motivation for loop shaping as a control design method, and LTR as a particular approach to achieving some desired loop shape. Using a simple one mode example, it is shown that the unstructured uncertainty is far too conservative to treat poorly modeled frequencies. It is concluded that in the case of a strict parameter uncertainty, such as an uncertain frequency, robustness should be checked by varying the parameter within the expected range, while examining the closed loop eigenvalues. A secondary, but crucial conclusion is that robustness is not necessarily determined by loop shape, except in the special case where the system component uncertainties are accurately described in terms of unstructured uncertainties.

Next a description of the LTR method is given, along with a discussion of some of its properties. Again, particular attention is paid to the implications of some of these properties for lightly damped, flexible structures. It is concluded that the LTR method does not always guarantee a robust system, even when the corresponding full-state feedback design is extremely robust, and should be used carefully in designing compensators for lightly damped, flexible systems. This is a result of the previously noted conclusion, that robustness is not necessarily a function of loop shape alone. The reasons for lack of robustness in LTR designs is examined and methods for using the extra degrees of freedom available in the non-square problem, to find a "better" LTR design for a given LQR loop shape are suggested.

After presenting the design methods, they are applied to a wrap-rib antenna model, in an attempt to achieve robustness in the face of frequency uncertainty, while maintaining a given loop shape. The antenna model is chosen because it is much more sensitive to frequency errors than other models we have tried. The results are compared with traditional LQG designs, traditional LTR designs and with a direct parameter optimization approach. In the conclusions, the implications of this comparison, and a general approach to using LTR to design robust control systems for non-square, lightly damped, flexible structures are discussed.

Background information may be found in the appendices, including a review of singular values, proofs of Theorems, and a discussion of numerical considerations in the application of the two LTR methods.

4.2.1 ROBUSTNESS MEASURES FOR MIMO FLEXIBLE SYSTEMS

One of the major reasons for the application of feedback control, is to minimize the effect of variations in plant dynamics (or equivalently, plant frequency response) on the system performance. Robustness is the study of exactly how large of a variation in plant dynamics can be tolerated, before a given feedback system goes unstable.

The basic work in single-input-single-output (SISO) feedback systems was done more than forty years ago by Nyquist, Bode [B01] and their colleagues. The most important robustness result is the Nyquist Stability Criterion, and the related concepts of gain margin and phase margin. These margins specify, in an exact sense, how much the gain and phase of the plant frequency response

30

can vary before the closed-loop system will go unstable. In particular the gain margin measures the amount by which the open-loop gain can be increased without causing instability, while the phase margin measures the amount by which the open-loop phase lag can be increased without causing instability. These essentially measure the closeness of the Nyquist plot to the -1 point, therefore generalizing the Nyquist Stability Criterion from a measure of absolute stability to one of relative stability.

The present work focuses on developing robust control methods for large, flexible, lightly damped structures. There are two aspects of these systems that cause some difficulty in analyzing robustness properties. The first is their lightly damped, flexible nature, which implies a highly oscillatory frequency response, making concepts such as gain and phase margin much more difficult to interpret. This difficulty, however, can still be handled within the context of classical control methods, though with some care. The second difficulty proves to be more fundamental, and stems from the existence of a number of inputs and outputs, all connected together. Since there is no longer one loop gain to be analyzed, classical methods cannot be applied directly. Furthermore, it has been shown that analyzing each loop of a multiple loop system separately, does not always give results that are valid for the overall system [DO1]. Fortunately the robustness of multivariable systems has been studied extensively in the last ten years. It is the purpose of this Section, to give a quick overview of the state-of-the-art in robustness of multiple-input-multiple-output (MIMO) feedback control systems.

An extremely general approach to MIMO robustness can be found in the work of Zames [ZA1,2] on cone bounded perturbations and Safonov [SA1,2] on even

31

more general perturbations. These results rely heavily on the mathematical field of functional analysis and are applicable to both non-linear and time-varying plants. The special case of linear, time-invariant plants, however, can be dealt with much more simply, and a number of more practical robustness Theorems have been developed. These Theorems can be divided into two groups, paralleling the two modern approaches to control theory mentioned in the last Section. The most popular approaches to describing the robustness of linear, time-invariant MIMO feedback control systems deal with a transfer function description of the plant uncertainty. It's the transfer function approach which leads to loop shaping as a method for obtaining robust control, and it will be dealt with first.

Transfer Function Approaches to Robustness

Consider the simple feedback system illustrated in Fig. 4.1, where:

R(s) - Command Signal
K(s) - Compensator
U(s) - Control signal to the plant
G'(s)- True, possibly unknown plant, described by a nominal
       plant, G(s), and some characterization of errors
Y(s) - Output variables (Measurements)

Dropping the dependence on s, some transfer functions describing the system can then be evaluated as follows:

$$Y = [(I+GK)^{-1}GK]R = [GK(I+GK)^{-1}]R \qquad (4.2.1)$$

$$E = R - Y = (I+GK)^{-1}R \qquad (4.2.2)$$

$$U = [(I+KG)^{-1}K]R = [K(I+KG)^{-1}]R \qquad (4.2.3)$$

Also define the following functions:
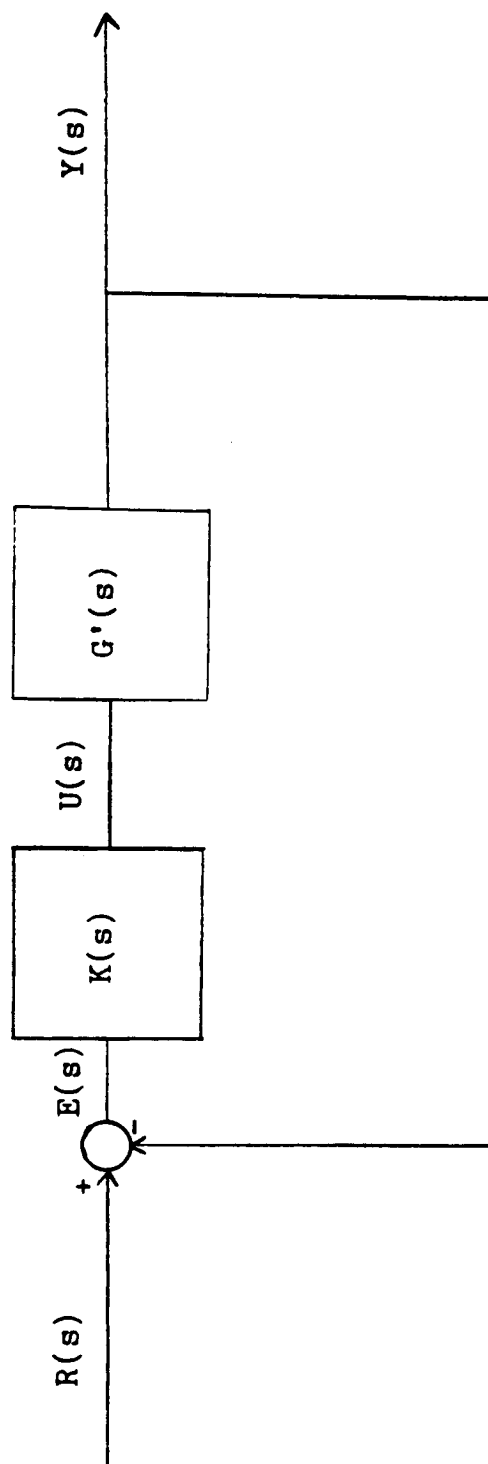
Figure 4.1 MIMO Feedback System Configuration

GK   - Output Loop Transfer Function

KG   - Input Loop Transfer Function

[I+GK]   - Output Return Difference

[I+KG]   - Input Return Difference

$[I+(GK)^{-1}]$ - Output Inverse Return Difference

$[I+(KG)^{-1}]$ - Input Inverse Return Difference

And make note of the following identities:

$$[I+(GK)^{-1}]^{-1} = GK[I+GK]^{-1} = [I+GK]^{-1}GK \qquad (4.2.4a)$$

$$[I+(KG)^{-1}]^{-1} = KG[I+KG]^{-1} = [I+KG]^{-1}KG \qquad (4.2.4b)$$

$$[I+(GK)^{-1}]^{-1} + [I+GK]^{-1} = I \qquad (4.2.5a)$$

$$[I+(KG)^{-1}]^{-1} + [I+KG]^{-1} = I \qquad (4.2.5b)$$

The first two identities show that the inverse return difference is simply the inverse of the closed loop transfer function. The second two identities show that the sum of the inverses of the return difference and inverse return difference is equal to the identity. The implications of this fact, in terms of fundamental limitations on design, are discussed in Ref. [SA3].

Note that the output loop and input loop transfer functions and related return differences are not in general the same for MIMO systems, though they are for SISO systems. In fact, if the number of inputs is not equal to the number of outputs, they will not even have the same dimensions. This property affects the way in which an uncertainty is described. In particular the true plant G'(s) might be described in terms of a nominal plant G(s) in one the following two ways:

$$G'(s) = L_o(s)G(s) \tag{4.2.6a}$$

or $\quad G'(s) = G(s)L_i(s)$ $\hfill$ (4.2.6b)

$L_o(s)$ will have the dimension of the plant output, and can be considered an uncertainty acting at the output, while $L_i(s)$ will have the dimension of the plant input, and can be considered an uncertainty acting at the input. $L_o(s)$ would provide the best error description for the output loop since $G'(s)K(s)=L_o(s)G(s)K(s)$, while $L_i(s)$ would provide the best error description for the input loop, since $K(s)G'(s)=K(s)G(s)L_i(s)$. The point at which the loop is "opened" to examine robustness will therefore depend on the way in which the error is described, and vice-versa. For simplicity, only errors acting at the plant input will be considered, but the results for errors acting at the output can be easily found by replacing $K(s)G(s)$ by $G(s)K(s)$ in the Theorems of the following Sections.

Unstructured Uncertainty

The most basic description of uncertainties in the form of (4.2.6a) or (4.2.6b) is the unstructured uncertainty introduced by Doyle and Stein [DO1] and by Lehtomaki [LE1,2,3,4]. An unstructured uncertainty is one that can be given no more structure than a bound on a suitable measure of its size. For matrices, singular values serve as such a measure. Singular values are discussed in Appendix A. It is assumed that the reader is familiar with the concept of maximum and minimum singular values as well as some of their properties.

Consider the following two[1] possibilities for $L(s) = L_i(s)$:

$$L(s) = [I+\Delta_m(s)] \quad \text{(multiplicative uncertainty)} \tag{4.2.7a}$$

$$\text{or} \quad L(s) = [I+\Delta_d(s)]^{-1} \quad \text{(divided uncertainty)} \tag{4.2.7b}$$

where in each case the perturbation can be bounded by frequency dependent functions l_m and l_d:[2]

$$\overline{\sigma}[\Delta_m(s)] \leq l_m(s) \tag{4.2.8a}$$

$$\text{and} \quad \overline{\sigma}[\Delta_d(s)] \leq l_d(s) \tag{4.2.8b}$$

THe function $l_m(s)$ and $l_d(s)$ are real and positive on the Nyquist D-contour.

The closed loop stability of the true system ($KG'[I+KG']^{-1}$) can be determined by the multivariable generalization of the Nyquist Criterion [RO1], which requires that the $\det[I+KG']$, evaluated on the standard Nyquist D-contour (denoted by $s\epsilon\Omega_R$), encircle the origin in a counter-clockwise direction, as many times as there are unstable open-loop poles of KG'. For most practical problems involving flexible structures, the only poles of G on the imaginary axis will be at the origin, and there will be an excess of poles over zeros, implying that $\lim_{s\to\infty} K(s)G(s)=0$. In this case the Nyquist D-contour reduces

----

[1] Two other unstructured uncertainty representations are the additive and subtracted representations, which are discussed in Ref. [LE1]. These, however, are equivalent to the multiplicative and divided disturbances respectively and will not be discussed here.

[2] Another method for bounding the uncertainties is the cone-bounded perturbation [DO4]. This essentially corresponds to a multidimensional scaling of the problem and is again equivalent to Eq. (4.2.8).

to the imaginary axis, with the possibility of an identation about the origin, and $s\varepsilon\Omega_R$ can be replaced by $j\omega$. Under the assumptions that G and G' have the same number of open-loop unstable poles, and that KG' and KG have identical open-loop poles on the $j\omega$-axis we have the following two results:

Theorem 4.1: (Multiplicative Disturbance) The closed loop system will remain stable for all allowable perturbations iff:

$$\overline{\sigma}[KG(s)(I+KG(s))^{-1}] < 1/l_m(s) \quad \forall s\varepsilon\Omega_R \qquad (4.2.9a)$$

or equivalently if KG is invertible:

$$\underline{\sigma}[I+(KG(s))^{-1}] > l_m(s) \quad \forall s\varepsilon\Omega_R \qquad (4.2.9b)$$

Theorem 4.2: (divided disturbance) The closed loop system will remain stable for all allowable perturbations iff both a) and b) are true:

a) L(s) has no zero or strictly negative real eigenvalues for any $s\varepsilon\Omega_R$

b) $\quad \overline{\sigma}[(I+KG)^{-1}] < 1/l_d(s) \quad \forall s\varepsilon\Omega_R \qquad (4.2.10a)$

or equivalently:

$$\underline{\sigma}[I+KG] > l_d(s) \quad \forall s\varepsilon\Omega_R \qquad (4.2.10b)$$

A proof of the above results is given in Appendix B.

It should be noted that these are not conservative results, given the error characterization of Eq. (4.2.8). In fact, if the above conditions are not met, there exists a perturbation, $\Delta_m(s)$ or $\Delta_d(s)$, whose maximum singular value

lies below $l_m(s)$ or $l_d(s)$ respectively, which will destabilize the system.

The unstructured uncertainty can however be unduly conservative in its characterization of error. If the error is known to have some structure it is quite possible that the particular $\Delta_m(s)$ or $\Delta_d(s)$ required to cause instability cannot occur.

One major difference between the above two results is the additional requirement, in the case of a divided uncertainty, that $L(s)$ have no zero or strictly negative real eigenvalues for $s\varepsilon\Omega_R$. This is needed to insure that the function $[I+\varepsilon\Delta_d]^{-1}$ remains continuous as ε varies from zero to one, and can be interpreted as indicating that Theorem 4.2 cannot guarantee robustness in the case where phase is completely arbitrary. See Appendix B and Ref. [LE1] for further details. This places a limit on the situations in which a divided disturbance can be used to study robustness. For most practical problems, however, the phase will be known to within ±180°, and both Theorems 4.1 and 4.2 are applicable. In this case the system can be made robust to multiplicative uncertainties by maintaining a large inverse return difference, or equivalently a small loop gain, while the same system can be made robust to divided uncertainties by maintaining a large return difference, or equivalently a large loop gain. The two representations therefore imply opposite requirements for achieving robustness, and together imply that a system can be made robust either by maintaining very high loop gains, or by maintaining very low loop gains, while it will be most sensitive to errors in the region of gain cross-over. This is a familiar result from classical control, corresponding to the fact that perturbations of the Nyquist plot far away from

the -1 point will not affect stability, and the unstructured uncertainties provide its MIMO generalization. One final note is that Eq. (4.2.5b) indicates that the return difference and inverse return difference are not independent, implying that a system cannot be made robust to both multiplicative and divided disturbances acting simultaneously at any fixed frequency.[3]

In applying the unstructured uncertainties to flexible structures, which will have an infinite number of possibly lightly damped and poorly modeled modes, the divided disturbance is not particularily useful. The reason for this is that if some set of modes at "low frequencies" are robustly controlled by maintaining a high loop gain in that frequency range, there there will necessarily exist a further set of modes at some "intermediate frequency" which will lie near cross-over. If the low frequency modes are inaccurately modeled, then the intermediate frequency modes will also be inaccurately modeled, and the system will not be robust to errors in these modes. The unstructured uncertainty, when applied to lightly damped flexible structures therefore implies that the loop gain must be kept below some level, whenever poorly modeled frequencies are present. To gain an appreciation for this limit, consider a very simple SISO flexible model.

----

[3] The divided disturbance is often considered most appropriate in dealing with low frequency errors, while the multiplicative disturbance is most appropriate when dealing with high frequency errors. This is because the divided disturbance indicates high loop gain, typically true at low frequencies, while the multiplicative disturbance indicates low loop gain, typically true at high frequencies. It should be emphasized that both are unstructured, with the only additional structure available in the divided disturbance being due to the fact that phase cannot be completely arbitrary.

39

Example of a Multiplicative Unstructured Uncertainty Approach

Since the unstructured uncertainty approaches are generalizations of classical SISO theory, they will work for more complicated systems only if they work for a simple SISO system. With this in mind consider a system consisting of a single, underdamped, flexible mode whose gain and damping ratio are known, but whose frequency is known only within given bounds. Such a system might be described as follows:

$$G'(s) = \frac{f'^2}{s^2 + 2\zeta f's + f'^2} \qquad\qquad G(s) = \frac{f_0^2}{s^2 + 2\zeta f_0 s + f_0^2} \qquad\qquad (4.2.11)$$

let $\Delta f = (f' - f_0)/f_0$

then
$$\Delta_m(s) = \frac{\Delta f s[(2 + \Delta f)s + 2\zeta f']}{s^2 + 2\zeta f's + f'^2} \qquad\qquad (4.2.12)$$

and
$$|\Delta_m(j\omega)| = |\Delta f|\omega \frac{(2+\Delta f)^2 + (2\zeta f')^2}{(f'^2 - \omega^2)^2 + (2\zeta f')^2\omega^2} \qquad\qquad (4.2.13)$$

This is the $l_m(\omega)$ for one particular error in frequency (Δf), but Δf is actually only known to be within certain bounds. The correct $l_m(\omega)$ would then take the worst case of the above bound for every possible Δf. An algorithm to find $l_m(\omega)$ for a set of bounds on Δf would, for every ω, calculate Eq. (4.2.12) for a sufficient number of Δf's between the bounds, and then plot the worst case.

Fig. 4.2a illustrates the result of such an algorithm. In this case $f_0 = 1$ rad/sec, $\zeta = .01$ and Δf is allowed to vary between $-.10$ and $+.10$.

$20\log_{10}(1/l_m(\omega))$ is plotted, taking the worst case of 200 different Δf's between $-.10$ and $+.10$ at 400 frequency points between .75 rad/sec and 1.25 rad/sec.

A computationally simpler approximation would be to consider only the two worst cases of Δf, ($\Delta f = -.10$ and $\Delta f = +.10$). The result of an algorithm that did this for the same number of frequency points is plotted in Fig. 4.2b. The plots are similar, though the shapes vary slightly between the limits on Δf. The second approach, might provide guidelines for a first cut design, though it would not strictly guarantee stability by Theorem 4.1.

The function $(1/l_m(\omega))$ places strict limitations on the bandwidth of the system, since the closed-loop gain must fall below it. This implies that the bandwidth is limited by the first time that $(1/l_m(\omega))$ falls below 0 db. This occurs when $l_m(\omega)$ first rises above 1, or when the errors in frequency response first rise above the nominal frequency response. It would be expected that this would occur at some frequency for any realistic plant but will it occur near a given uncertain natural frequency? In the cases plotted in Figs. 4.2a and 4.2b $(1/l_m(\omega))$ actually dropped to about -20 db. Theorem 4.1 would therefore imply that a SISO feedback system with with a 1% damping ratio and 10% frequency error would be required to have a loop gain that fell below -20 db at that frequency, sharply limiting bandwidth and therefore performance.

To get a rough idea of the extent of the limits imposed on such a system by Theorem 4.1, consider an approximation of Eq. (4.2.13). Assume that ζ and Δf
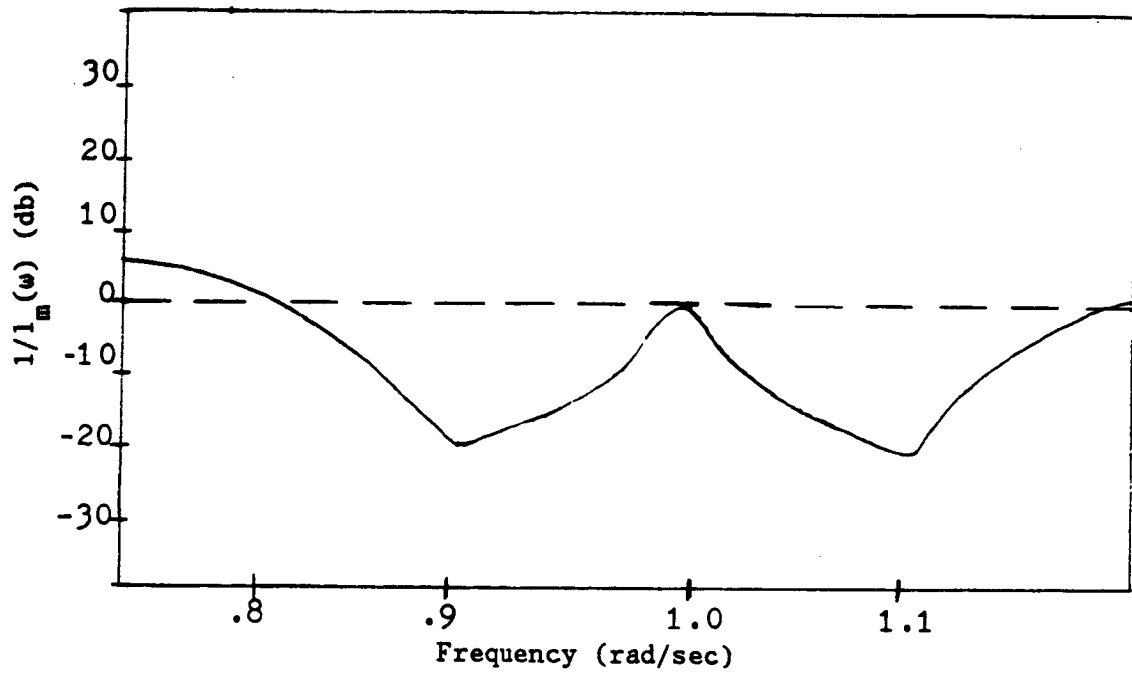
Figure 4.2a $1/1_m(\omega)$ for $-0.1 \leq \Delta\omega \leq +0.1$
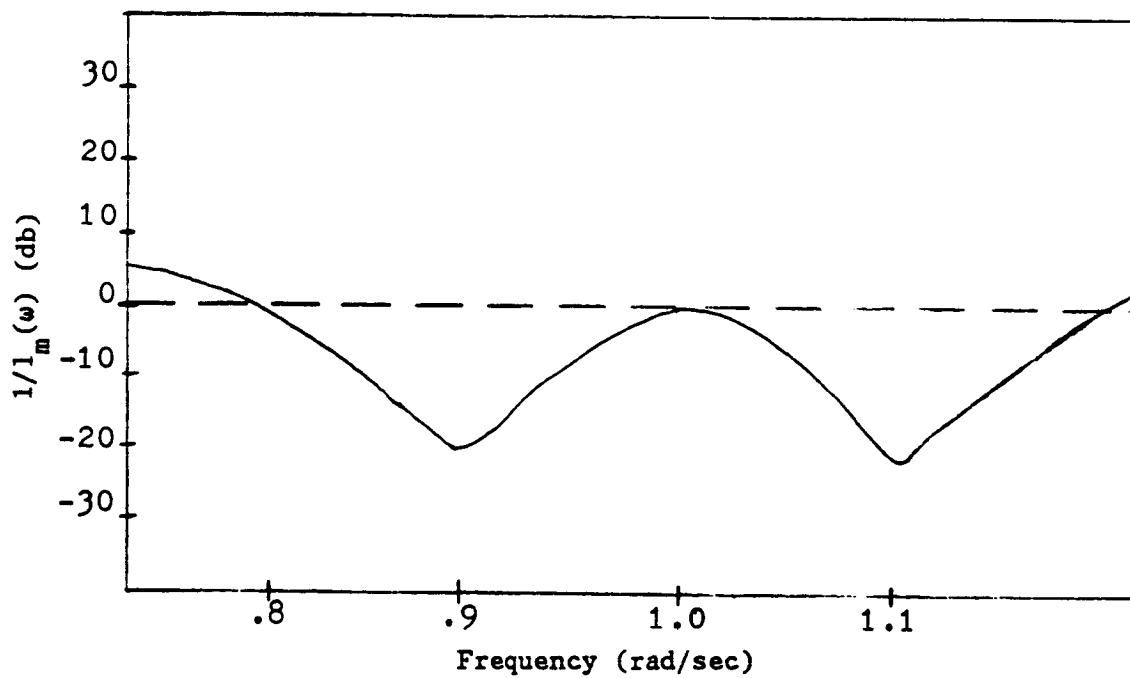
Figure 4.2b $1/1_m(\omega)$ for $\Delta\omega = -0.1$ and $+0.1$

are both small as compared to 1, and that the function reaches a maximum at $\omega = f'$. Then:

$$|\Delta(j\omega)|_{max} \simeq \Delta f/\zeta \qquad\qquad (4.2.14)$$

This indicates that relative frequency errors on the order of the damping ratio will limit the system closed-loop bandwidth. This is a relatively strict limitation, since if the damping ratio in a particular mode is 1%, a reasonable value for flexible space structures, a 1% frequency error might destabilize a system whose bandwidth included that mode.

This limit seems overly restrictive, but to gain a more concrete appreciation of the conservativeness of the unstructured uncertainty for this particular system consider a simple constant gain controller in the feedback loop. The closed-loop characteristic equation of the system is:

$$s^2 + 2\zeta f's + (1+k)f'^2 = 0 \qquad\qquad (4.2.15)$$

This is clearly stable for all $k > -1$, for all $\zeta > 0$ and for all f'. The bandwidth of the closed-loop system can therefore be increased without bound, for arbitrary error in frequency and arbitrary non-zero damping ratios, in conflict with the requirements implied by Theorem 4.1. The reason that the unstructured uncertainty is so conservative, even for this very simple, SISO system, is that it doesn't take into account any information on the phase of the system. Essentially it defines limits on the gain error, while allowing completely arbitrary phase error. For this system though, the phase error is uniquely determined by the gain error, so that the exact phase shifts that would be necessary to destabilize the system for a given gain shift can never

occur. The unstructured uncertainty is therefore not a good characterization of error due to uncertain frequencies in the modeled modes of a lightly damped, flexible structure. Next apply Theorem 4.2 to the same problem.

Application of Theorem 4.2 to the Example Problem

In applying Theorem 4.2, the first step is to ascertain that $L(s)$ is never zero, or strictly negative on $s \varepsilon \Omega_R$, or equivalently that the phase of $L(j\omega)$ never reaches $\pm 180^\circ$. For the example:

$$L(j\omega) = \frac{f'^2[(f_0^2-\omega^2)(f'^2-\omega^2)+4\zeta^2 f_0 f' \omega^2 + 2\zeta\omega[f_0(f'^2-\omega^2)-f'(f_0^2-\omega^2)]j]}{\omega^2[(f'^2-\omega^2)^2+4\zeta^2 f'^2 \omega^2]} \quad (4.2.16)$$

$L(j\omega)$ is equal to zero or strictly negative only when the imaginary part of eq. (4.2.16) is identically equal to zero. This in turn is true only when $\zeta=0$ or when $\omega^2=-f_0 f'$, so unless $\zeta=0$, there is no real frequency at which $L(j\omega)$ is either zero or negative real, indicating that Theorem 4.2 is applicable.[*] For the example the divided disturbance is given as follows:

$$\Delta_d(s) = \frac{\Delta f s[(2+\Delta f)s+2\zeta f_0]}{s^2+2\zeta f_0 s+f_0^2}, \quad \text{where } \Delta f=(f_0-f')/f' \quad (4.2.17)$$

$|\Delta_d(j\omega)|$ will reach a maximum near $\omega=f_0$, so: $|\Delta_d(j\omega)|_{max} \simeq \Delta f/\zeta$

Theorem 4.2 therefore implies that whenever the frequency error is on the order of the damping ratio, loop gain at that frequency must lie above 0db, or

----

[*] Actually, for small ζ and large Δf the phase of $L(j\omega)$ asymptotically reaches $\pm 180^\circ$, but it is never exactly equal to $\pm 180^\circ$.

equivalently, that sufficiently high gain will stabilize the system. Theorems 4.1 and 4.2 together indicate that a feedback control for this example can be made robust by either introducing very high gains, or very low gains, while in the case where $\Delta f > \zeta$ there will exist a zone of intermediate gains which will not be robust, as was pointed out in the previous Section. This is a conservative result since it has been ascertained that the above example is robust to arbitrary frequency errors for any positive feedback gain.

In conclusion, errors in the frequency of a lightly damped oscillator provide a highly structured parameter variation and the unstructured uncertainties of Doyle and Lehtomaki provide an overly conservative characterization of these errors. This further implies that due to their conservativeness unstructured uncertainties are not particularly useful for determining the robustness of flexible systems with poorly modeled frequencies. An implication of this observation will be dicussed further in the context of LTR design methods (Section 4.2.4).

4.2.2 ASYMPTOTIC LOOP TRANSFER RECOVERY (LTR) CONTROL DESIGN

LTR is an appealing approach to control design for two basic reasons. The first is that it can be used to recover the gain and phase margins of a Linear Quadratric Regulator (LQR) at the plant input, or of a Kalman Bucy Filter (KBF) at the plant output. This is sometimes called robustness recovery [DO2] or sensitivity minimization [KW1], but these are somewhat misleading terms since they suggest that the loop recovered system will have the same robustness properties as the full state feedback LQ regulator or the KB filter. This is not necessarily true as will be indicated more specifically later.

The second appeal of the LTR approach is its applicability to loop shaping as a more general control design method. The idea of loop shaping is most clearly spelled out in Ref. [DO1], where it is pointed out that a number of system properties, including performance, sensitivity, noise rejection, "robustness" and control effort, depend on the system loop shape (maximum and minimum singular values of the system transfer function matrix). The LTR loop shaping approach involves first designing an LQR loop or a KBF loop with desired characteristics, and then recovering that loop shape by LTR methods. Again there is an assumption in the loop shaping approach that all systems with the same loop shape will behave identically. This is true for the nominal plant, but when the plant parameters are perturbed, the two loops may no longer be identical and the system response (and stability) may vary considerably. In a later Section, a number of examples will be given of systems with identical loop shape, but different robustness characteristics.

For simplicity, the input loop recovery procedure of Doyle and Stein [DO1,2] will be considered, noting that output loop recovery [KW1] is simply its dual. After describing the procedure it will be interpreted for SISO systems, and for 1-input, m-output systems. This interpretation will lead to a polynomial (pole/zero cancellation) approach to loop recovery. Methods for using the extra degrees of freedom available in the loop recovery procedure to find an "optimal" loop recovered system will be considered in Section 4.4.

Input Loop Recovery

The LQR loop has excellent robustness properties. In particular an LQ regulator with diagonal input weighting matrix R is guaranteed to have at

least an infinite gain margin, a gain reduction margin of 1/2 and a phase margin of ±60°, simultaneously in all the feedback loops [LE1,2]. The idea of input loop recovery is to design an LQ regulator with a desired loop shape and then use an asymptotic procedure to design a KB filter that recovers that loop shape. Since gain and phase margins are a function of loop shape, the output feedback system, using a KB filter to estimate the plant states, will have the identical gain and phase margins as the LQR loop. For this reason, input loop recovery is sometimes called robustness recovery. This is the point of view taken in Ref. [DO2]. Another advantage of the loop recovery approach is that it is relatively simple to specify the LQR loop shape at low frequencies by carefully choosing the weightings in the LQR cost functional [HA1]. Loop Transfer Recovery (LTR) can then be used to achieve the identical loop shape for an output feedback system. This is the loop shaping control approach, and is the point of view taken in Ref. [DO1].

To see how loop transfer recovery works, consider a full-state feedback control law, $u=-Kx$. The input loop transfer function for this system will be $K(sI-A)^{-1}B$. Now consider a state estimator of the form,

$$\dot{\hat{x}} = A\hat{x} + Bu + G(y - C\hat{x}) \qquad (4.2.18)$$

and a control law based on the state estimate $\hat{x}$, $u=-K\hat{x}$. In this case the compensator transfer function is,

$$K(s) = K(sI - A + BK + GC)^{-1}G \qquad (4.2.19)$$

and the input loop transfer function for the output feedback system is:

$$K(s)G(s) = K(sI - A + BK + GC)^{-1}GC(sI - A)^{-1}B \qquad (4.2.20)$$

To get loop recovery choose an estimator gain matrix G, such that,

$$K(sI-A+BK+GC)^{-1}GC(sI-A)^{-1}B \rightarrow K(sI-A)^{-1}B \qquad (4.2.21)$$

In Refs. [DO1,2] it is indicated that any G matrix that asymptotically satisfies

$$G \rightarrow qBW \qquad (4.2.22)$$

for some arbitrary symmetric, positive definite matrix W, will recover the loop shape. q is a large scalar parameter which is increased to achieve asymptotic loop recovery. To illustrate this result, note that the transfer function between y and ŷ in the state estimator can be written as follows,

$$\hat{y} = (I + C\bar{\Phi}G)^{-1}C\bar{\Phi}Gy \qquad (4.2.23)$$

where $\bar{\Phi}$ denotes $(sI - A + BK)^{-1}$. This leads to the following alternate representation of K(s),

$$K(s) = K[\bar{\Phi} - \bar{\Phi}(I + C\bar{\Phi}G)^{-1}C\bar{\Phi}]G \qquad (4.2.24)$$

which after some further manipulation can be rewritten as:

$$K(s) = K\bar{\Phi}G(I + C\bar{\Phi}G)^{-1} \qquad (4.2.25)$$

Now let $G \rightarrow qBW$ which means that,

$$K(s) \rightarrow K\bar{\Phi}B(C\bar{\Phi}B)^{-1}. \qquad (4.2.26)$$

Using the identity, $\bar{\Phi}B = \Phi B(I + K\Phi B)^{-1}$, where $\Phi = (sI - A)^{-1}$ Eq. (4.2.26) becomes,

$$K(s) \rightarrow K\Phi B(C\Phi B)^{-1} \qquad (4.2.27)$$

and,

$$K(s)G(s) \rightarrow K\Phi B(C\Phi B)^{-1}C\Phi B = K\Phi B \qquad (4.2.28)$$

This shows explicitly how loop recovery inverts the plant dynamics from the left and replaces them by the full-state feedback dynamics.

So far there has been no requirement that K be derived from an LQR problem, nor that the estimator be a KB-filter. In fact any appropriate method (e.g.,

pole placement) could be used to select the control gains K, and any estimator (e.g., an observer) which both asymptotically satisfies Eq. (4.2.22) and stabilizes the plant, could be used to calculate the asymptotic estimator gains G. However, the choice of an LQR approach for finding K has the advantage that the resulting loop will have desirable properties, and the use of a KB-filter to recover that loop shape has the advantage of guaranteeing a stable plant at every stage in the asymptotic loop recovery procedure.

To use a KB filter for the LTR, the first step involves appending additional columns to the B matrix until the plant is square. The only requirement on these columns is that the resulting plant be minimum phase, and within this constraint the extra columns can be viewed as free design variables. Once the system is "squared up," a KB filter is found, where the measurement noise covariance N is an arbitrary positive definite matrix, and the state noise covariance has the following special form,

$$M = M_o + q^2 BWB^T \qquad (4.2.29)$$

where M_o is some nominal noise covariance, q is the parameter which will be increased to achieve recovery and W is an arbitrary positive definite matrix. Note that the B matrix in Eq. (4.2.29) includes the appended columns, so the rank of BWB^T is equal to the number of plant outputs.

To show that this KB filter will asymptotically satisfy Eq. (4.2.22), consider the Riccati equation:

$$AP + PA^T - PC^TN^{-1}CP + M_o + q^2 BWB^T = 0 \qquad (4.2.30)$$

and divide by q^2:

$$A(P/q^2) + (P/q^2)A^T - q^2(G/q^2)N(G/q^2)^T + (M_o/q^2) + BWB^T = 0 \qquad (4.2.31)$$

Now let $q \to \infty$, under the assumption that the plant be minimum phase, to get:

$$-(G/q)N(G/q)^T + BWB^T \to 0 \qquad (4.2.32)$$

The KBF estimator gains will therefore have the following asymptotic property:

$$G \to qBW^{\frac{1}{2}}TN^{-\frac{1}{2}} \qquad (4.2.32)$$

Where T is an orthonormal matrix (ie. $TT^T = T^TT = I$). This of course satis-fies Eq. (4.2.22) and the KB filter will asymptotically recover the loop shape as q is made to approach infinity.

One quick note before continuing to an interpretation of loop recovery for SISO systems, is that the estimator gain matrix G may become very large before loop recovery is achieved. This may cause some computational problems and may not provide the best solution for a robust compensator, as will be discussed further in Section 4.2.3. A related problem concerns the convergence of esti-mator functional gains. As G increases in size, the performance of the esti-mator increases, implying that the number of modes necessary to achieve con-vergence of the estimator functional gains also increases. Asymptotic LTR therefore implies a large system model if the estimator is expected to con-verge to the optimal infinite dimensional estimator, as measured by functional gains. This issue still needs to be looked into. Next the SISO case will be examimed to gain a more intuitive understanding of the LTR procedure.

SISO Interpretation of Loop Recovery

The SISO loop recovery problem is as follows. Given a SISO

$G(s) = n(s)/d(s)$, find a proper (or strictly proper) $K(s) = N(s)/D(s)$ such that $K(s)G(s) = G(s)K(s) \simeq \gamma(s)/d(s)$ for some specified $\gamma(s)$. The obvious solution is to let $N(s) = \gamma(s)$ and $D(s) = n(s)D_1(s)$, where $D_1(s)$ consists of enough poles to make $K(s)$ proper (or strictly proper), and these poles are placed far enough into the l.h.p. that they do not significantly affect the loop shape in the design region. This interpretation also clarifies the minimum phase condition, since if $G(s)$ is non-minimum phase, this procedure will result in a pole/zero cancellation in the r.h.p., that will destabilize the closed loop system.

The asymptotic LTR procedure does not calculate an exact pole/zero cancellation, but achieves this cancellation asymptotically. It is clear, however, that it is possible to achieve loop recovery by specifying a compensator that does achieve exact cancellation, without going through an asymptotic process. In both cases the cancellation will be close to exact before loop recovery is achieved, so it will be assumed that it is exact.

This interpretation indicates the essential difference between the true LQR loop and the LTR loop. While both loops may look identical over any given frequency range, the LTR loop will contain a number of hidden pole/zero cancellations. These cancellations do not show up for the nominal plant, but as soon as the plant changes, they will no longer be exact and the LQR and LTR loop shapes may be considerably different. This is especially evident for lightly damped systems, since the plant zeros in this case will lie close to the imaginary axis. Very small errors in the plant zeros will therefore produce very large errors in the LTR loop shape. It is because of this property that an LTR design will in general not have the same robustness characteris-

tics as the corresponding LQR design.

Some Comments on the MIMO Case

LTR is a more interesting and less obvious design procedure in the MIMO case, but the same basic properties carry through. In this case the designer would choose the following compensator,

$$K(s) = K\Phi B(C\Phi B)^{-1}/D_1(s) \qquad\qquad (4.2.34)$$

where $D_1(s)$ would have the same interpretation as the SISO case. Eq. (4.2.34) can be rewritten by dividing out the common factor $\det[sI - A]$ to get,

$$K(s) = [Kadj(sI-A)B][Cadj(sI-A)B]^{-1}/D_1(s) \qquad\qquad (4.2.35)$$

where $Kadj(sI-A)B$ is the MIMO generalization of $\gamma(s)$ and $Cadj(sI-A)B$ is the MIMO generalization of $n(s)$.

For the special case of 1-input and m-outputs $[Cadj(sI-A)B]$ will be a square matrix where only the first column is fixed and the next $m-1$ columns are at the designers discretion (within the constraint of a non-minimum phase plant). Thinking again in terms of the SISO problem, this is somewhat like having an $n(s)$ at the designer's discretion, corresponding to some freedom in the placement of compensator poles. Once the poles are picked, however, loop recovery will specify the compensator zeros. Keeping this in mind an algebraic, direct pole/zero cancellation, design of a LTR compensator for a 1-input, m-output plant will be considered.

4.2.3 ALGEBRAIC LOOP TRANSFER RECOVERY

As indicated in the previous Section, loop recovery can be achieved for a SISO system by defining a compensator that exactly cancels the plant zeros and replaces them by a set of "optimal" zeros corresponding to the LQR loop. For the case of a 1-input, m-output plant, a similar procedure can be carried out, but now the designer has a set of free design variables. This freedom can be used in a variety of ways. Some possibilities include choosing a minimum order loop recovery compensator or specifying the location of the compensator poles. For the purposes of this discussion a minimal order compensator for which the compensator poles can be chosen arbitrarily will be considered, and an algebraic procedure to find the compensator numerator polynomials, or equivalently the compensator zeros will be used to achieve a given input loop shape. It should be emphasized that this is not a requirement of the algebraic LTR approach. Lower order compensators might be found by removing the freedom to specify pole location, while higher order compensators would allow the designer a number of free parameters which could be adjusted so as to meet some other criteria, possibly via an optimization process. The choice considered for this discussion, however, allows one to examine the important effect of compensator pole location, without adding excess variables to the formulation.

A 1-input, m-output plant and compensator will have the following special form:

$$G(s) = \begin{bmatrix} g_1(s) \\ g_2(s) \\ . \\ . \\ g_m(s) \end{bmatrix} = \begin{bmatrix} n_1(s) \\ n_2(s) \\ . \\ . \\ n_m(s) \end{bmatrix} / d(s) \qquad (4.2.36a)$$

$$K(s) = [k_1(s) \; k_2(s) \; \ldots \; k_m(s)] = [N_1(s) \; N_2(s) \; \ldots \; N_m(s)]/D(s)$$

$$(4.2.36b)$$

The input loop transfer function will be:

$$K(s)G(s) = \sum_{i=1}^{m} n_i(s)N_i(s)/d(s)D(s) \qquad (4.2.37)$$

To achieve loop recovery it is necessary that:

$$K(s)G(s) = \sum_{i=1}^{m} n_i(s)N_i(s)/d(s)D(s) = \gamma(s)/d(s)D_1(s) \simeq \gamma(s)/d(s) \qquad (4.2.38)$$

where $\gamma(s)$ is the numerator polynomial for the LQR input loop. $D_1(s)$ is again a set of poles required to maintain a proper (or strictly proper) compensator, where these poles are kept far enough out in the l.h.p. that they don't significantly affect the loop shape in the design region. Then $D(s)=D_c(s)D_1(s)$, where $D_c(s)$ must be cancelled out by the input loop numerator. Once the compensator poles are selected, the following equation must be solved to find the compensator numerator polynomials:

$$\sum_{i=1}^{m} n_i(s)N_i(s) = \gamma(s)D_c(s) \qquad (4.2.39)$$

Next consider the minimal order compensator that can satisfy Eq. (4.2.39).

Let n_γ be deg($\gamma(s)$), n_c be the deg($D_c(s)$), n_1 be deg($D_1(s)$) and n_N be

deg($N_i(s)$). The degree of the left side of Eq. (4.2.39) will be $n_N + n_n$,

while the degree of the right side of Eq. (4.2.39) will be $n_\gamma + n_c$, so the

first requirement on n_N is that:

$$n_N + n_n = n_\gamma + n_c \qquad\qquad (4.2.40)$$

The second requirement on n_N is that there must exist enough degrees of free-

dom to satisfy Eq. (4.2.39) for arbitrary $\gamma(s)D_c(s)$. The number of free par-

ameters is $m(n_N+1)$, while the number of polynomial coefficients that must be

satisfied is $n_\gamma+n_c+1$, this implies that:

$$m(n_N+1) = n_\gamma + n_c + 1 \qquad\qquad (4.2.41)$$

Combining Eqs. (4.2.41) and (4.2.42) gives the following result for n_N:

$$n_N = (n_n/(m-1)) - 1 \qquad\qquad (4.2.42)$$

For a strictly proper compensator, the order of the compensator is

$n_c + n_1 = n_n/(m-1)$. So a 1-input, 2-output plant has a strictly proper loop

recovery compensator of the same order as the degree of the plant numerator

polynomials, while a 1-input, 3-output plant has a loop recovery compensator

of half that order, etc.. This approach therefore leads to lower order com-

pensators than the asymptotic, observer based approach described in the previ-

ous Section. In fact, as m increases, the order of the compensator can become

very small, while still achieving loop recovery.

Once the order of the compensator and the location of the compensator poles

are chosen, the compensator numerator polynomials are found by the solution of

a set of $m(n_n+1)$ linear equations. Let the ith plant numerator polynomial be written as follows:

$$n_i(s) = n_{i,n_n} s^{n_n} + \ldots + n_{i,1}s + n_{i,0} \qquad (4.2.43a)$$

and similarily let the ith compensator numerator polynomial be:

$$N_i(s) = N_{i,n_N} s^{n_N} + \ldots + N_{i,1}s + N_{i,0} \qquad (4.2.43b)$$

Then:

$$
\begin{bmatrix}
n_{1,0} & 0 & \ldots\ldots & 0 & \ldots\ldots & n_{m,0} & 0 & \ldots\ldots & 0 \\
n_{1,1} & n_{1,0} & \ldots\ldots & 0 & \ldots\ldots & n_{m,1} & n_{m,0} & \ldots\ldots & 0 \\
\cdot & \cdot & & \cdot & & \cdot & \cdot & & \cdot \\
\cdot & \cdot & & \cdot & & \cdot & \cdot & & \cdot \\
n_{1,n_n} & n_{1,n_n-1} & \cdot\cdot & \cdot & \ldots\ldots & n_{m,n_n} & n_{m,n_n-1} & \cdot\cdot\cdot & \cdot \\
0 & n_{1,n_n} & \ldots & \cdot & \ldots\ldots & 0 & n_{m,n_n} & \ldots\ldots & \cdot \\
\cdot & \cdot & \ldots\ldots & \cdot & \ldots\ldots & \cdot & \cdot & \ldots\ldots & \cdot \\
\cdot & \cdot & \ldots\ldots & \cdot & \ldots\ldots & \cdot & \cdot & \ldots\ldots & \cdot \\
0 & 0 & \ldots\ldots & n_{1,n_n} & \ldots\ldots & 0 & 0 & \ldots & n_{m,n_n}
\end{bmatrix}
\begin{bmatrix}
N_{1,0} \\ N_{1,1} \\ N_{1,n_n} \\ \cdot \\ \cdot \\ \cdot \\ N_{m,0} \\ \cdot \\ N_{m,n_n}
\end{bmatrix}
=
\begin{bmatrix}
d_0 \\ d_1 \\ \cdot \\ \cdot \\ \cdot \\ \cdot \\ \cdot \\ \cdot \\ d_{n_n+n_{nn}}
\end{bmatrix}
\qquad (4.2.44)
$$

or symbolically, $Nn = d$, where d_i is the ith coefficient of $\gamma(s)D_c(s)$. The above algorithm is easily implemented on digital computer whenever a unique solution to Eq. (4.2.39) exists, or equivalently whenever the matrix N is non-singular.

4.2.4 ROBUSTNESS OF LTR DESIGNS

The purpose of this Section is to present a discussion of particular aspects of LTR designs which relate to robustness.

One observation concerns the relationship between loop shape and robustness implied by Theorems 4.1 and 4.2. Specifically, if model errors are accurately described by unstructured uncertainties, then LTR methods can be used to ensure that the conditions of Theorems 4.1 and 4.2 are met, thereby guaranteeing robust stability. This constitutes the ideal case for applying Loop Transfer Recovery, since specifying constraints on the loop shape is a necessary and sufficient condition for robustness. On the other hand, some model errors are not well described by unstructured uncertainties. In particular frequency errors in the model of a lightly damped flexible structure fall into this category (see Section 4.2.1), as do most cases of strict parameter variations. In this case Theorems 4.1 and 4.2 give sufficient but not necessary conditions for robust stability, and a design based upon constraining loop shape on the basis of unstructured uncertainties will be conservative, resulting in low performance. In the case of lightly damped structures the implied constraints on loop shape would require that uncertain flexible modes not be actively controlled (again see Section 4.2.1). Therefore, the robustness of designs which actively control flexible modes cannot be analyzed by examining loop shape alone. In fact, for a given loop shape, a whole family of LTR designs may exist, where the robustness of these designs varies. In conclusion, the application of LTR methods to lightly damped structures with uncertain frequencies cannot be blindly approached in terms of conditions implied on the loop shape. A major emphasis of the current study has been to identify

57

conditions which are important. These results will be illustrated by the examples presented in Section 4.2.5.

As noted in Section 4.2.2, one variable among a family of LTR designs with the same loop shape is the location of pole/zero cancellations. Whenever these cancellations occur near the imaginary axis a small perturbation in the plant, resulting in a small shift of the plant zeros, will cause a very large variation in the open-loop frequency response. It would therefore be reasonable to expect that an LTR design which tries to avoid pole/zero cancellations near the imaginary axis will be more robust than one that does not. One way to reduce the number of plant zeros, and therefore the number of cancellations, is to add measurements. A second order flexible system, with m-inputs and m-displacement outputs, can have at most (n-2m) transmission zeros [ED1][1]. Remembering that in the asymptotic LTR approach, each additional measurement entails an additional artificial input, this implies that every measurement removes a pair of transmission zeros. In the version of the algebraic approach used at this point, additional measurements are used to reduce the compensator order, so it is unclear whether any robustness improvement might result.

A method for shifting the cancellations away from the imaginary axis in the asymptotic approach would be to use the extra degrees of freedom available in the choice of artificial inputs to shift the plant transmission zeros to the left. The best way to do this is still under investigation. This idea is also the motivation behind the algebraic LTR approach, which allows the desig-

----

[1] For velocity outputs the maximum number of finite transmission zeros is (n-2m+1)

ner to place the pole/zero cancellations as far into the left half plane as desired. The general question of how to choose the most robust LTR compensator for a given LQR loop shape is certainly not closed, and one method which we will continue to study is the optimal sensitivity approach described in Sec. 4.4.

One final comment on the robustness of LTR designs is a short discussion of Ref. [SH1], which deals specifically with the robustness problems associated with any compensator design that incorporates very high estimator gains. Asymptotic LTR designs can result in extremely high (on the order of 10^6 or higher) gains in the estimator Kalman gain matrix G. Two difficulties may arise. The first involves the case where a plant perturbation changes the structure of the plant transmission zeros at infinity. This is a perturbation that affects the excess of poles over finite transmission zeros[2]. An example in which this occurs for a realistic flexible system is as follows: Consider the system illustrated in Fig. 4.3, consisting of two disks (of inertia 1), stacked one on top of the other, connected by a rod (of length 1) which acts as a rotational spring (of spring constant 1/2). The input is a torque applied to the lower disk. The nominal output is the rotation of the upper disk. The nominal transfer function is:

$$G(s) = \frac{1/2}{s^2(s^2+1)} \qquad (4.2.45)$$

----

[2] Note that this is not the same as the finite transmission zeros added when neglected dynamics are appended to the design plant. In this case the number of poles increases along with the number of transmission zeros, indicating that the excess does not change, and the structure of the zeros at infinity therefore does not change.

59

An LQR design which minimizes the mechanical energy, plus the rotation of the lower disk squared, plus the control input squared, results in the following control gain vector (in modal coordinates):

$$K = [\ 1.0000 \quad 2.0555 \quad 1.6124 \quad 0.6325\ ] \qquad (4.2.46)$$

An asymptotic LTR design can be achieved by setting the process noise covariance equal to $(1 \times 10^{12})BB^T$, resulting in the following Kalman Filter gains:

$$G = \begin{bmatrix} 98,255.0 \\ 1,000,000.0 \\ 98,116.0 \\ 995,170.0 \end{bmatrix} \qquad (4.2.47)$$

This design is relatively robust with respect to frequency variations (withstands ±30% errors in the flexible frequency), but consider an error corresponding to a manufacturing defect which places the rotation sensor at a point ε below the top disk. The true transfer function would then become:

$$G'(s) = \frac{\varepsilon s^2 + 1/2}{s^2(s^2+1)} \qquad (4.2.48)$$

Therefore, while the nominal plant has no finite zeros, the true plant has a pair at $\pm\sqrt{-1/2\varepsilon}$, satisfying the conditions referred to in Ref. [SH1]. The asymptotic LTR design defined by Eqs. (4.2.46) and (4.2.47) will be unstable for $\varepsilon > 0.04$,[3] which produces finite zeros at ±3.54j or lower on the imaginary axis. This might be a troublesome robustness problem in some applications, but it can occur only under very special circumstances. For any square flexi-

----

[3] It will also be unstable for $\varepsilon < -0.01$, but this corresponds to a measurement location above the disk and is not physically feasible.

ble structure with displacement outputs, the maximum number of finite transmission zeros is (n-2m) [ED1]. If the nominal plant has this maximum number of transmission zeros, then no perturbation in plant parameters can result in the conditions required by Ref. [SH1] for robustness problems.

In conclusion the robustness problems associated with LTR control exposed in Ref. [SH1] depend on a nominal plant which is chosen such that there exists a perturbation in plant parameters which will increase the number of finite transmission zeros by at least 2. This possibility can always be ruled out by ensuring that the nominal (design) plant has the maximum possible number of finite transmission zeros, which will be the case in most practical problems. In particular the antenna model studied in this report always has the maximum number of transmission zeros and is not affected by the robustness problems exposed in Ref. [SH1]. The extension of these ideas to infinite-dimensional systems is not considered in Ref. [SH1] and has not been addressed in the present work. This would, however, provide an interesting topic for future examination.

The second observation in [SH1] is that, due to the very high gains involved, a small error in the realization of the compensator could destabilize the system. The authors suggest that a compensator be realized directly from the transfer function $K(sI-A+GC+BK)^{-1}G$. This issue also has not been considered in detail, but it will be examined later.
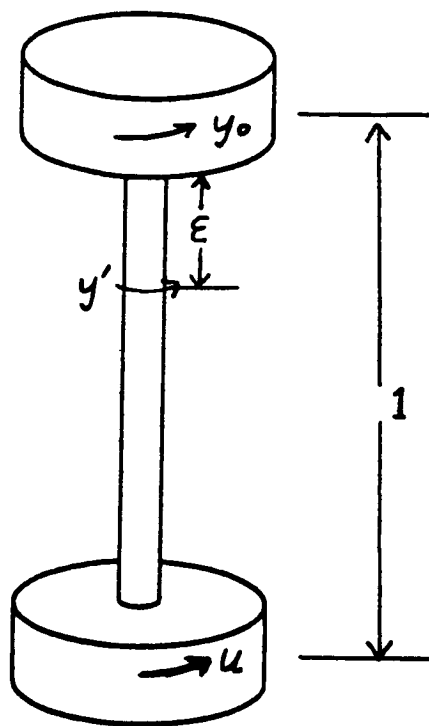
Figure 4.3 Two Disk System

4.2.5 EXAMPLES OF THE LTR APPROACH

Antenna Model

The methods developed in the previous Section are applied to the wrap-rib antenna described in Chapter 2. The system is modeled by a component mode method, ie. mode shapes of the beams and the mesh Sections are found separately, and the "modal" representations are then combined to form a model for the 90° sector. A subset of six modes are selected from this very large model to constitute a design model for one quadrant of the antenna Frequencies, modal input influence coefficients, and modal output influence coefficients for the six modes included in the design model are listed in Table 4.2.1.

Damping is assumed to be visco-elastic (ie. the damping matrix is proportional to the stiffness matrix)[1], but the model allows different damping coefficients[2] for the beam and the mesh portions of the sector model. This implies that damping is added at the component mode stage, and furthermore that the damping matrix, after combining the beam and mesh component mode models and calculating the overall modal representation, will include off-diagonal terms. The final antenna model, in a second-order modal represensation, will have the following form:

$$\ddot{\phi} + D\dot{\phi} + \Lambda^2\phi = Bu, \quad y = C\phi \tag{4.2.49}$$

where Λ^2 is the diagonal matrix of the natural frequencies squared, while D is

- - - - - - - - - - - - - - - - - - -

[1] Visco-elastic damping implies that the damping ratio of a mode increases proportionally with the frequency of that mode. Higher frequency modes will therefore be more highly damped. This is a realistic situation for most materials, particularily in the higher modes.

[2] The damping coefficient is a scalar number which multiplies the stiffness matrix, resulting in the damping matrix.

symmetric, positive-semidefinite, but is diagonal only in the case when the damping coefficients in both the beam and the mesh are identical. The particular model studied here has higher damping in the mesh, and the damping matrix is therefore not diagonal, though the off-diagonal terms are in general an order of magnitude smaller than the diagonal terms. The entire damping matrix is listed in Table 4.2.1.

Table 4.2.1 Antenna Modal Data

Mode #	1	2	3	4	5	6
ω	0.	6.95	18.95	36.57	51.89	55.32
ζ	0.	.0105	.0302	.0589	.0519	.0537
B_o	.093	-.122	-.285	-.511	-.120	-.111
C_1	.093	-.122	-.285	-.511	-.120	-.111
C_2	.0	.243	.183	.617	.201	.115
C_3	.0	.002	.183	.341	.099	.052
C_4	.0	.001	.129	.241	.070	.037
C_5	.0	.000	.019	.068	.027	.020
C_6	.0	.172	.129	.437	.142	.081

Damping Matrix

$$
\begin{bmatrix}
0.0 & 0.0 & 0.0 & 0.0 & 0.0 & 0.0 \\
0.0 & 0.146 & -0.030 & -0.050 & -0.016 & -0.009 \\
0.0 & -0.030 & 1.144 & -0.151 & -0.096 & -0.049 \\
0.0 & -0.050 & -0.151 & 4.308 & -0.009 & -0.095 \\
0.0 & -0.016 & -0.096 & -0.009 & 5.385 & 0.099 \\
0.0 & -0.009 & -0.049 & -0.095 & 0.099 & 5.940
\end{bmatrix}
$$

Simpler models, including series of connected masses and springs, as well as a beam/hub model have also been studied, but the difficulty in achieving robust control designs has been much greater for the antenna sector model. It is hypothesized that this is due largely to the addition of mesh modes to the beam/hub model, resulting in a densely packed set of frequencies, and some very slightly controllable/observable modes. From the point of view of con-

trol design, the important aspect of this particular model is that it is difficult to control robustly, and therefore poses a challenging problem.

The number of available measurements (or plant outputs) is not fixed at this time. There must be at least one measurement relative to inertial space, to insure that the rigid body mode is observable. This measurement is provided by a rotation sensor colocated with the hub torque input. To effectively control the shape of the antenna, measurements on the antenna surface must also be taken. Possible locations for these measurements are labeled and numbered on Fig. 4.4, where all these measurements are relative to the central hub position. The modal output influence coefficients are listed in Table 4.2.1. In the compensator design stage, the measurements used will be referred to by the corresponding number found on Fig. 4.4. For the examples presented here, only one other measurement will be used. That measurement corresponds to position #2, at the tip of the beam which lies perpendicular to the axis of rotation.

One final note on the measurement locations is that all seven measurements are not necessarily independent for a given mathematical model. This means that, for a particular mathematical model studied, the value of one measurement may be directly related to that of another measurement. As an example, consider measurement locations 2 and 6. The complete mathematical model of the antenna sector includes symmetric beam modes (the two beams move together in the same direction) and asymmetric beam modes (the motion of one beam exactly opposes the motion of the other). With no mesh, the asymmetric modes are uncontrollable, and even with the mesh they are only very slightly controllable. These modes were therefore neglected in the mathematical design
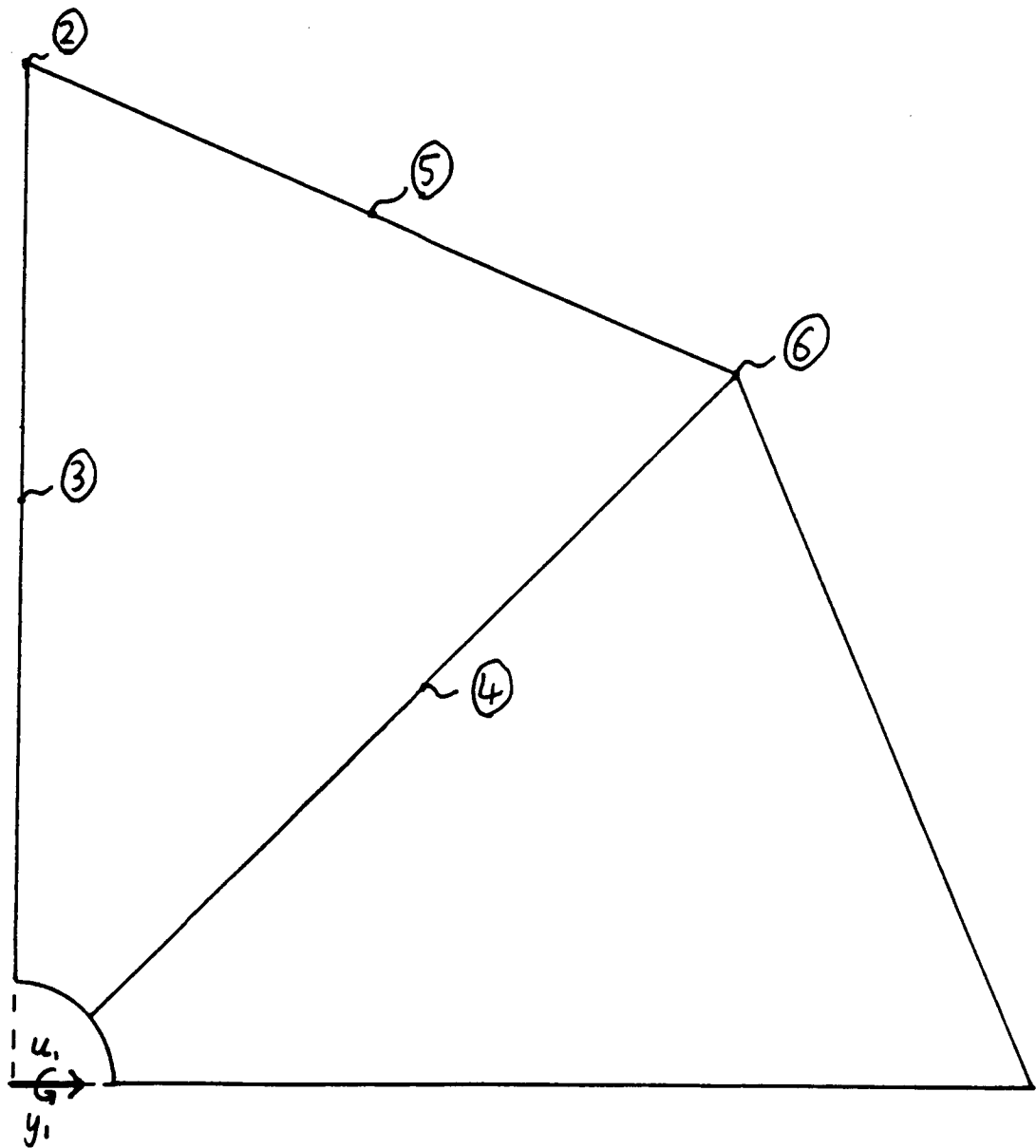
Figure 4.4 Antenna Quadrant Model

model, since they do not have much affect on the control problem. This, however, implies that in terms of the mathematical design model, the two beams will always move together, and the measurements at locations 2 and 6 will be linearly dependent upon each other. This points to an important consideration in determining the independence of measurements. The fact that measurements are independent for a physical system or for some mathematical model does not imply that they are independent for every possible, reduced order, mathematical model. Measurements 2 and 6 are clearly independent for the overall mathematical (and the physical) antenna model, but due to the exclusion of asymmetric modes, they are not independent for the reduced order mathematical design model studied here, due to the exclusion of asymmetric modes. In terms of this study, the implication is that adding measurement number 6 to number 2 will not result in any further information on the state of the system. This is particularily important with respect to the algebraic design method which must assume independence of all the measurements used.

LQR Design Problem

The first step in a Loop Transfer Recovery (LTR) control design is the choice of a full-state feedback control law, or equivalently the matrix K of control gains. The matrix K can be found by a number of methods, including pole placement, but, perhaps the most advantageous is by solving a Linear Quadratic Regulator (LQR) problem. The statement of the LQR problem is as follows:

Given $\dot{x} = Ax + Bu$ (4.2.50)

Minimize the following cost functional:

$$J = \int_0^\infty (x^T Q x + u^T R u) dt \qquad (4.2.51)$$

where Q is symmetric, positive semi-definite and R is symmetric, positive definite. The solution to the problem, for full state feedback is:

$$u = -Kx \qquad (4.2.52)$$

where $K = R^{-1}B^T P$ and P satisfies the following Riccati equation:

$$PA + A^T P - PBR^{-1}B^T P + Q = 0 \qquad (4.2.53)$$

The LQR approach has a number of positive features, including guaranteed gain and phase margins [LE1,2][3], the ability to shape the loop gain at low frequencies [HA1] and the simplicity of the approach. The designer "simply" chooses the Q and R matrices and the computer does the rest.

For the antenna problem, the input is a scalar, so without loss of generality R can be replaced by 1. The problem then reduces to finding a Q matrix in the following form:

$$Q = q_c Q_o \qquad (4.2.54)$$

where q_c is a scalar parameter which is increased to increase system performance (and loop gain), and Q_o is a matrix which specifies the form of the cost weighting on the states. There are a number of bases for choosing Q. One might wish to achieve a particular loop shape, or a particular closed loop

----

[3] This constitutes a large part of the appeal of the LTR control design approach

68

pole configuration, or there might be some considerations in terms of a physically meaningful objective function to be minimized. For instance, one might want to minimize the mechanical energy in the system, or a pointing error, or perhaps the RMS error of a surface or signal.

Three LQR designs will be presented for the antenna. The first minimizes the RMS surface error, since this provides a good meausure of antenna performance. The second minimizes the mechanical energy in the antenna, plus a term corresponding to the rigid body mode (this is necessary since there is no mechanical energy corresponding to rigid body rotation). The third minimizes RMS error, plus the rate of change of RMS error. All three LQR designs remain stable for combined frequency errors of -99% or +100%. Any robustness difficulties in the LTR designs therefore are not due to similar difficulties in the corresponding LQR design.

LQR Design #1

The first LQR design penalizes the RMS surface error of the antenna. This was chosen because the antenna performance is expected to be closely related to the surface error. The Q matrix which penalizes RMS error has the following form:

$$Q_1 = \begin{bmatrix} Q_r & 0 \\ 0 & 0 \end{bmatrix} \tag{4.2.55}$$

The elements of Q_r are given in Table 4.2.2. Notice that the weightings on the rigid body mode and the first three flexible modes are approximately equal, while the weightings on the last two modes are higher by approximately

69

a factor of 5. Q_r therefore approximately weights the position of the rigid

body mode and the first three flexible modes equally, places a little more

emphasis on the last two modes, and places no weighting on the modal veloci-

ties. The resulting closed loop pole configuration, as q_c is increased from

.01 to 100, is illustrated in Fig. 4.5. An asterisk is placed by the closed

loop poles for $q_c = 100$, and the loop gain for this case is illustrated in

Fig. 4.6. This loop gain indicates flexible modes both above and below 0db.

This is a desirable, yet realistic situation, since if all modes were below

0db they would essentially be uncontrolled, while if an modes were above 0db,

there would have to be some modes (of the true system) below 0db.

Table 4.2.2 Matrix Q_r

$$
\begin{bmatrix}
2166.16 & 385.25 & -313.39 & -754.52 & -5980.06 & -4880.05 \\
385.25 & 1618.56 & -632.98 & 42.80 & -5976.23 & -3724.72 \\
-313.39 & -632.98 & 1598.49 & -771.90 & 6803.32 & 3031.96 \\
-754.52 & 42.80 & -771.90 & 2539.28 & -5295.22 & 1537.05 \\
-5980.06 & -5976.23 & 6803.32 & -5295.22 & 98137.61 & -2965.06 \\
-4880.05 & -3724.72 & 3031.96 & 1537.05 & -2965.06 & 102461.54
\end{bmatrix}
$$

LQR Design #2

The second LQR design penalizes the mechanical energy (kinetic +

potential), plus a term corresponding to the rigid body mode. For a

mechanical system the kinetic energy is given by $x^T M x$, where M is the mass

matrix, and the potential energy is given by $x^T K x$, where K is the stiffness

matrix. The appropriate Q matrix to weight the mechanical energy is

therefore:

POLE CONFIGURATION
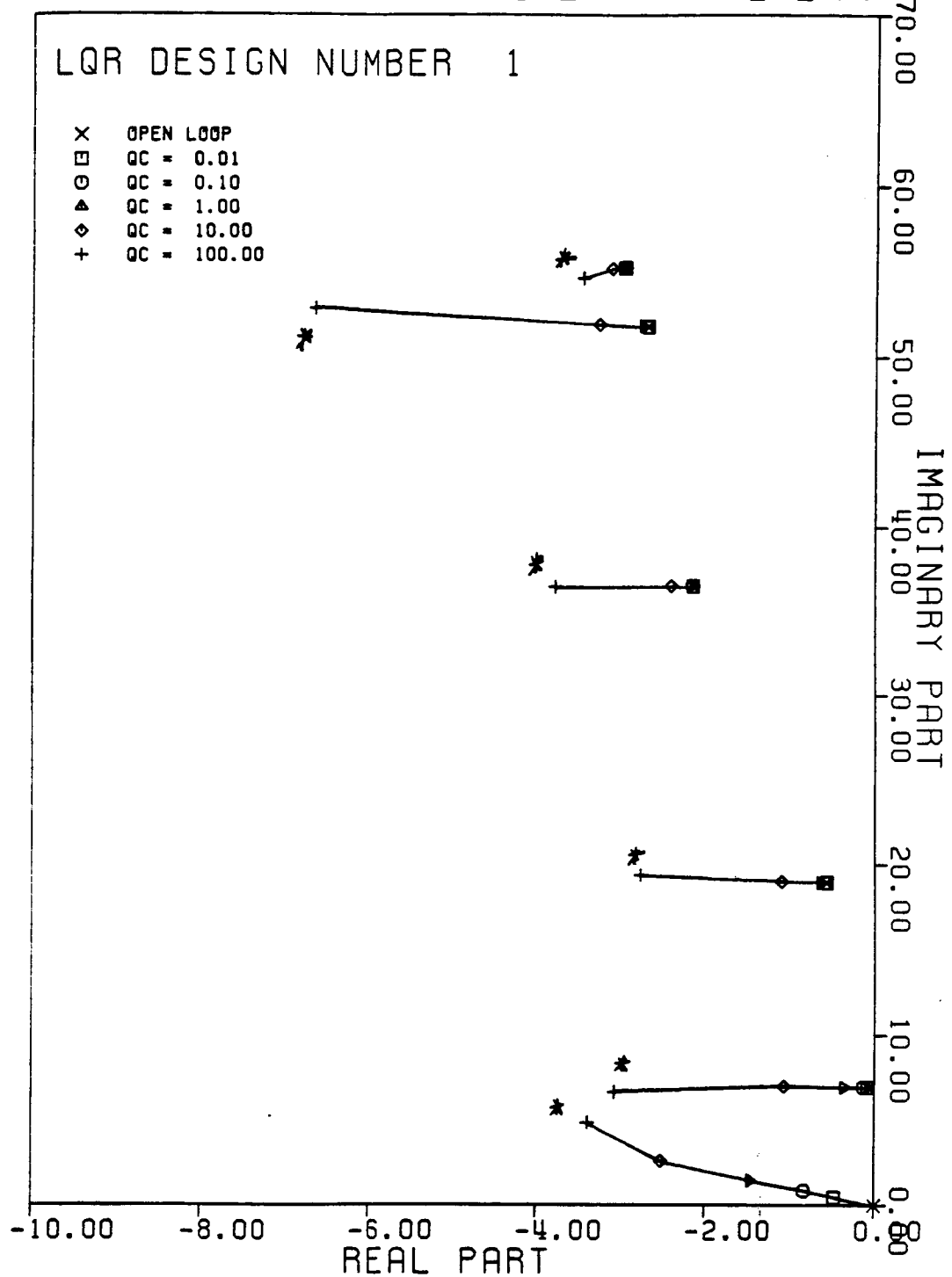
Figure 4.5   Pole Configuration for LQR Design #1

71
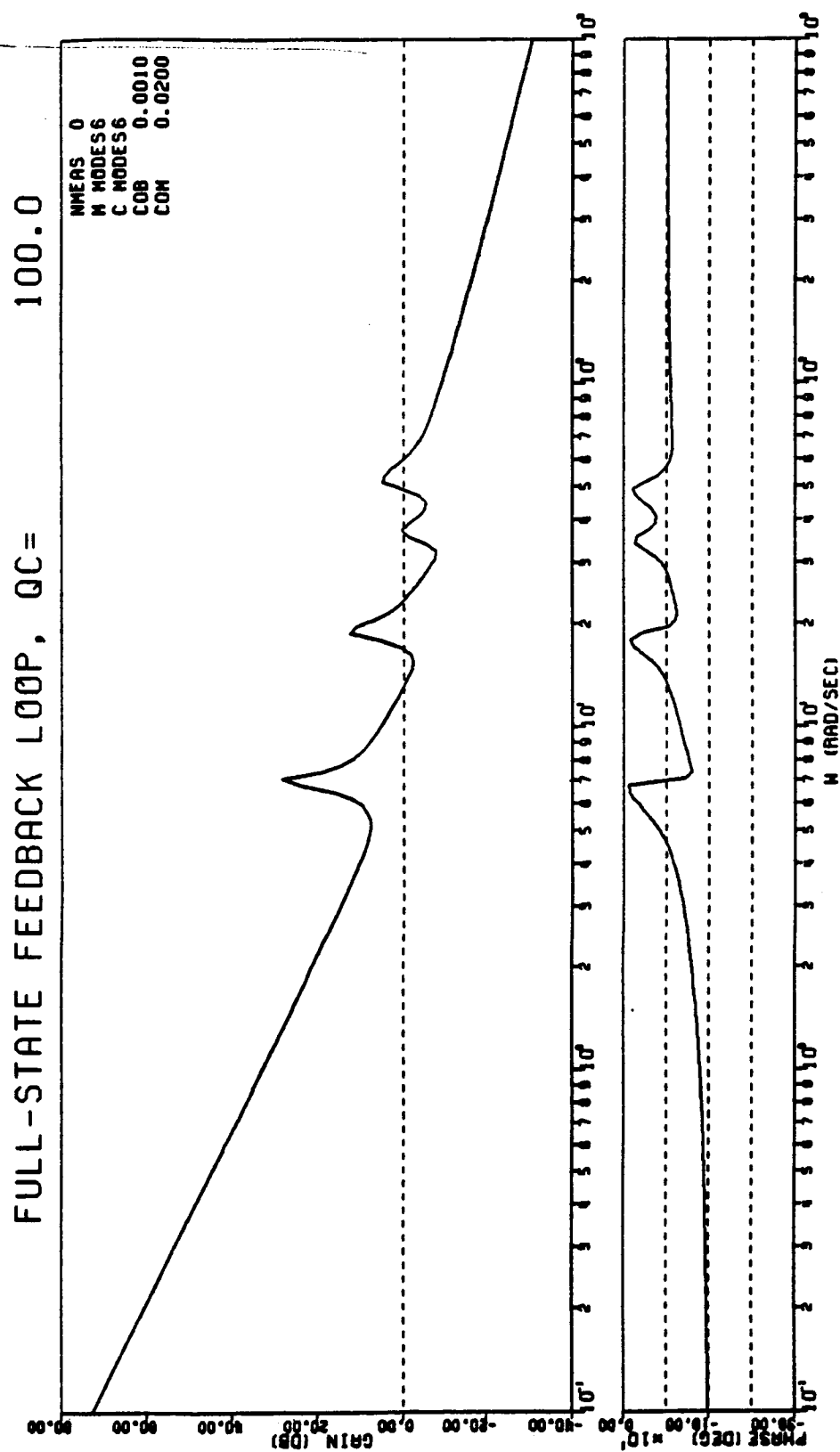
Figure 4.6 Input Loop Gain for LQR Design #1

$$Q_e = \begin{bmatrix} K & 0 \\ 0 & M \end{bmatrix}$$ (4.2.56)

If the rigid body coordinate is the first state variable, K will have a zero first row and first column, indicating that there is no potential energy corresponding to rigid body motion. The resulting control law would therefore fail to control rigid body motion, so some weighting on the rigid body motion must be added to the K matrix. The new K matrix will be identical with the addition of a scalar parameter q_b in the (1,1) position (q_b can be used to vary the relative weighting on the rigid body motion). In transforming the system to modal coordinates both K and M will be premultiplied by T^T and postmultiplied by T, where T is the matrix of eigenvectors for the 2nd order problem. Since the input influence coefficient matrix Bs'o (see Table 4.2.1) is equal to $T^T b$, where b is a vector with a 1 in the first position and zeros in all other positions, the resulting Q matrix in modal coordinates will be:

$$Q_2 = \begin{bmatrix} \Lambda^2 + q_b B_o B_o^T & 0 \\ 0 & I \end{bmatrix}$$ (4.2.57)

For the purposes of this report the relative rigid body weighting factor q_b has been set to 50. The resulting $\Lambda^2 + q_b B_o B_o^T$ matrix is listed in Table 4.2.3.

Table 4.2.3 Potential Energy + Rigid Body Weighting Matrix

$$\begin{bmatrix}
.43 & -.57 & -1.33 & -2.38 & -.93 & -.52 \\
-.57 & 49.07 & 1.75 & 3.13 & 1.23 & .68 \\
-1.33 & 1.75 & 363.11 & 7.28 & 2.85 & 1.59 \\
-2.38 & 3.13 & 7.28 & 1350.40 & 5.10 & 2.84 \\
-.93 & 1.23 & 2.85 & 5.10 & 2694.60 & 1.11 \\
-.52 & .68 & 1.59 & 2.84 & 1.11 & 3061.30
\end{bmatrix}$$

Note that this matrix places considerably higher emphasis on the higher

modes. This is because the matrix Λ^2 places a cost proportional to the square

of the modal frequency. The other important difference between this weighting

matrix and Q_r is that a penalty is now placed on modal velocities. The closed

loop pole configuration, as q_c varies from 100 to 10,000, is illustrated in

Fig. 4.7. An asterisk is placed next to the poles corresponding to

$q_c = 1,000$, and the loop gain for this case is plotted in Fig. 4.8. As

expected, the control law resulting from Q_2 places less emphasis on the rigid

body modes, and more emphasis on the flexible modes, than does that resulting

from Q_1. This is indicated, both in the closed loop pole configuration, and

in the loop gain. While LQR Design #1 pushed the rigid body poles further to

the left than either of the first two sets of poles corresponding to flexible

modes, LQR Design #2 pushes all the flexible mode poles further to the left

than the rigid body poles. In comparing the two loop gains, that resulting

from Design #1 shows a continual decrease in loop gain throughout the fre-

quency range where flexible modes are being actively controlled, while the

loop gain resulting from Design 2 indicates a non- decreasing loop gain

through the same frequency range (though the gain is decreasing for both

higher and lower frequencies). It is important to note though, that both

designs actively control the flexible modes and have approximately the same

bandwidth, though Design #1 does have a higher gain at low frequencies. Later

in this Section it is found that the robustness properties of LTR designs

based on these two different LQR designs vary considerably. The real rea-

sons for this remain a topic for further investigation.

74

PØLE CØNFIGURATIØN
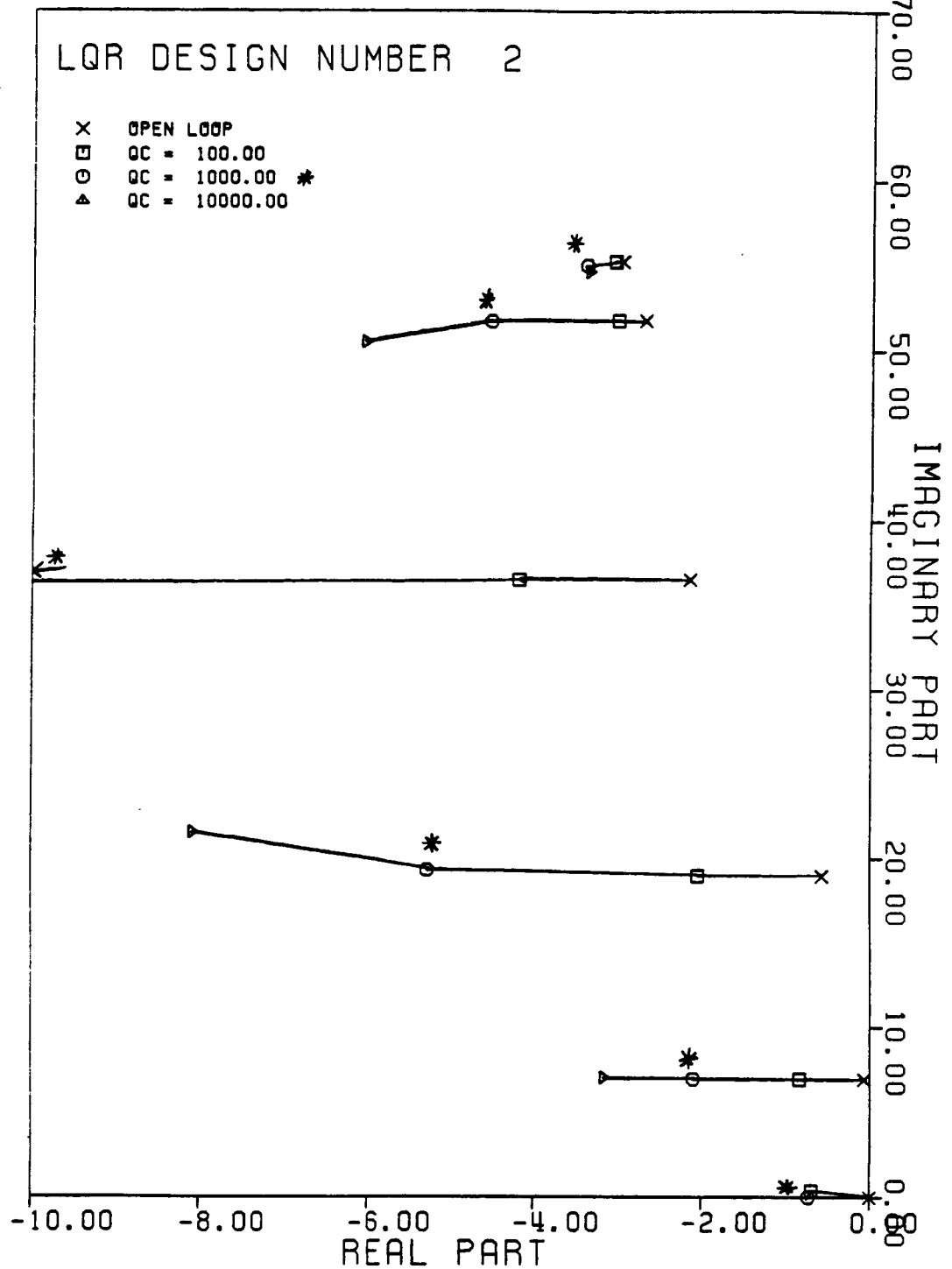
Figure 4.7   Pole Configuaration for LQR Design #2
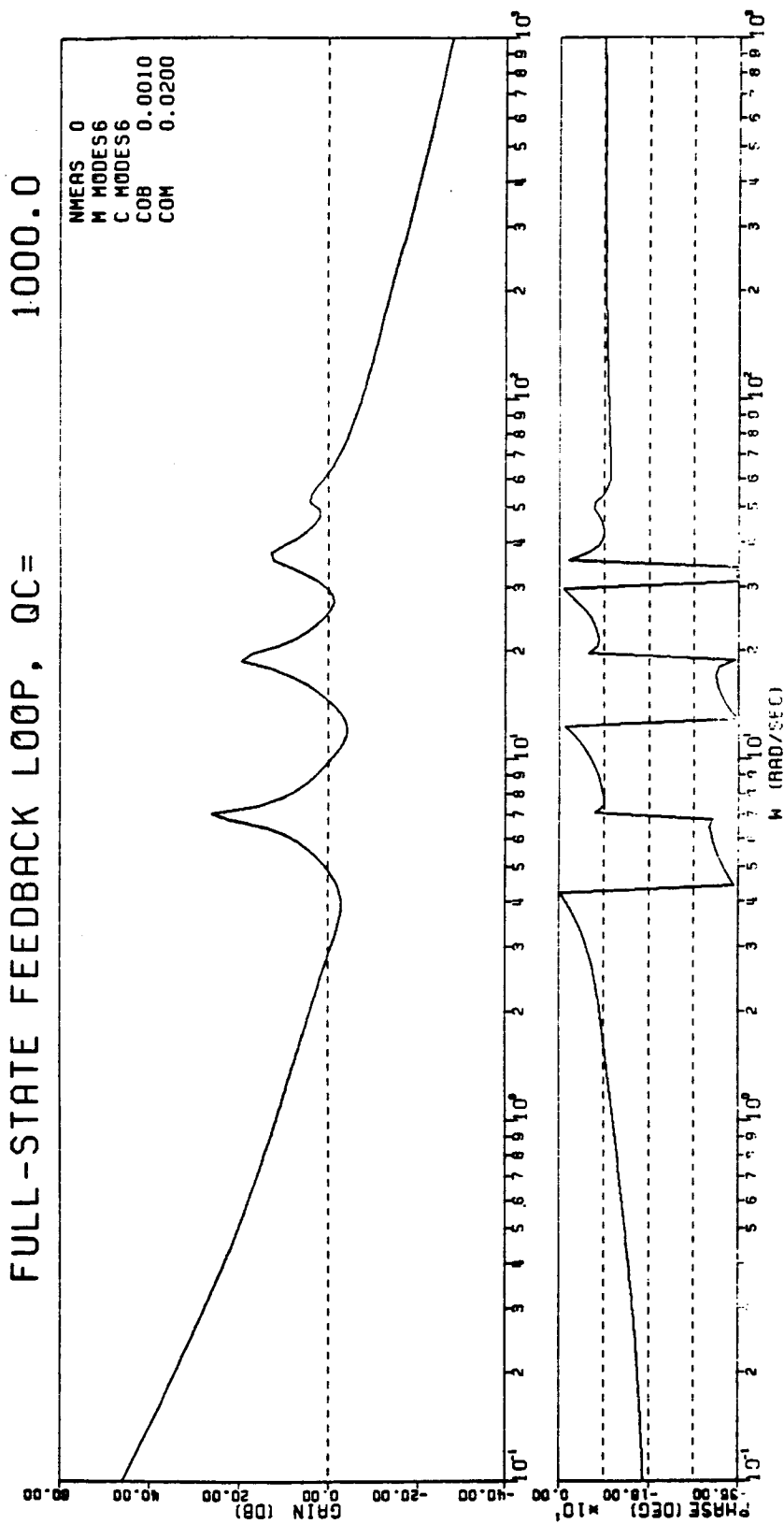
Figure 4.8 Input Loop Gain for LQR Design #2

LQR Design #3

There are two basic differences between Designs #1 and #2. The first is that Design #2 places much more emphasis on the higher frequency modes, while the second is that Design #2 places a penalty on modal velocities as well as modal displacements, while Design #1 does not. To separate these two effects, Design #3 uses the same penalties on modal position as #1 while adding identical penalties to modal velocity. The resulting Q matrix is as follows:

$$Q_3 = \begin{bmatrix} Q_r & 0 \\ 0 & Q_r \end{bmatrix} \tag{4.2.58}$$

The corresponding closed loop pole configuration as q_c varies from .01 to 10 is illustrated in Fig. 4.9. An asterix is placed next to the poles corresponding to $q_c = 1$, and the loop gain for this case is plotted in Fig. 4.10.

Next results for asympototic LTR designs, corresponding to each of the LQR designs, will be presented.

Asymptotic LTR Designs

There are a number of design variables in the asymptotic LTR procedure. These are the elements of the appended columns to the B-matrix, and a scalar parameter q, which is increased until loop recovery is achieved. Since only the case of two measurements is studied at this point there will be only one appended column to the B matrix. This is chosen as a scalar parameter r_s times a vector corresponding to an input collocated with the second output[*].

----

[*] The input influence coefficients corresponding to an input collocated with

PØLE CONFIGURATION

LQR DESIGN NUMBER 3

X   OPEN LOOP
□   QC = 0.01
○   QC = 0.10
△   QC = 1.00
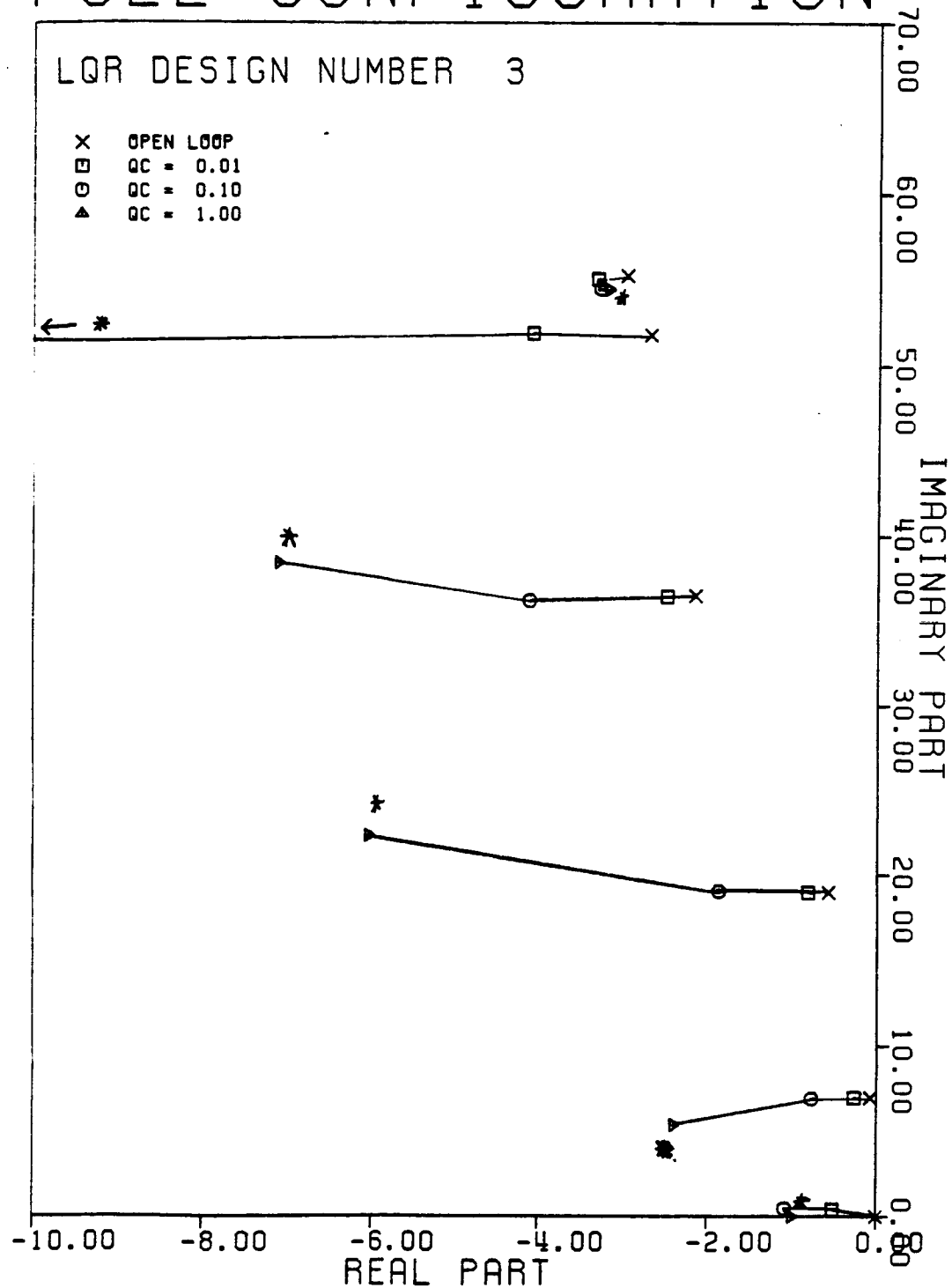
Figure 4.9   Pole Configuration for LQR Design #3

FULL-STATE FEEDBACK LOOP, QC= 1.0
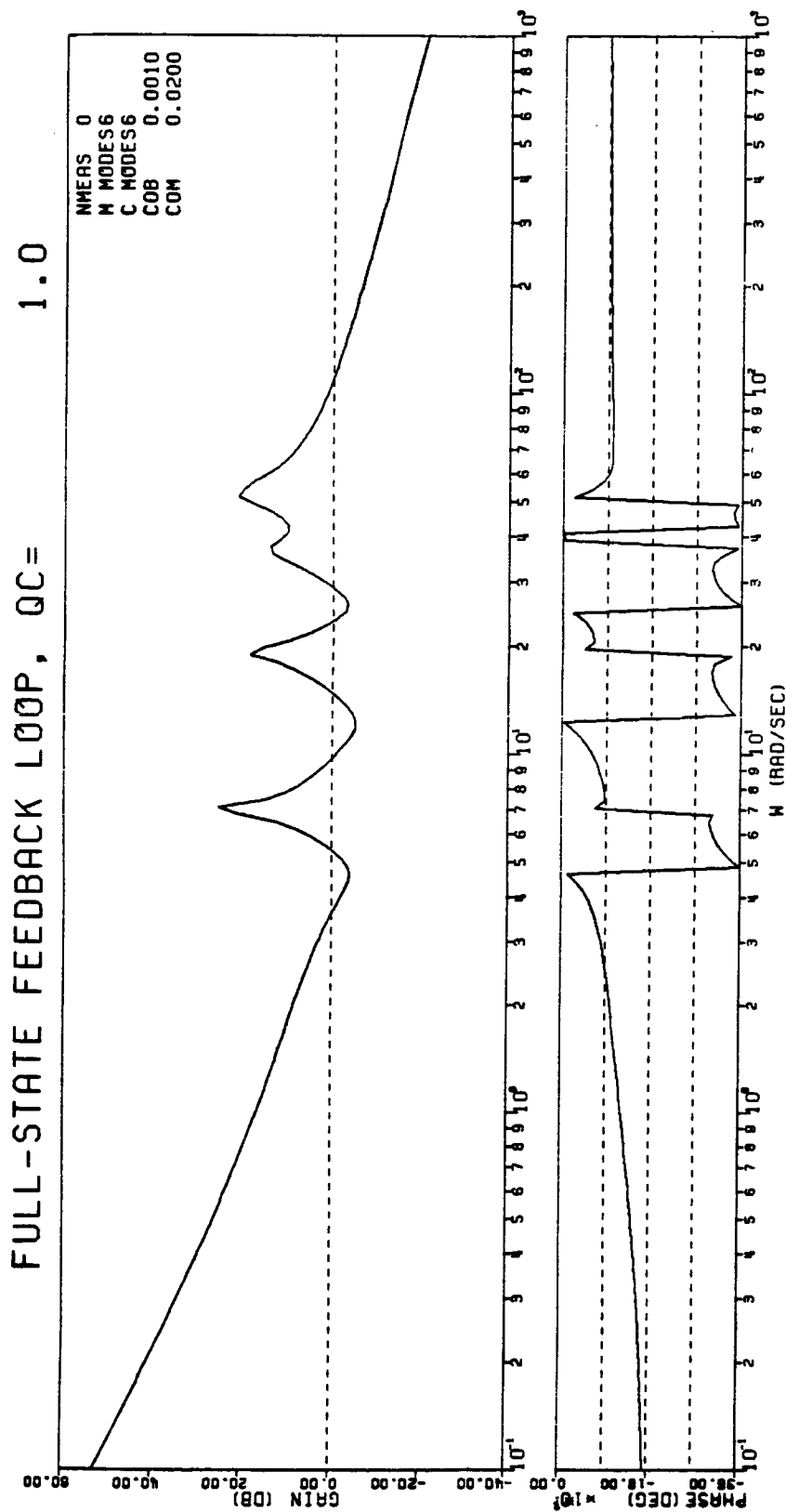
Figure 4.10 Input Loop Gain for LQR Design #3

79

The reason that a collocated input location is chosen is that this guarantees a minimum-phase system for $r_s = 1$. The case $r_s = 0$ is equivalent to not adding any columns to the B-matrix, and does not strictly satisfy the conditions for asymptotic loop recovery outlined in Refs. [DO1,2]. However, loop recovery is achieved for this case so it will be considered as a design possibility.

Asymptotic LTR compensators corresponding to each of the three LQR designs are presented. In each case the loop gain for both the final step in loop recovery and the preceding step are plotted.

The point at which loop recovery is achieved is somewhat of a relative measure. As the parameter q is increased, three effects take place simultaneously. First the loop shape begins to converge as pole/zero cancellations line up, second the overall loop gain increases and third the uncancelled compensator poles move out into the l.h.p. on 45° rays. Loop recovery is achieved when the overall shape and gain of the compensated plant loop match the full-state feedback loop and the decrease in loop gain due to the uncancelled poles shifts past the point where loop gain has dropped below 0db. This will be clearer when the loop gain plots are presented in Figs. 4.11-4.17. The parameter q (listed as QEST on the figures) is actually multiplied by 10^{10} to produce the results presented. This scaling was found to produce loop recovery for reasonable values of q. q is increased by steps of a factor of ten at a time, until it is judged, by visual inspection, that

----

the 2nd measurement wil be identical to the output influence coefficients for the 2nd measurement, listed in Table 4.2.1.

80

loop recovery has been achieved.

The tables describe robustness results. The first column gives the LQR design #, the second column the LQR parameter q_c, the third column the LTR parameter q and the fourth column the 2nd input scaling factor r_s. The robustness results indicate stability or instability of the closed loop system when all the frequencies are varied by the percentage indicated. An S indicates a stable closed loop system, while a U indicates an unstable closed loop system. This was chosen as a rough measure of robustness since the compensators we tested seemed to be most sensitive to a shift of all the frequencies in the same direction. This is also a realistic possibility since a variation in mass or stiffness properties would produce just such a result. In a final analysis stage a more complex study of robustness (for all possible sets of frequency errors) would have to be carried out, but the data presented in Tables 4.2.5-4.2.7 give an easily read and meaningful measure of robustness.

Asymptotic LTR for LQR design #1

In this case loop recovery was achieved for q=100. The loop gains for the case of q=10 and q=100 are plotted in Figs. 4.11 and 4.12 respectively. A number of different values of the scalar parameter r_s were tested and loop recovery was achieved in every case. Robustness results are presented for two cases: $r_s=1$ and $r_s=0$. Neither case proved to be robust, but while the case with $r_s=1$ indicated stability only for a 10% increase in frequency, the case with $r_s=0$ indicated stability only for a 10% decrease in frequency. This does

suggest that the choice of the appended B-matrix columns will affect robustness. Note that increasing q to get loop recovery does not seem to improve robustness. In fact, the results do not change. However, increasing q does increase bandwidth and low frequency loop gain, thereby increasing performance while maintaing robustness.

Table 4.2.4 Robustness of Asymptotic LTR Design for LQR Design #1

Q#	q_c	q	r_s	-40%	-30%	-20%	-10%	+10%	+20%	+30%	+40%
1	100	10	1	U	U	U	U	S	U	U	U
1	100	100	1	U	U	U	U	S	U	U	U
1	100	10	0	U	U	U	S	U	U	U	U
1	100	100	0	U	U	U	S	U	U	U	U

Asymptotic LTR for LQR Design #2

For the second LQR design, loop recovery was achieved for q=10. The loop gain for q=1 and q=10 are plotted in Figs. 4.13 and 4.14 respectively. for this case different values of r_s were not tested since the LTR desing was extremely robust for r_s=1. In fact Table 4.2.5 indicates stability for ±40% variations in frequency at both steps in the loop recovery. This is an excellent robustness result, but we do not yet have a rigorous explanation for it.

Table 4.2.5 Robustness of Asymptotic LTR Design for LQR Design #2

Q#	q_c	q	r_s	-40%	-30%	-20%	-10%	+10%	+20%	+30%	+40%
2	1000	1	1	S	S	S	S	S	S	S	S
2	1000	10	1	S	S	S	S	S	S	S	S

Figure 4.11 Input Loop Gain for Asymptotic LTR on LQR Design #1 (q=10)
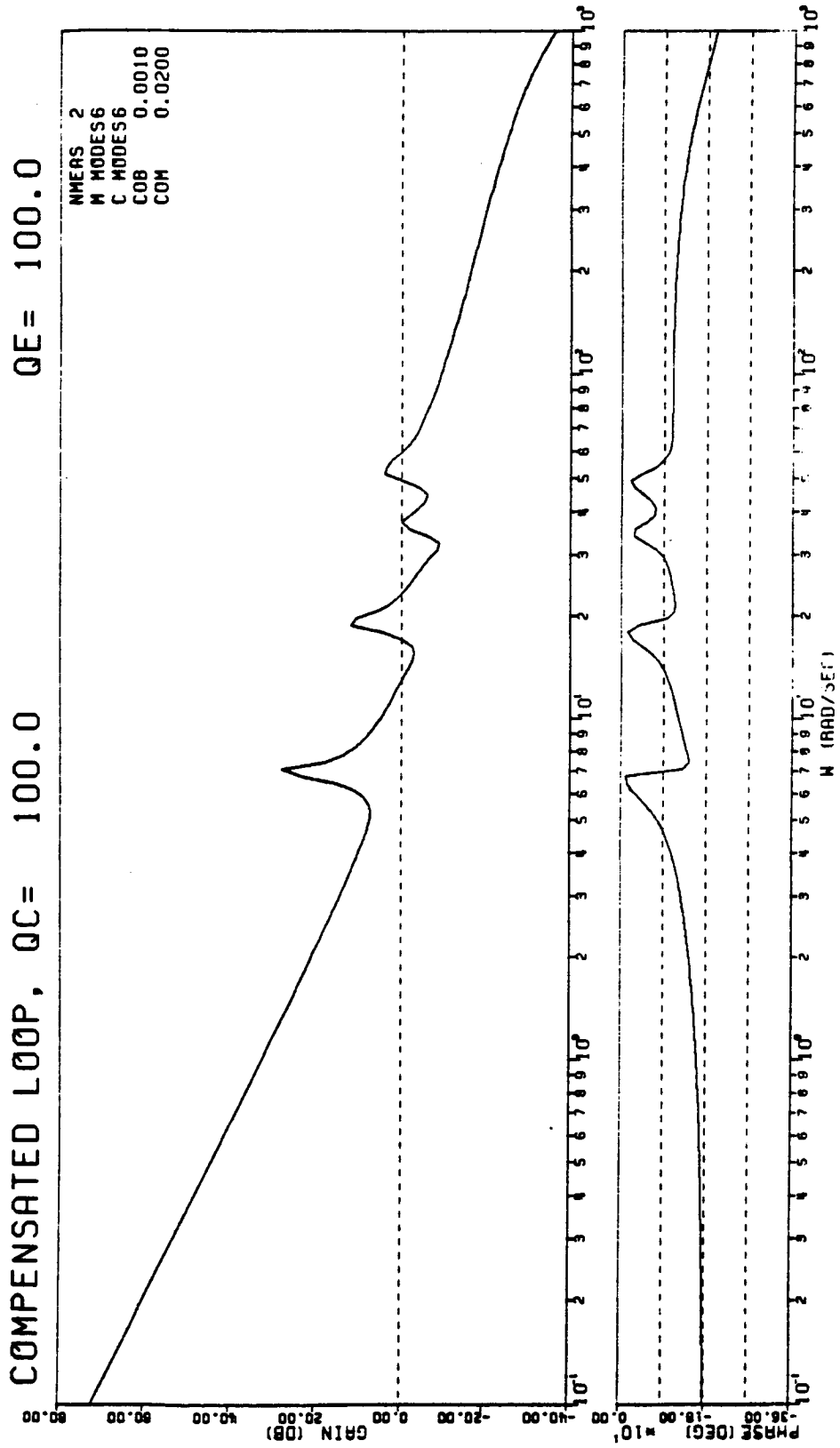
Figure 4.12 Input Loop Gain for Asymptotic LTR on LQR Design #1 (q=100)

As indicated earlier, one difference between the two designs is that design #2 pushs all the closed loop poles corresponding to flexible modes further into the l.h.p. than poles corresponding to the rigid body mode, while design #1 does not. This indicates that the second design does not attempt to move the antenna rigid body mode too quickly, but it does pay a great deal of attention to the flexible modes. The first design, on the other hand, has a very high gain at low frequencies (indicating a fast response to errors in the rigid body mode), but does not pay much attention to the flexible modes. The performance of the second design, in terms of fast reduction in the RMS error or of the rigid body displacement error, will be less than that of the first. Though there is clearly a trade-off between performance and robustness, this does not entirely explain the difference in robustness, since much lower per-formance designs based on RMS error were also tried and no large increase in robustness was observed. This is still very much in the area of hand-waving, but a more rigorous understanding of the great increase in robustness observed for the second LQR loop shape, will be a major part of our effort in 1986.

Asymptotic LTR for LQR Design #3

LQR design #3 was concocted to separate the effect of the two major differ-ences between designs #1 and #2. That is the increased cost on the high fre-quency modal displacements and the cost on modal velocities. The modal dis-placement cost in design #3 is identical to that of design #1, while a rate of change of RMS term is added to weight modal velocities. In this case, loop recovery was achieved for q=100. Loop gains for q=10 and q=100 are plotted in Figs. 4.15 and 4.16 respectively. Robustness results are presented in Table
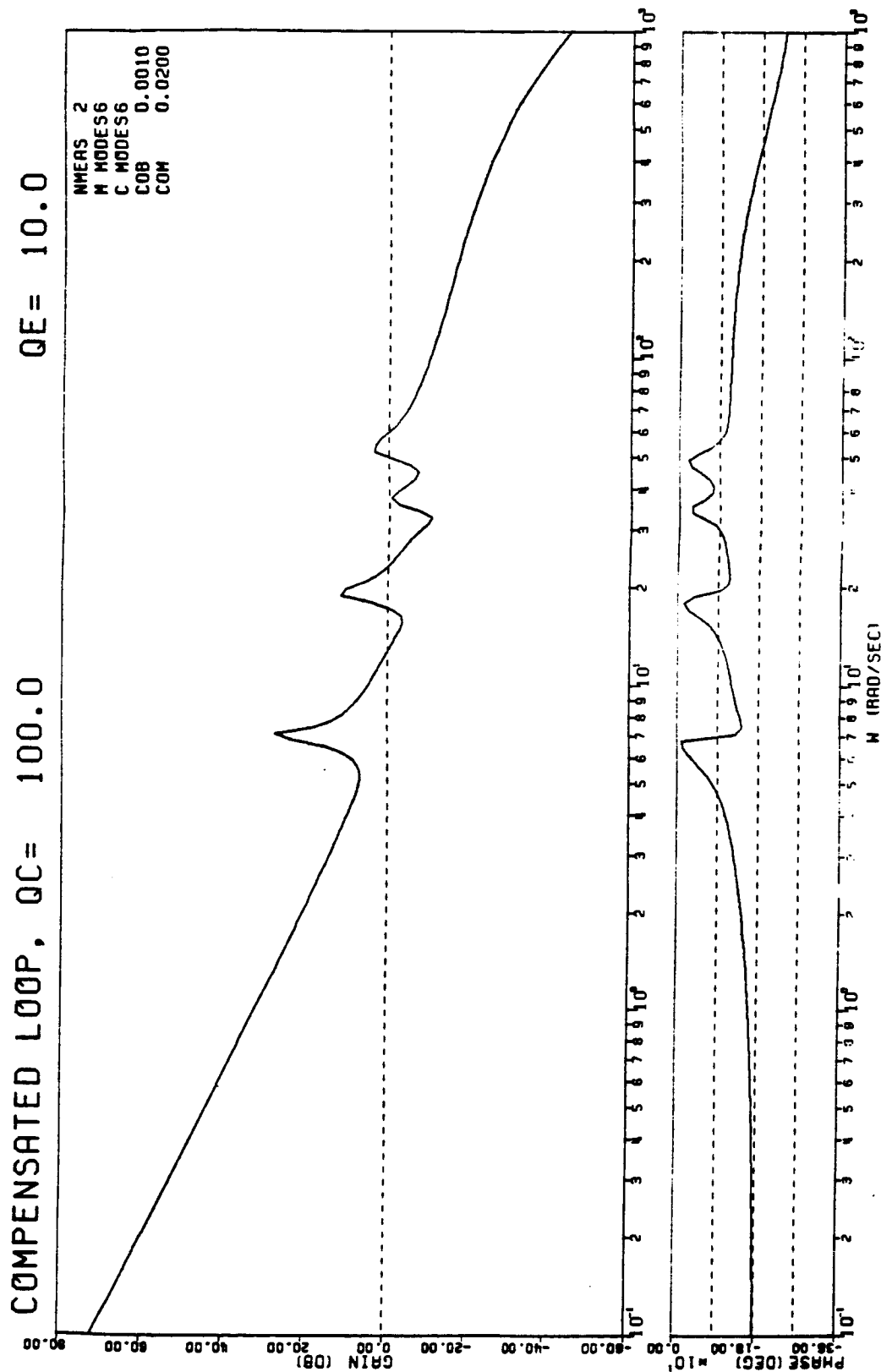
Figure 4.13 Input Loop Gain for Asymptotic LTR on LQR Design #2 (q=1)
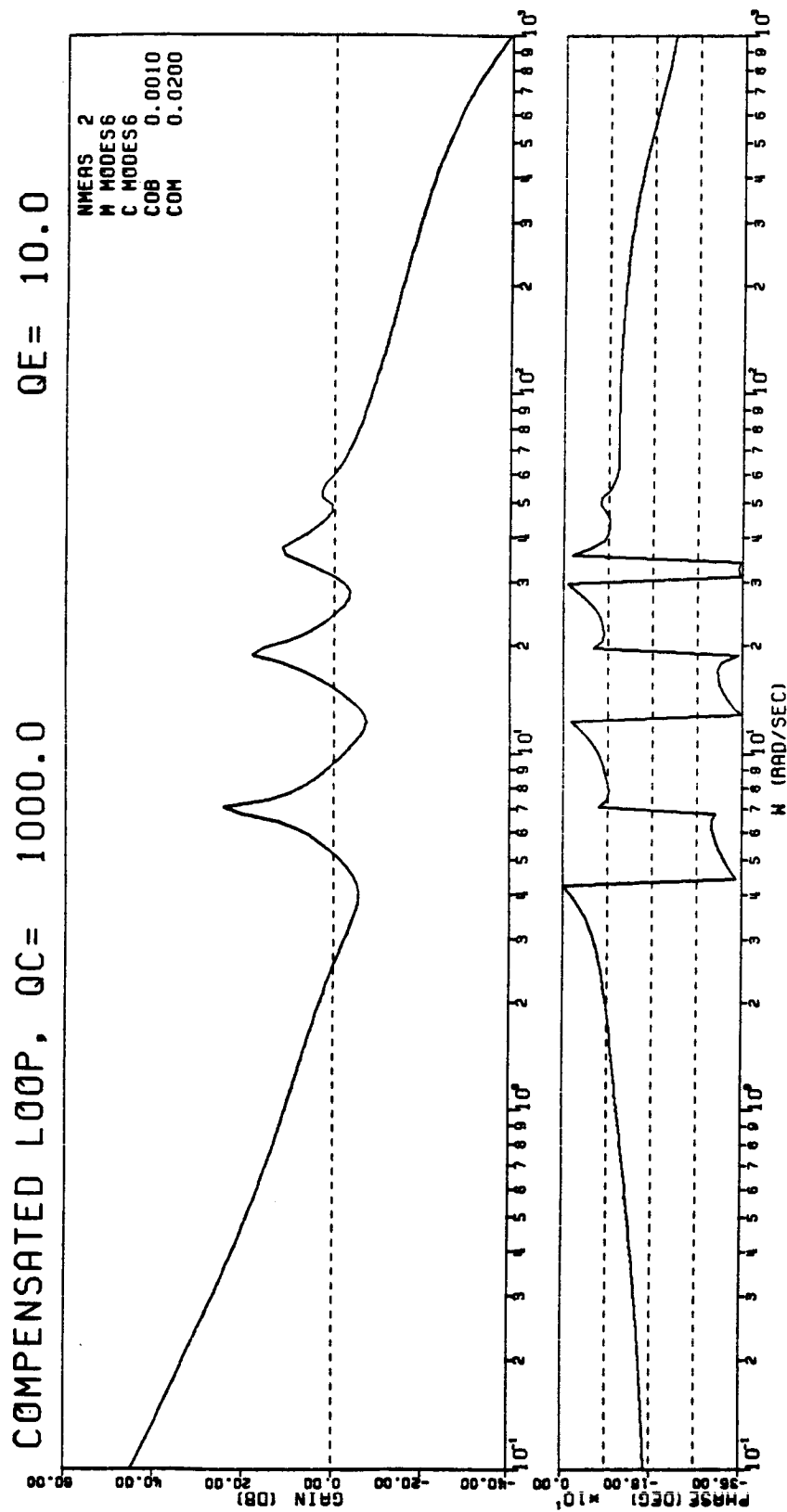
Figure 4.14 Input Loop Gain for Asymptotic LTR on LQR Design #2 (q=10)

4.2.6. This design is considerably more robust than #1, but not quite as robust as #2. Again, we do not have a rigorous explanation of this fact, and this will remain an area of active research. Also note that increasing q does not improve robustness, but it does improve performance.

Table 4.2.6 Robustness of Asymptotic LTR Design for LQR Design #3

Q#	q_c	q	r_s	-40%	-30%	-20%	-10%	+10%	+20%	+30%	+40%
3	1	1	1	S	S	S	S	S	S	S	U
3	1	10	1	S	S	S	S	S	S	S	U
3	1	100	1	S	S	S	S	S	S	S	U

Algebraic LTR Designs

The design variables in the Algebraic LTR approach are the locations of the compensator poles. The compensator order is fixed by the maximum degree of the plant numerator polynomials (n_n) and the number of measurements (m). For the 6-mode antenna model with two measurements this will be order ten, or two orders less than an estimator based design. Of the ten poles available, eight will be cancelled and two will not. The positions of the uncancelled poles is set at $-200\pm200j$. This is far enough away from the controlled flexible frequencies that the loop shape in the design region is not significantly affected. To examine the effect of varying pole locations, four sets of pole locations were chosen. These are listed in Table 4.2.7.
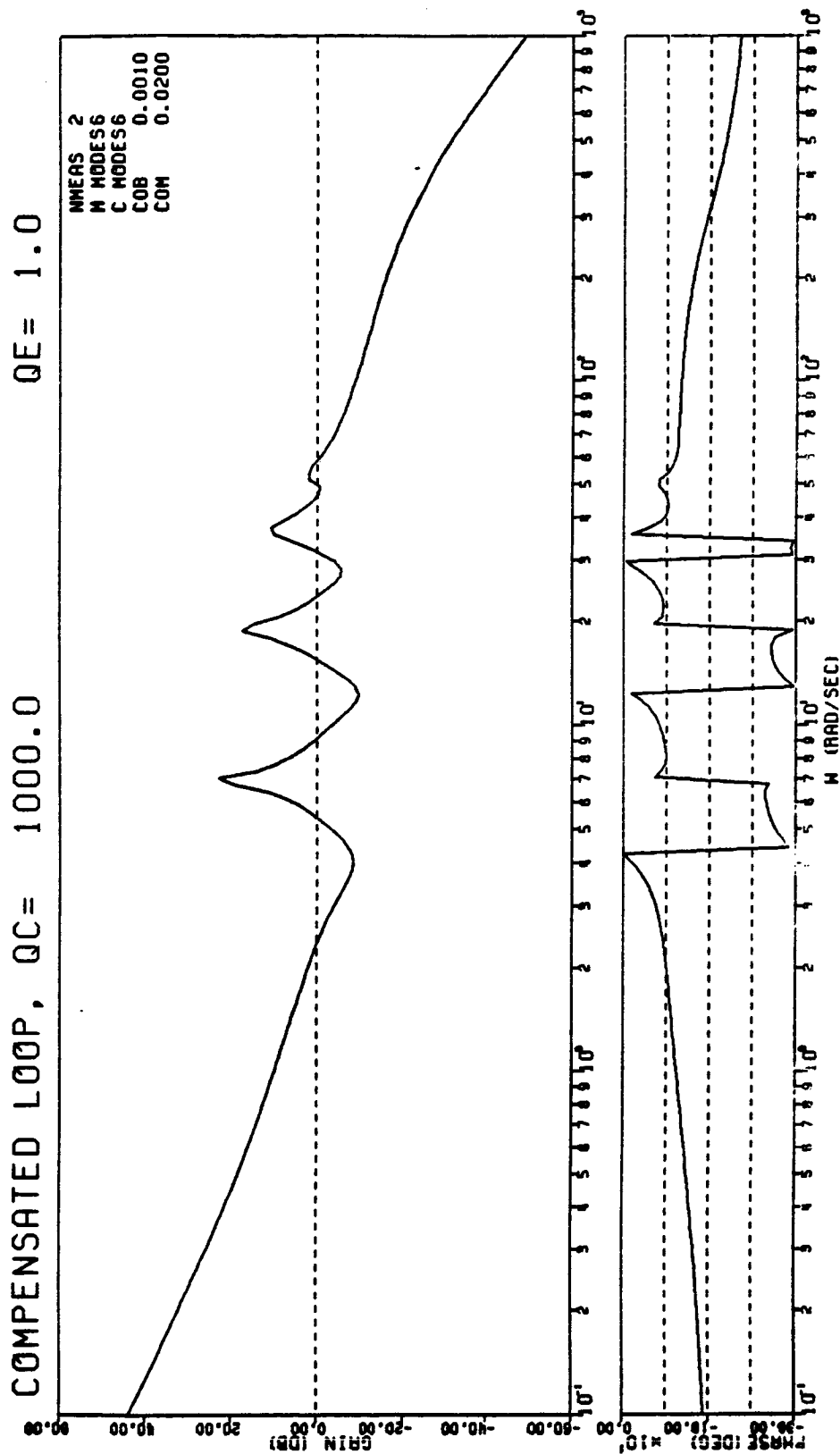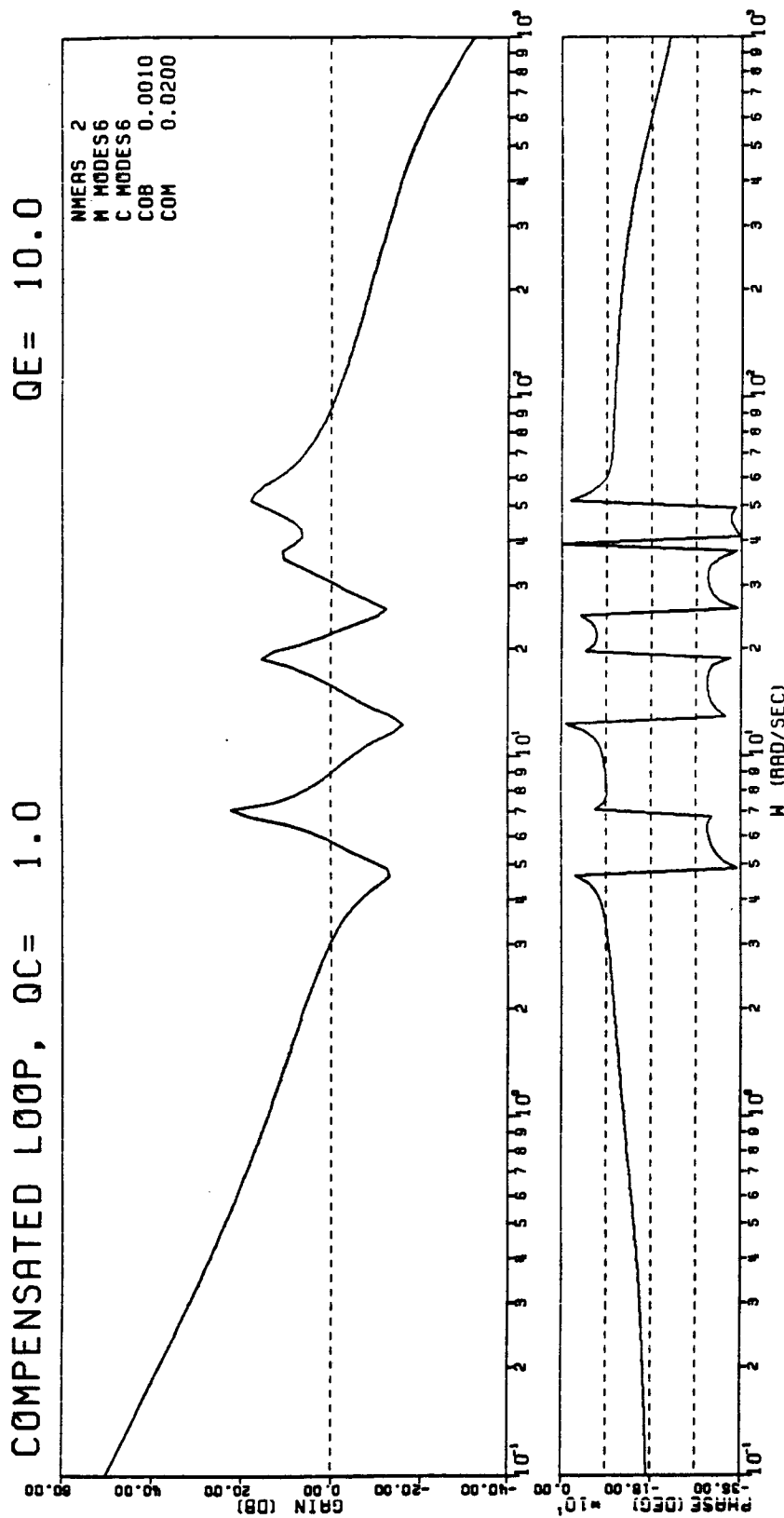
Figure 4.15 Input Loop Gain for Asymptotic LTR on LQR Design #3 (q=10)
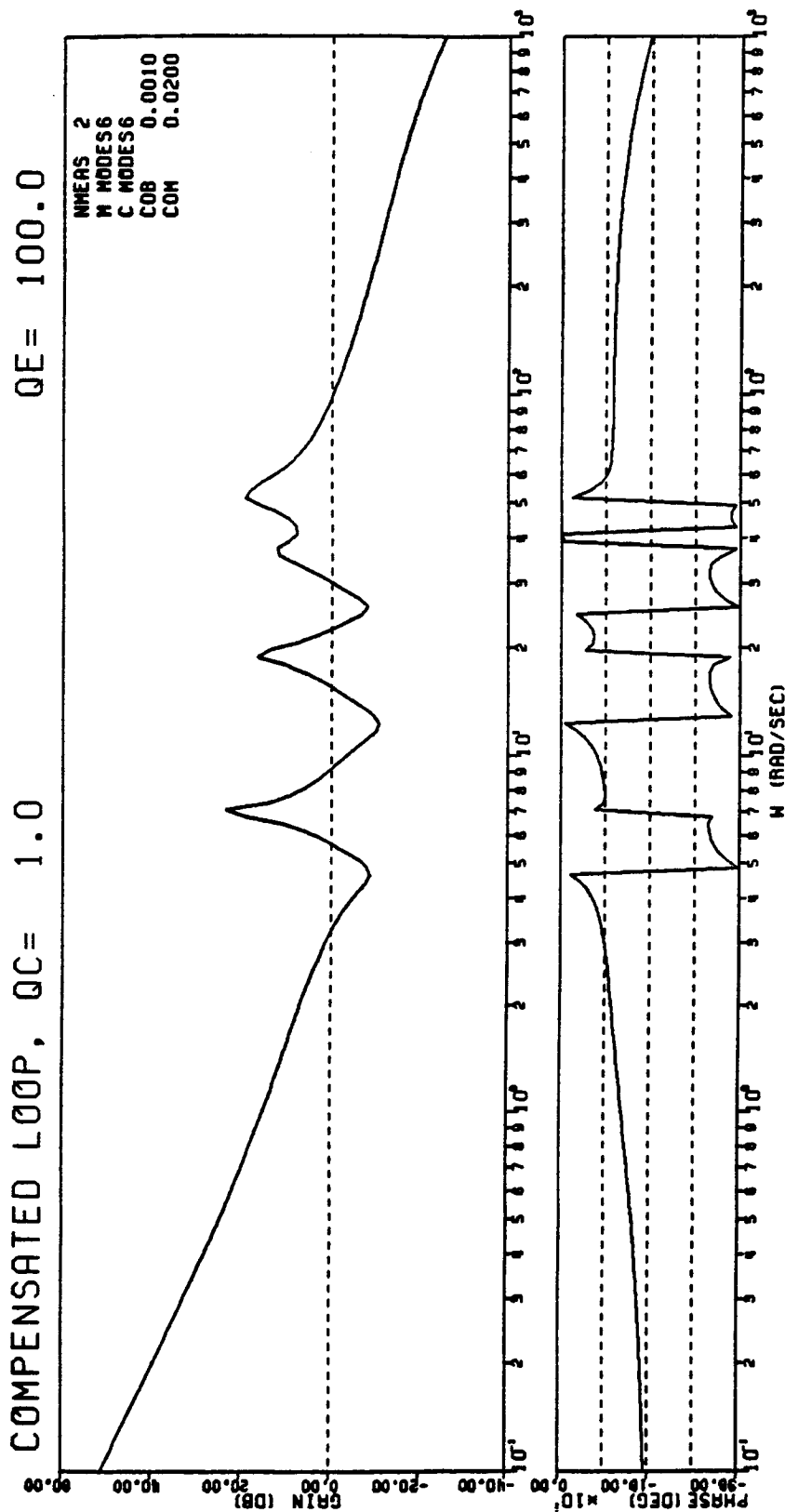
Figure 4.16 Input Loop Gain for Asymptotic LTR on LQR Design #3 (q=100)

C-2

Table 4.2.7 Compensator Pole Locations

#	Pole #1	Pole #2	Pole #3	Pole #4
1	-1±1j	-2±2j	-3±3j	-4±4j
2	-10±10j	-20±20j	-30±30j	-40±40j
3	-.15±10j	-1.5±25j	-2.5±50j	-3.0±55j
4	-1.9±9.8j	-5.5±8.3j	-8.3±5.5j	-9.8±1.9j

The first two sets of poles lie on 45° rays from the origin. The next set are located close to the plant zeros in both channels. This is done in the spirit of the asymptotic approach which cancels plant transmission zeros. The fourth set of poles are placed in a Butterworth filter pattern with a cut-off frequency of 10 rad./sec..

Loop recovery was satisfactorily achieved in every case, but robustness results were not particularily positive. Table 4.2.8 lists those results for all three LQR designs and all four sets of compensator poles. Only LQR design #2 in conjuction with pole location #2 showed any respectable robustness results. Again, a rigorous interpretation of these results has not yet been made, but the number of possible cases for pole locations has not been exhausted. Once an ideal LQR Loop shape is found an optimizing routine might be applied to find the "best" pole locations.

Table 4.2.8 Algebraic LTR Designs

Q#	q_c	PL	-40%	-30%	-20%	-10%	+10%	+20%	+30%	+40%
1	100	1	U	U	U	U	U	U	U	U
1	100	2	U	U	U	U	S	U	U	U
1	100	3	U	U	U	U	U	U	U	U
1	100	4	U	U	U	U	U	U	U	U
2	1000	1	U	U	U	U	U	U	U	U
2	1000	2	S	S	S	S	S	S	U	U
2	1000	3	U	U	S	S	U	U	U	U
2	1000	4	U	U	U	U	U	U	U	U
3	1	1	U	U	U	U	U	U	U	U
3	1	2	U	U	U	U	U	U	U	U
3	1	3	U	U	U	U	U	U	U	U
3	1	4	U	U	U	U	U	U	U	U

4.3 SENSITIVITY OPTIMIZATION

Our second approach to robust compensator design is to use parameter optimization (nonlinear programming) to minimize various measures of the sensitivity of the closed-loop system to parameter errors in the model. Initially, we augmented the quadratic performance index in the optimal linear regulator problem with terms penalyzing the gradient of the closed-loop response (sensitivity) with respect to uncertain parameters. While the resulting optimal control problem could not be solved via the solution of a Riccati equation, the function and gradient evaluations for parameter optimization involved solution of Liapunov matrix equations, which can be solved rather efficiently by well known methods. Unfortunately, this approach proved ineffective because we were unable to find a quadratic performance index involving sensitivity vectors such that the compensator that minimized the performance index was robust.

A much more successful approach has been to minimize an objective functional involving the gradients of the real parts of the closed-loop eigenvalues with respect to uncertain parameters; i.e., minimize the sensitivity of the closed-loop eigenvalues. The closed-loop system has the form

$$\left\{ \begin{matrix} z \\ \hat{z} \end{matrix} \right\} = A_{cl} \left\{ \begin{matrix} z \\ \hat{z} \end{matrix} \right\}$$

where

$$A_{cl} = \begin{bmatrix} A & -BK \\ GC & (A-BK-GC) \end{bmatrix} .$$

Our typical sensitivity objective functional has the form

$$J_s = \Sigma[dRe(\lambda_i)/da_j]^2$$

where the λ_i's are the eigenvalues of A_{cl} and the a_j's are the uncertain parameters in A, B and C. The uncertain parameters usually are natural frequencies and damping ratios. The design variables for this optimization problem are the control and estimator gains K and G.

Usually, we obtain the initial gains as the solution to an optimal LQG problem, and then use sensitivity optimization to improve the robustness of the closed-loop system. We use standard formulas [KA2,Ch.II.2] for computing $d\lambda_i/da_j$ in terms of the eigenvectors and eigenvalues of A_{cl} and dA_{cl}/da_j, and we have found that the computation is much more efficient if done entirely in real arithmetic.

For our beam-hub model, we have been able to take an initial LQG compensator that allows less than 10% variation in the natural frequencies before the closed-loop system becomes unstable and obtain a sensitivity-optimized compensator that allows more than 20% variation in the frequencies while maintaining closed-loop stability.

The following two tables list the dominant closed-loop eigenvalues of the antenna and two compensators based on a six- mode antenna model. The first compensator is optimal for an LQG problem in which state weighting Q penalizes

94

the r.m.s. surface error of the antenna and the disturbance is white noise distributed uniformly over the antenna, along with white noise entering through the actuator. This compensator allows less than 10% error in the open-loop plant frequencies before the closed-loop system becomes unstable. With the LQG compensator as the initial guess, our sensitivity optimization program found the second compensator, which allows more than 20% error in the open-loop frequencies while maintaining closed-loop stability.

Table 4.3.1. Dominant Closed-loop Eigenvalues with LQG Compensator

For correct frequencies	For +10% error in all frequencies	For +20% error
-1.2 ± .2j	-2.0	-10.7
	-1.1	- 1.0
-3.3 ± 4.8j	-4.8 ± .5j	- 1.6 ± 1.3j
-3.0 ± 6.7j	- .4 ± 6.0j	- .06 ± 5.6j
-1.1 ± 7.0j	-2.7 ± 7.0j	-2.50 ± 7.0j
- .6 ± 19.j	+ .4 ± 17.j	+ .80 ± 16.j
-2.8 + 20.j	- 3.5 ± 20.j	- 3.8 ± 19.j
-3.8 + 30.j	- .5 ± 33.j	+ 0.2 ± 36.j

Table 4.3.2. Dominant Closed-loop Eigenvalues with Sensitivity Optimized Compensator

For correct frequencies	For +10% error in all frequencies	For +20% error
-1.3	-1.6	-2.2
- .6	- .6	- .6
-3.4 ± 4.8j	-4.1 ± 4.0j	-4.5 ± 2.5j
- .6 ± 6.9j	- .6 ± 6.0j	- .6 ± 5.2j
-3.0 ± 6.7j	-2.5 ± 6.7j	-2.1 ± 6.8j
-2.8 ± 19.j	- .3 ± 17.j	-.05 ± 16.j
- .7 ± 20.j	-3.2 ± 20.j	-3.6 ± 20.j
-2.2 ± 36.j	-1.3 ± 33.j	- .7 ± 29.j

We have found that the form of the operator Q in the optimal control problem affects robustness significantly. The Q for the preceding LQG compensator penalized the rigid-body displacement primarily and did not penalize energy at all. Table 4.3.3 gives the dominant closed-loop eigenvalues produced by the LQG compensator for a Q which penalizes both the rigid-body angle and the total energy in the antenna. We chose the Q-to-R ratio so that the real part (-.65) of the least stable closed-loop eigenvalue with this compensator is comparable to the real part (-.6) of the least stable eigenvalue with the previous LQG compensator (which resulted from the Q that penalized the antenna surface error). In this case, sensitivity optimization did not improve the robustness of the LQG compensator significantly.

Table 4.3.3. Dominant Closed-loop Eigenvalues
with Second LQG Compensator

For correct frequencies	For ±10% error in all frequencies	For ±20% error
-0.65 ± 0.13j	-0.56 ± 0.17j	-0.53 ± 0.18 j
-0.70 ± 0.33j	-0.76 ± 0.42j	-0.76 ± 0.48 j
-0.78 ± 6.94j	-1.36 ± 6.83j	-1.50 ± 6.92 j
-0.84 ± 6.96j	-0.27 ± 7.81j	-0.13 ± 8.46 j
-1.13 ± 18.9j	-2.49 ± 18.8j	-2.61 ± 18.9 j
-2.05 ± 18.9j	-0.71 ± 21.1j	-0.59 ± 22.8 j

4.4 OPTIMIZED LOOP RECOVERY DESIGNS

Another approach to improving robustness combines the Loop Transfer Recovery methods described in Section 4.2 with the sensitivity optimization methods described in Section 4.3. This is the optimal Loop Transfer Recovery approach, and is currently under investigation.

The idea of the approach is to take advantage of the robustness improvement inherent in the sensitivity optimization methods, while maintaining a fixed loop shape. This guarantees that robustness is not achieved at the cost of a reduced loop gain, or equivalently reduced performance. As noted in Section 4.2.2, the loop recovery compensator for a given full state feedback loop shape is not unique when a plant has more outputs than inputs. In the asymptotic LTR approach, this non-uniquenss corresponds to the choice of artificial columns in the B-matrix. This allows the designer some freedom in the placement of finite plant transmission zeros, which in turn determine the location of the compensator poles. In the algebraic LTR approach the degrees of freedom depend on a number of factors including the desired compensator order,[1] but for the specific algorithm described in Section 4.2.3, the compensator order is fixed and the degrees of freedom translate directly into the location of the compensator poles.

Consequently two optimal LTR approaches are suggested. The first finds an optimal set of elements for the artificial columns of the B-matrix in an asymptotic LTR design. The second finds an optimal set of compensator pole

----

[1] As compensator order is increased, the number of degrees of freedom in the algebraic loop recovery design also increases.

locations in an algebraic LTR design. In both cases the sensitivity of the real parts of each closed loop pole to variations in plant frequency are evaluated. The objective function is equal to the sum of the squares of these sensitivities. This objective function is used since it gave excellent results in the more general sensitivity optimization approach described in Section 4.3.

Since the data presented in Section 4.2.5 suggests that the asymptotic LTR designs provide greater robustness than the algebraic designs, the optimal approach is being applied first to the asymptotic design method. Currently the software is written and preliminary results are expected early in 1986.

Two other applications of optimization to the LTR approach are also being considered. The first is based upon the conjecture that the lack of robustness exhibited by LTR designs relative to the equivalent LQR designs, is a function of pole/zero cancellations close to the imaginary axis. As noted in Section 4.2.4, small variations in plant parameters can result in very large variations in loop shape whenever pole/zero cancellations occur close to the imaginary axis. An optimization routine could therefore be used to choose artificial columns of the B-matrix so as to shift finite plant transmission zeros away from the imaginary axis. A second possibility depends on the fact that the LTR estimator design is largely independent of the full-state feedback LQR control gain matrix K. An optimization routine could therefore leave the LTR estimator design fixed while varying the elements of K so as to minimize closed loop pole sensitivity. Unlike the other optimal approaches described in this Section, this approach would not maintain a given loop shape, and performance might be reduced, but it may produce some further

insight into the relationship betweeen full-state feedback loop shape and LTR robustness.

These optimal LTR approaches to achieving robust control of the antenna will be studied more extensively in 1986.

5.0 CONTROL DRIVEN FINITE ELEMENTS

5.1 A COMPARISON OF THREE FINITE ELEMENT SCHEMES FOR APPROXIMATING THE SOLUTION TO THE OPTIMAL LINEAR REGULATOR PROBLEM FOR A FLEXIBLE STRUCTURE

The Control System

One end of the Euler-Bernoulli beam in Figure 5.1.1 is attached rigidly (cantilevered) to a rigid disc which is free to rotate about its center, point O, which is fixed. Also, a point mass m_1 is attached to the other end of the beam. The control is a torque u applied to the disc, and all motion is in the plane.

Figure 5.1.1
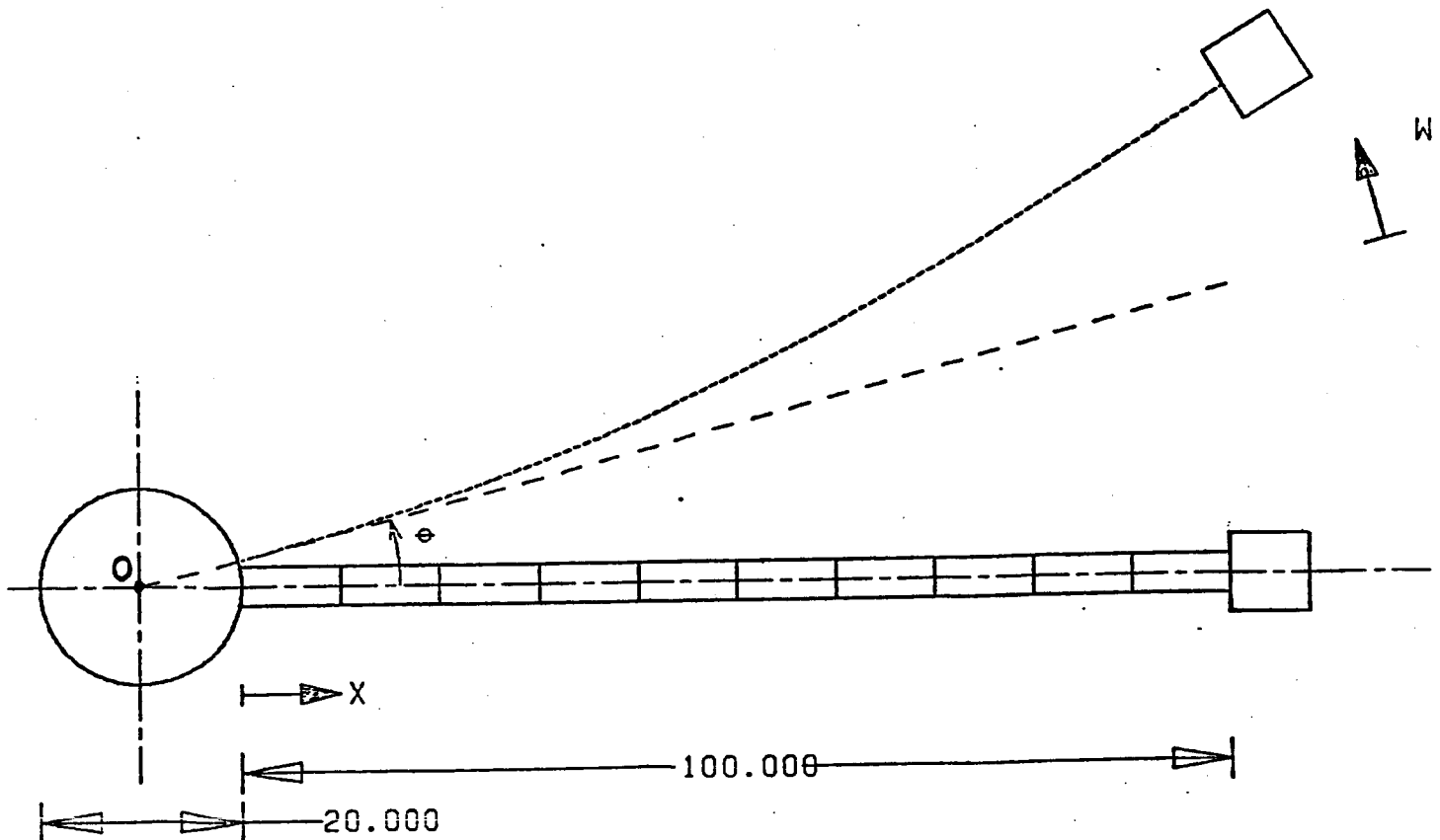
Table 5.1.1. Structural Data

r = hub radius   10 in

l = beam length   100 in

I_0 = hub moment of inertia about axis

       perpencilar to page through 0   100 slug in^2

m_b = beam mass per unit lingth   .01 slug/in

m_1 = tip mass   1 slug

EI = product of elastic modulus and

second moment of cross Section for beam   13,333 slg in^3/sec^2

fundamental frequency of undamped structure   .9672 rad/sec

The angle θ represents the rotation of the disc (the rigid- body mode), w(t,s) is the elastic deflection of the beam from the rigid-body position, and w_1(t) is the displacement of m_1 from the rigid-body position. The control problem is to stabilize rigid-body motions and linear (small) transverse elastic vibrations about the state $\theta = 0$ and $w = 0$. Our linear model assumes not only that the elastic deflection of the beam is linear but also that the axial inertial force produced by the rigid-body angular velocity has negligible effect on the bending stiffness of the beam. The rigid-body angle need not be small.

This system can be written in the form (3.1.1) with the generalized displacement vector

$x = (\theta, w, w_1)$ $H = R \times L_2(0,1) \times R.$ (5.1.1)

We assume that the beam has Voigt-Kelvin viscoelastic damping, so that the damping operator in (3.1.1) is

$$D_0 = c_0 \, A_0 \qquad\qquad\qquad (5.1.2)$$

where $c_0 = 10^{-4}$. For the details of the energy-space formulation of this problem and the operators in (3.1.1), see [GI1].

The Optimal Control Problem

In the optimal control problem, we take $Q = I$ in the performance index in (3.2.1). This means that the state weighting term $<Qz,z>_E$ is twice the total energy in the structure plus the square of the rigid-body rotation. Since there is one input, the control weighting R is a scalar, and we take $R = .05$.

The functional control gains in (3.3.2) have the form

$$f = (\alpha_f, \phi_f, \beta_f), \qquad\qquad\qquad (5.1.3)$$

$$g = (\alpha_g, \phi_g, \beta_g), \qquad\qquad\qquad (5.1.4)$$

where the α's and β's are scalar gains for the hub and tip mass and ϕ_f and ϕ_g are functions which define the feedback law for the beam. Because the strain energy in the beam involves the second spacial derivative of w, $\phi_f{}''$ appears in the the control law in (3.3.2), rather than ϕ_f.

Approximation

To approximate the solution to the optimal control problem, we solve a sequence of finite dimensional optimal control problems as described in Chap-

ter 3.4. To illustrate the convergence of the approximating feedback control laws, we will plot the distributed functional gain components ϕ_f'' and ϕ_g.

We compare three approximation schemes; i.e., three different sets of basis vectors e_i for the approximation to the generalized displacement in (3.4.1). The first approximation of the structure is based on a finite element approximation of the beam which uses cubic Hermite splines [ST1] as basis functions, the second approximation scheme uses cubic B-splines to approximate the beam, and the third approximation scheme uses the natural mode shapes of the structure as the basis vectors in the approximating optimal control problems. Recall that cubic B- splines require the displacement, slope and second derivative to be continuous at the nodes, while cubic Hermite splines require only the displacement and slope to be continuous at the nodes. To get the natural modes of the structure, we used 24 elements in the Hermite spline approximation to get the first 12 modes of undamped, free vibration.

Figure 5.1.2 shows the distributed functional gain components computed using the Hermite splines, Figure 5.1.3 shows the distributed functional gain components computed using the B-splines, and Figure 5.1.4 shows the distributed functional gain components computed using the natural mode shapes. For both spline schemes, we get convergence with ten elements and very near convergence with eight elements. Also, we get convergence with ten modes and very near convergence with eight modes.

Now note that if n_e is the number of elements, then the number of degrees of freedom in the Hermite spline scheme is $2n_e + 1$, while the number of

degrees of freedom in the B-spline scheme is $n_e + 1$. This means that the B-splines and natural mode shapes are almost equally efficient for computing the control gains and that the Hermite splines require almost twice as many degrees of freedom. This is important because the dimension of the Riccati matrix equation that must be solved in each approximate optimal control problem is twice the number of degrees of freedom in the approximation scheme.

We experimented with varying the location of the nodes for the Hermite splines and B-splines. While we found that we could improve the rate of convergence slightly, we felt that the improvement was not sufficient to justify the elaborate procedure. The improvement in convergence rate obtained by varying the node locations was insignificant compared to the improvement obtained by using modes or B-splines instead of Hermite splines.

Figure 5.1.2a

CONTROL FUNCTIONAL GAINS
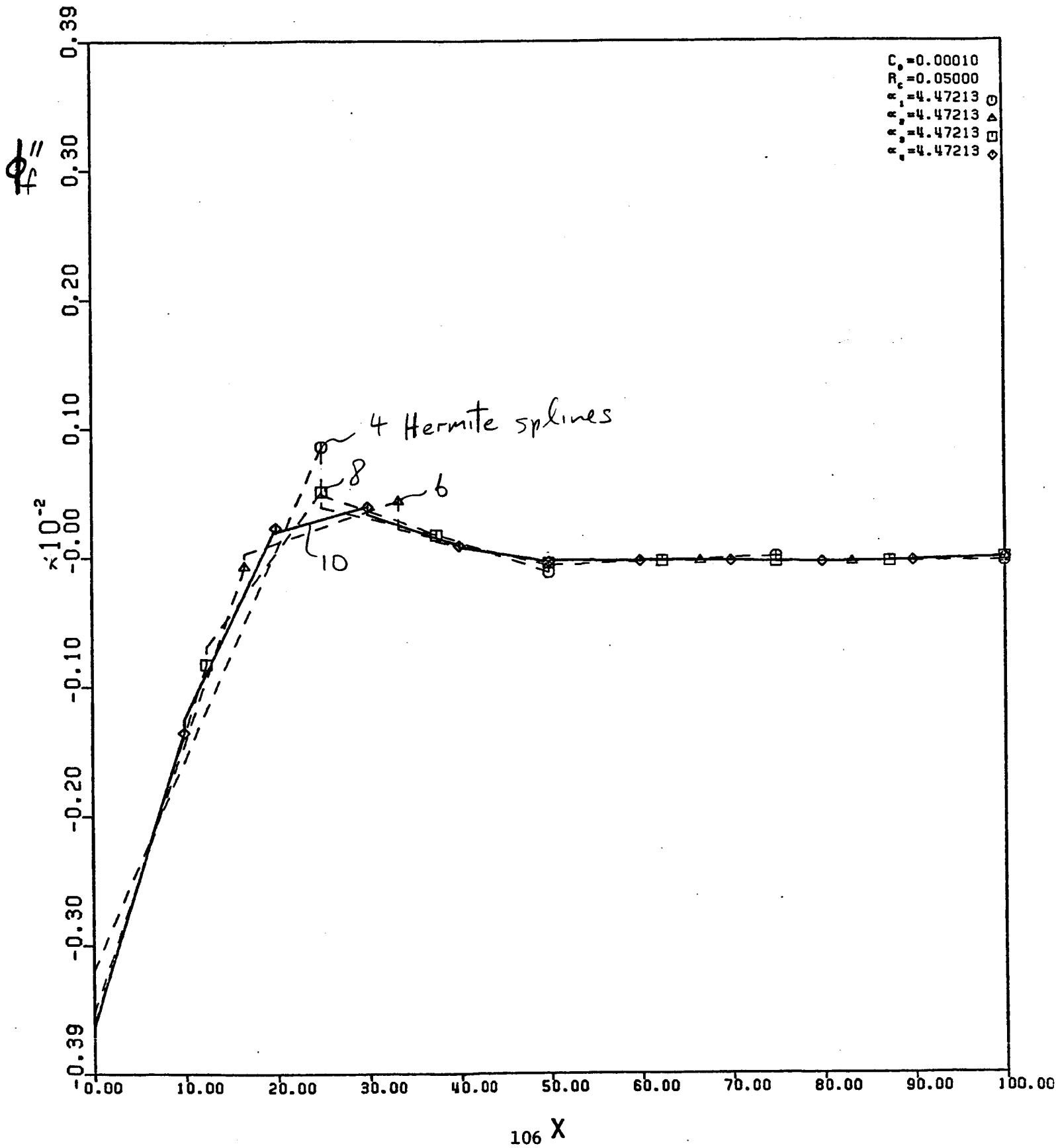
Figure 5.1.2b

CONTROL FUNCTIONAL GAINS

$C_o = 0.00010$
$R_c = 0.05000$
$B_1 = 1.24400$ ⊙
$G_1 = -133.87$
$B_2 = 1.29728$ △
$G_2 = -139.69$
$B_3 = 1.31063$ ▢
$G_3 = -141.15$
$B_4 = 1.31413$ ◇
$G_4 = -141.54$

4 Hermite splines

6

8

10

ϕ_9

X
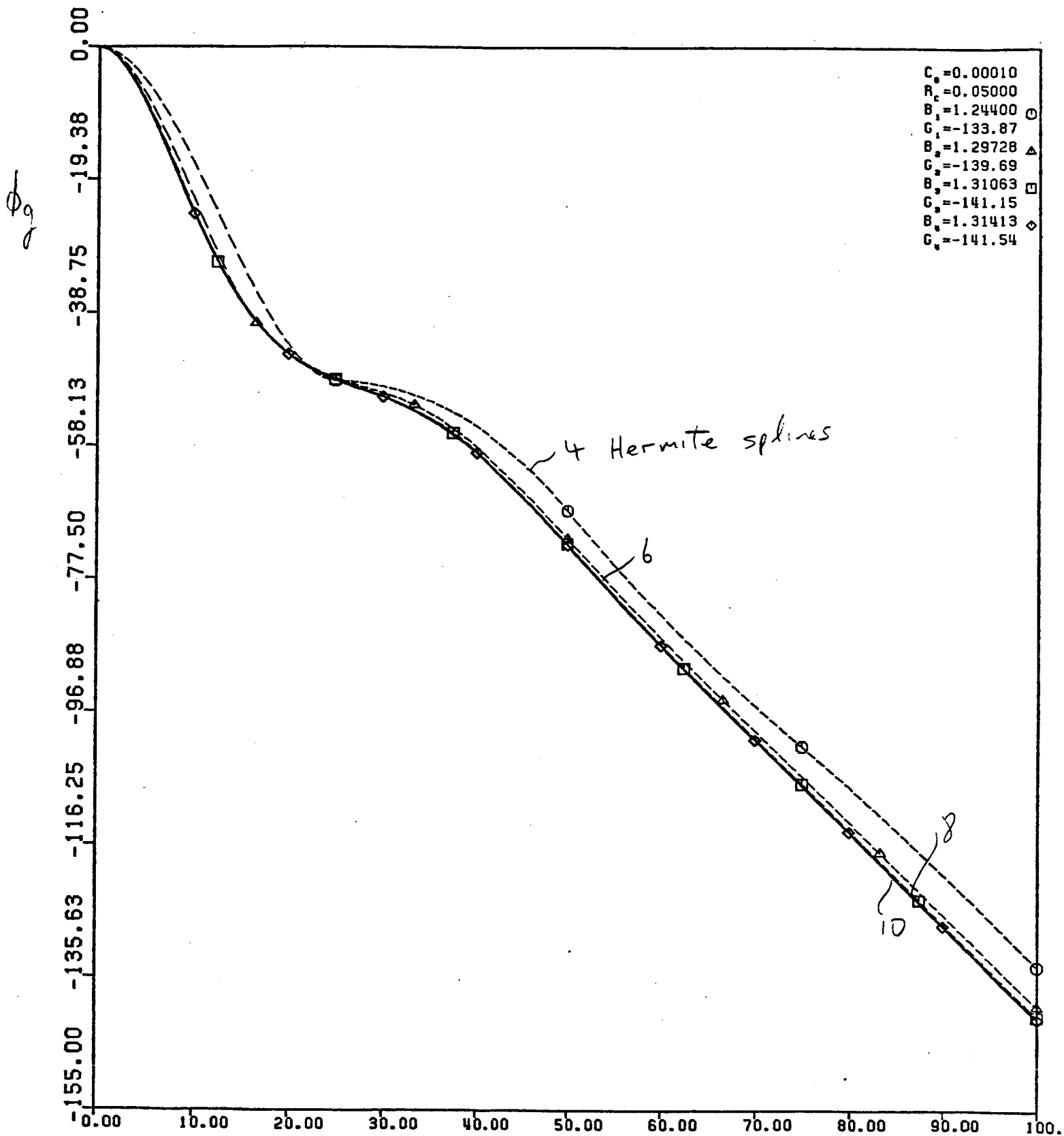
Figure 5.1.3a

CONTROL FUNCTIONAL GAINS
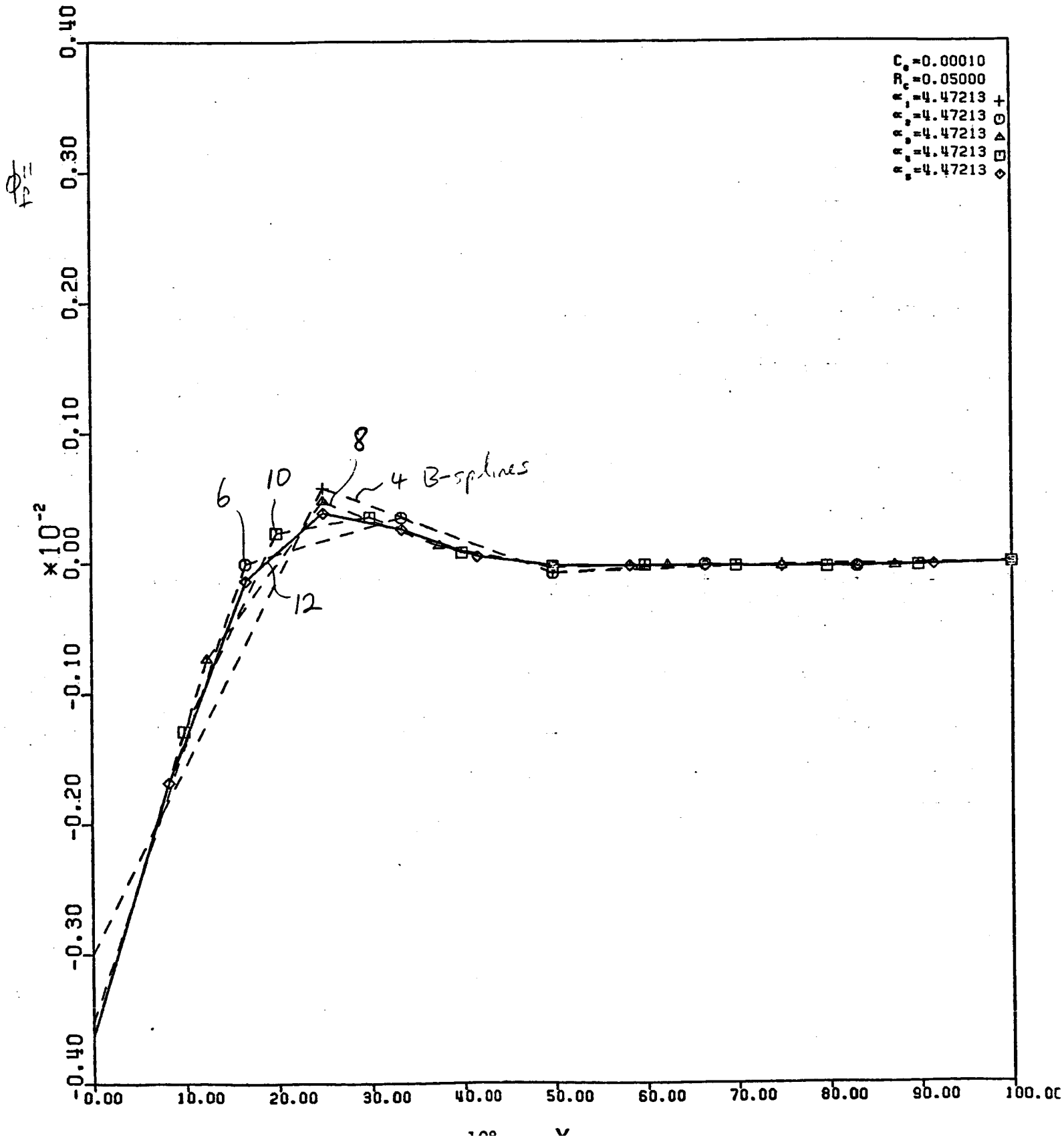
Figure 5.1.3b

CONTROL FUNCTIONAL GAINS

$C_c = 0.00010$
$R_c = 0.05000$
$B_1 = 1.13657$ +
$G_1 = -121.87$
$B_2 = 1.28174$ ⊙
$G_2 = -137.98$
$B_3 = 1.30785$ △
$G_3 = -140.85$
$B_4 = 1.31346$ ▢
$G_4 = -141.46$
$B_5 = 1.31515$ ◇
$G_5 = -141.65$

4 B-splines

6

8

10,12
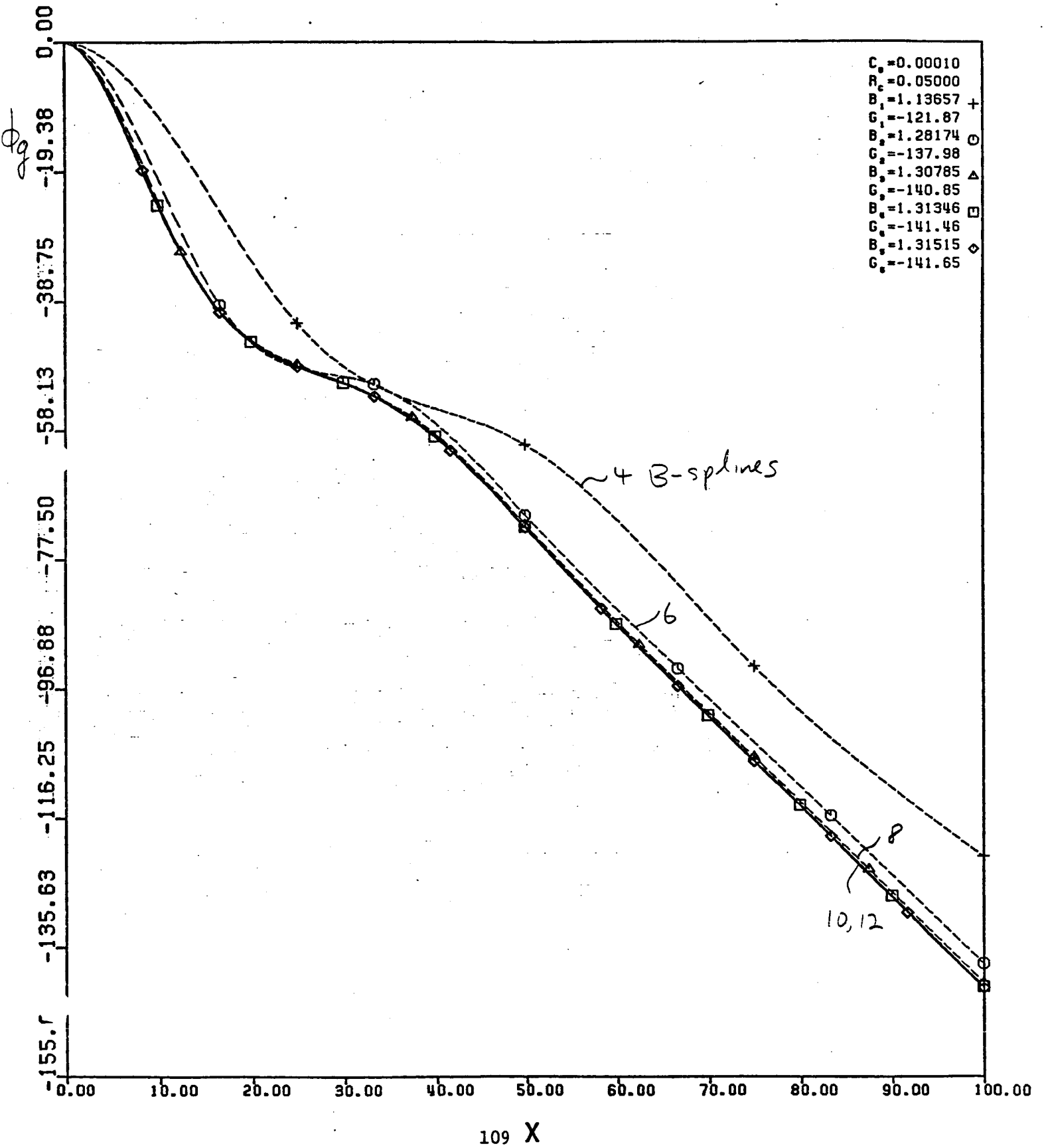
Figure 5.1.4a

CONTROL FUNCTIONAL GAINS

Figure 5.1.4b

CONTROL FUNCTIONAL GAINS

Legend:

$C_s = 0.00010$
$Q_s = 1.00000$
$R_c = 0.05000$
$B_1 = 1.11907$ +
$G_1 = -119.78$
$B_2 = 1.28170$ ⊙
$G_2 = -137.90$
$B_3 = 1.30926$ △
$G_3 = -140.99$
$B_4 = 1.31434$ ⊡
$G_4 = -141.56$
$B_5 = 1.31566$ ◇
$G_5 = -141.71$

4 modes

6

8

10

y-axis: ϕ_q — 0.00, -19.38, -38.75, -58.13, -77.50, -96.88, -116.25, -135.63, -155.00

x-axis: X — 0.00, 10.00, 20.00, 30.00, 40.00, 50.00, 60.00, 70.00, 80.00, 90.00, 100.00

5.2 DIRECT APPROXIMATION OF HAMILTONIAN SYSTEM

We have investigated approximation of the solution to the optimal control problem for the distributed model of the space stucture by constructing direct finite element approximations of the infinite dimensional Hamiltonian system. To date, our numerical solution of the LQG optimal control problem for the distributed model of the space antenna has been based on an approximation scheme that is indirect in that we first approximate the open-loop system with a sequence of finite dimensional systems and then solve a finite dimensional optimal control problem for each approximating system. The solutions to these finite dimensional problems converge to the solution to the infinite dimensional problem. However, for certain space structures, direct approximation of the solution to the infinite dimensional problem may allow better choices for the basis elements used in the approximation.

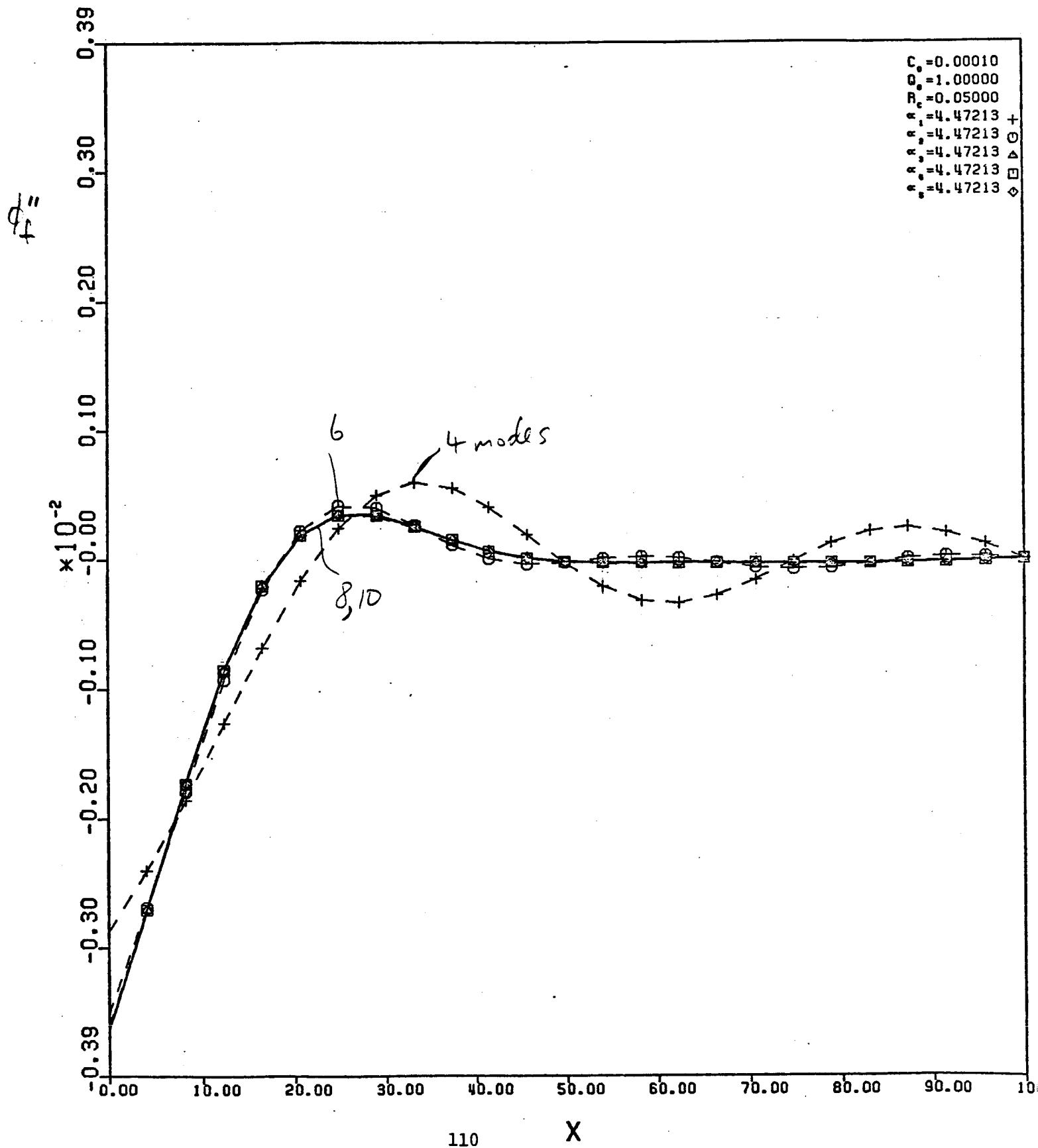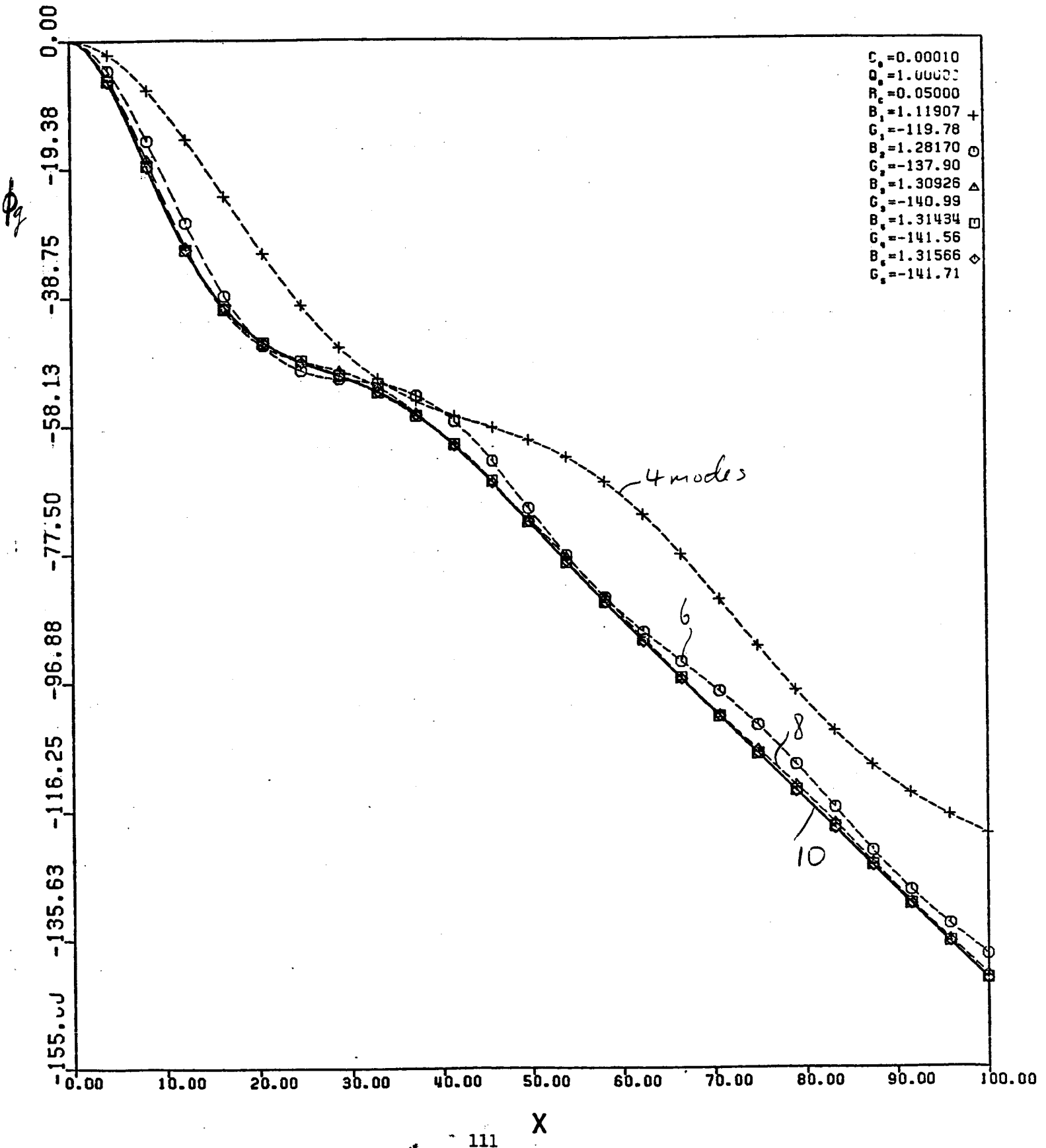The Hamiltonian operator involved in the solution to the optimal regulator problem is

$$\begin{bmatrix} A & -BB^* \\ -Q & -A^* \end{bmatrix} \tag{5.2.1}$$

where A is the open-loop semigroup generator, B the input operator, and Q the state-weighting operator in the optimal control problem. Recently, we began studying the extension of an idea used at JPL for solving static state estimation problems. As applied to the control problem, the idea is to choose a finite element scheme to approximate the infinite dimensional Hamiltonian operator directly with operators of the form

$$\begin{bmatrix} A_n & -C_n \\ -Q_n & -A_n^{\perp} \end{bmatrix} \qquad \qquad (5.2.2)$$

Here, $A_n^{\perp}$ is not necessarily the adjoint of A_n. In particular, two different

sets of basis vectors may be used in approximating A and A^*.

For the models of flexible structures and the finite element schemes that
we have used to date, direct approximation yields the same finite dimensional
Hamiltonian operator as does indirect approximation, but for more complicated
structure models, this should not be the case. Direct approximation of the
infinite dimensional Hamiltonian operator may be most useful for structures in
which some of the materials are viscoelastic with history-dependent damping.
For discussion of history-dependent viscoelastic effects see [CO1,FU1]. Such
structures lack the basic selfadjointness of more common structures, and the

operators A and A^* have very different domains. Hence different finite ele-

ment basis vectors are needed for approximating A and A^*. These basis vectors
should be chosen to produce appropriate convergence of the direct approxima-
tions to the Hamiltonian system and the corresponding direct approximations to
the solution of the infinite dimensional optimal control problem.

6.0 SUMMARY AND CONCLUSIONS

The work described in this report further develops aspects of modern control theory which make it better able to deal with issues of modeling and implementation. The report represents an extension of previous work done for JPL in which elements of distributed parameter control theory and finite dimensional control theory have been synthesized into a design approach which simultaneously produces both a model which is appropriate for the control problem at hand, and an "optimal" controller based on that model. The interaction of modeling and controller design is central to the approach. The techniques developed have been applied to a space antenna to demonstrate their performance on space systems of realistic complexity.

A major focus of the work carried out during 1985 was robustness. Robustness refers to the ability of a control system to perform satisfactorily even when the model used for the design is an imperfect representation of the actual system. There are two types of modeling errors which are of major concern in designing control systems for large space structures (LSS). Much of the work on functional gains is aimed at one particular type of modeling problem: model truncation. Parameter errors are another important source of modeling error. Work during the current year emphasized the development of LSS controller designs which are relatively insensitive to parameter errors but still maintain a satisfactory level of system performance. For antenna structures of the type considered, this is a difficult problem which does not easily yield to standard techniques.

As a general rule, an improvement in robustness can only be achieved at the cost of a reduction in some measure of performance. In order to achieve a

proper balance between performance and robustness, some constraints must be imposed. In the loop recovery approach, the open loop and closed loop frequency responses are constrained to approximate those of the full state feedback LQR design. Thus, the performance of the system is first determined in the context of the LQR design, and then one tries to obtain an estimated state feedback implementation which has similar performance and also adequate robustness. The sensitivity optimization approach also begins with the solution of an LQR problem and designs an estimated state feedback implementation. In this case, however, there is no constraint to retain the LQR frequency response. Instead, the goal is to minimize the sensitivity of the closed loop eigenvalues to parameter errors. A constraint must be imposed to keep the closed loop regulator and estimator eigenvalues sufficiently far in the left half plane otherwise the optimization routine would generate a very low performance control system. Designs based on sensitivity optimization tend to be more robust than LTR designs, but their loop gains are also lower.

Both of these approaches rely heavily on the statement of the LQR problem which serves as a starting point for the designs. The state weighting operator in the performance index for the LQR problem discussed in Chapter 3 is Q. Generally, scaling up Q while holding the control weighting matrix R fixed leads to larger control gains and a less robust compensator. The numerical examples presented in Sections 4.2 and 4.3 indicate that in addition to the magnitude of Q, the relative penalization that Q specifies among the different components of the state vector can affect robustness dramatically. For example, Q's which penalize only the RMS surface error of an antenna model were found to lead to designs which were not very robust. However, Q's which penalize the energy or the RMS surface error plus the rate of change of RMS

error, were found to be quite robust. While the interpretation of these results is not entirely clear at this point, some observations can be made. Penalizing RMS surface error alone leads to controllers which try to reduce rigid body displacement much faster than elastic deformations. This means that the closed loop eigenvalues for the rigid body mode are substantially to the left of those for the lowest flexible modes. In this case, large control torques are produced to control the rigid body mode, and the system is not robust because these torques strongly excite the flexible modes which may be inaccurately known. The other two Q's mentioned above penalize the rigid body and flexible modes more equally. The real parts of of the closed loop eigenvalues, and hence the decay rates, for the rigid body mode and lowest elastic modes are approximately equal and the compensator is more robust. In our continuing research effort, we plan to pursue further the relationship between the selection of Q and robustness.

Another factor which has a strong effect on robustness in the number an position of the measurements. In the case of the beam-hub model, control designs based on two measurements were much more robust than those based on one measurement. The implications of the number of measurements for the antenna model will be studied more extensively in 1986.

Sensitivity optimization appears to be a successful approach for designing robust compensators for complex structures, but we need more analysis and numerical experimentation to determine the best objective functionals and the most effective methods of optimization. We have experimented with objective functionals involving both first and second-order gradients of eigenvalues with respect to uncertain parameters, and found that minimizing the second

gradients also does not improve robustness significantly. Also, we are comparing performance of the optimization routines using analytic as opposed to numerical gradients with respect to the design variables.

The results in Section 5.1 demonstrate that a well chosen finite element scheme can greatly reduce the order of approximation required to design an optimal compensator for a flexible structure. It should not be surprising that the natural mode shapes are at least among the best basis vectors for approximating the optimal functional gains. It is more interesting that the cubic B-splines are almost as efficient in the example that we worked; they are much better than the cubic Hermite splines, which are most common in engineering finite element approximations of beams. This suggests that further research on control driven finite elements could produce significantly more efficient numerical methods for the design of controllers for large flexible structures.

Since we know now that some approximation schemes are more efficient than others for numerical solution of distributed optimal control problems, it seems natural to try to develop a scheme especially for the approximate solution of the optimality conditions for the infinite dimensional LQG problem for the distributed model of a flexible structure. These optimality conditions are embodied in the infinite dimensional Hamiltonian operator discussed in Section 5.2, where we propose the direct approximation of this operator instead of the indirect approximation that usually is used. For the kinds of material models and finite element schemes that we have used so far, the direct and indirect approximations are identical, but for materials with memory (particularly history-dependent damping) the direct approximation of

118

the Hamiltonian operator would be different and should be investigated.

REFERENCES

BA1) Balakrishnan, A.V., _Applied Functional Analysis_, Springer-Verlag, 1981

BA2) Balas, M.J., "Feedback Control of Flexible Systems," _IEEE Trans. Auto. Contr._, Vol. AC-23, pp. 673-679, 1978

BA3) Balas, M.J., "Modal Control of Certain Flexible Dynamic Systems," _SIAM J. Control Opt._, Vol. 16, pp. 450-462, 1978

BO1) H.W. Bode, _Network Analysis and Feedback Amplifier Design_, Van Nostrand, New York, 1945

CH1) Chen, C.T., _Linear System Theory and Design_, Holt, Rinehart and Winston, New York, 1984

CO1) Coleman, B.D., Mizel, V.J, "On the Stability of Solutions of Functional Differential Equations," _Arch. Rat. Mech. Anal._, Vol. 30, pp. 173-196, 1969

CU1) Curtain, R.F., Pritchard, A.J., _Infinite Dimensional Linear Systems Theory_, Springer-Verlag, 1978

DO1) Doyle, J.C., Stein, G., "Multivariable Feedback Design: Concepts for a Classical/Modern Synthesis," _IEEE Trans. Auto. Contr._, Vol. AC-26, No. 1, pp. 4-16, 1981

DO2) Doyle, J.C., Stein, G., "Robustness with Observers," _IEEE Trans. Auto. Contr._, Vol. AC-24, No. 4, pp. 607-611, 1979

ED1) Edmunds, R.S., "Robust Control Design Techniques for Large Flexible Space Structures having Non-Colocated Sensors and Actuators," Ph.D. Thesis, UCLA, June, 1982

EL1) El-raheb, M.L., Wagner, P., "Static and Dynamic Characteristics of Large Deployable Reflector," Paper No. 81-0503-pc., presented at AIAA Specialists Conference at Atlanta, GA, April 1981

FR1) Freudenberg, J.S., Loose, D.P., "Relations between properties of Multivariable Feedback Systems at Different Loop-Breaking Points: Part I," Proc. 24th Conf. Dec. Contr., pp. 250-256, 1985

FU1) Fung, Y.C., _Foundations of Solid Mechanics_, Prentice-Hall, 1965

GI1) Gibson, J.S., "An Analysis of Optimal Modal Regulation: Convergence and Stability," _SIAM J. Control Opt._, Vol. 19, No. 5, 1981

GI2) Gibson, J.S., "The Riccati Integral Equations for Optimal Control Problems on Hilbert Spaces," _SIAM J. Control Opt._, Vol. 17, 1979

GI3) Gibson, J.S., Adamian, A., "Approximation Theory for LQG Optimal Control of Flexible Structures," to appear.

HA1) Harvey, C.A., Stein, G., "Quadratic Weights for Asymptotic Regulator Properties," IEEE Trans. Auto. Contr., Vol. AC-23, No. 3, pp. 378-387, 1978

HR1) HR Textron Report #956541-Final, September, 1984

HR2) HR Textron Report #956541-Final Extension, February, 1985

KA1) Kailath, T., Linear Systems, Prentice-Hall Inc., New Jersey, 1980

KA2) Kato, T., Perturbation Theory for Linear Operators, 2nd Edition, Springer-Verlag, New York, 1984

KL1) Klema, V.C., Laub, A.J., "The Singular Value Decomposition: Its Computation and Some Applications," IEEE Trans. Auto. Contr., Vol. AC-25, No. 2, pp. 164-176, 1980

KO1) Kouvaritakis, B., Postlethwaite, I., "Principal Gain and Phases: Insensitive Robustness Measures for Assessing Closed-Loop Stabliity Property," IEE Proc., Vol. 129, No. 1, pp. 233-241, 1982

KW1) Kwakernaak, H., "Optimal Low-Sensitivity Linear Feedback Systems," Automatica, Vol. 5, pp. 279-285, 1969

LA1) Laub, A.J., "Numerical Linear Algebra Aspects of Control Design Computations," IEEE Trans. Auto. Contr., Vol. AC-30, No. 2, pp. 97-108, 1985

LE1) Lehtomaki, N.A., "Practical Robustness Measures for Multivariable Control System Analysis," Ph.D. Thesis, Massachusetts Institute of Technology, May, 1981

LE2) Lehtomaki, N.A., Sandell, N.R., Jr., Athans, M., "Robustnesss Results in Linear-Quadratic Gaussian Based Multivariable Control Designs," IEEE Trans. Auto. Contr., Vol. AC-26, No. 2, pp. 75-92, 1981

LE3) Lehtomaki, N.A., Castanon, D., Levy, B., Stein, G., Sandell, N.R., Jr., Athans, M., "Robustness Tests Utilizing the Structure of Modelling Error," Proc. 20th IEEE Conf. Dec. Contr., pp. 1173-1190, 1981

LE4) Lehtomaki, N.A., Castanon, D.A., Levy, B.C., Stein, G., Sandell, N.R., Jr., Athans, M., "Robustness and Modeling Error Characterization," IEEE Trans. Auto. Contr., Vol. AC29, No. 3, pp. 212-220, 1984

LO1) "Space Technology, Lockheed Tests Large Space Antenna," Aviation Week and Space Technology, April 30th, 1984

PO1) Postlethwaite, I., "Gain and Phase Margins for Linear Multivariable Feedback Systems," Proc. 18th Allerton Conf. on Comm., Contr. and Comp., pp. 396-403, 1980

RO1)   Rosenbrock, H.H., "The Stability of Mutivariable Systems," IEEE Trans. Auto. Contr., Vol. AC-17, No. 2, pp. 105-107, 1972

SA1)   M.G. Safonov, Stability and Robustness of Multivariable Feedback Systems, MIT Press, Cambridge Massachusetts, 1980

SA2)   Safonov, M.G., "Robustness and Stability Aspects of Stochastic, Multivariable Feedback System Design," Ph.D. Thesis, Massachusetts Institute of Technology, May 1977

SA3)   Safonov, M.G., Laub, A.J., Hartmann, G.L., "Feedback Properties of Multivariable Systems: The Role and Use of the Return Difference Difference Matrix," IEEE Trans. Auto. Contr., Vol. AC-26, No. 1, pp. 47-65, 1981

SA4)   Safonov, M.G., Athans, M., "Gain and Phase Margin for Multiloop LQG Regulators," IEEE Trans. Auto. Contr., Vol. AC-22, No. 2, pp. 173-179, 1977

SH1)   Shaked, U., Soroka, E., "On the Stability Robustness of Continuous Time LQG Optimal Control," IEEE Trans. Auto. Contr., Vol. AC-30, No. 10, pp.1039-1043, 1985

ST1)   Strang, G., Fox, G.J., An Analysis of the Finite Element Method, Prentice-Hall, Englewood Cliffs, NJ, 1973

ST2)   Stewart, G.W., Introduction to Matrix Computations, Academic Press, New York, 1973

SU1)   Sundararajan, N., Joshi, S.M., Armstrong, E.S., "Robust Controller Synthesis for a Large Flexible Space Antenna," Proc. 23rd Conf. Dec. Contr., pp.202-208, 1984

ZA1)   Zames, G., "On the Input-Output Stability of Time-Varying Nonlinear Feedback Systems - Part I: Conditions Derived Using Concepts of Loop Gain, Conicity, and Positivity," IEEE Trans. Auto. Contr., Vol. AC-11, No. 2, pp. 228-238, 1966

ZA2)   Zames, G., "On the Input-Output Stability of Time-Varying Nonlinear Feedback Systems - Part II: Conditions Involving Circles in the Frequency Plane and Sector Nonlinearities," IEEE Trans. Auto. Contr., Vol. AC-11, No. 3, pp. 465-476, 1966

Appendix A: Singular Values

Singular values measure the "size" of a complex matrix, and are equivalent to the concept of the modulus of a complex scalar. The singular values of a matrix transfer function can therefore be thought of as the MIMO equivalents of the gain of a scalar transfer function.

Any n x m complex matrix A can be decomposed in the following fashion:

$$A = U\Sigma V^* = \sum_{i=1}^{k} \sigma_i u_i v_i^*$$

where:

$k = \min(n,m)$

$\sigma_i = \sqrt{\lambda_i[AA^*]} = \sqrt{\lambda_i[A^*A]}$,

$\sigma_i \geq \sigma_{i+1}$

$U = [u_1\ u_2\ \ldots\ u_n], \quad UU^* = U^*U = I$

$V = [v_1\ v_2\ \ldots\ v_n], \quad VV^* = V^*V = I$

The σ_i's are the singular values of A, the vectors u_i are the left singular vectors of A and the vectors v_i are the right singular vectors of A. The largest singular value σ_1 is denoted by $\bar{\sigma}$ and the smallest singular value σ_k by $\underline{\sigma}$. $\bar{\sigma}[A]$ is the l_2 induced operator norm of A in the following sense:

123

$$\overline{\sigma}[A] = \max_{x \neq 0} \frac{\|Ax\|_2}{\|x\|_2} = \max_{\|x\|_2 = 1} \|Ax\|_2$$

while $\underline{\sigma}[A]$ is a measure of the closeness of A to singularity in the following sense:

$$\underline{\sigma}[A] = \min_{x \neq 0} \frac{\|Ax\|_2}{\|x\|_2} = \min_{\|x\|_2 = 1} \|Ax\|_2$$

$\underline{\sigma}[A]$ is the only computationally reliable tool for the determination of near singularity, or rank of a matrix [KL1,LA1].

The following table includes a number of useful properties of singular values:

1) $\underline{\sigma}[A] > 0 \qquad \underline{\sigma}[A] = 1/\overline{\sigma}[A^{-1}]$

2) $\sigma_i[\alpha A] = |\alpha| \sigma_i[A]$

3) $\underline{\sigma}[A] \leq |\lambda_i[A]| \leq \overline{\sigma}[A]$

4) $A = A^* \implies \sigma_i[A] = |\lambda_i[A]|$

5) $A = A^* \geq 0 \implies \sigma_i[A] = \lambda_i[A]$

6) $\overline{\sigma}[A + B] \leq \overline{\sigma}[A] + \overline{\sigma}[B]$

7) $\overline{\sigma}[AB] \leq \overline{\sigma}[A]\overline{\sigma}[B]$

8) $\underline{\sigma}[AB] \geq \underline{\sigma}[A]\underline{\sigma}[B]$

9) $\underline{\sigma}[A] - 1 \leq \underline{\sigma}[I + A] \leq \underline{\sigma}[A] + 1$

10) $\overline{\sigma}[E] < \underline{\sigma}[A] \qquad \sigma[A + E] > 0$

11) $\overline{\sigma}[A] < 1 \qquad \underline{\sigma}[I + A] \geq 1 - \overline{\sigma}[A]$

Another slight variation on the singular value decompostion is the polar decompostion, used extensively by Postlethwaite [PO1,2,KO1]. Write the singular value decompostion as:

$$A = U\Sigma V^* = UV^*(V\Sigma V^*) = (U\Sigma V^*)UV^*$$

where $U\Sigma V^*$ is the usual singular value decomposition, $UV^*(V\Sigma V^*)$ is the right polar decomposition and $(U\Sigma U^*)UV^*$ is the left polar decomposition. Postlethwaite defines the principal gains as the eigenvalues of $V\Sigma V^*$ or $U\Sigma U^*$, which are of course just the singular values of A, and the principal phases as the arguments of the eigenvalues of the unitary matrix UV^*. This decomposition is useful in separating a transfer function into a gain part and a phase part and will be used the proof of Theorems 2.1 and 2.2 in Appendix B.

Appendix B: Proof of Unstructured Uncertainty Theorems

Theorem 4.1 will be proved in detail. The changes that need to be made for Theorem 4.2 will not be extensive and will be described in less detail.

Theorem 4.1:

The Multivariable Nyquist Criterion requires that $\det[I + KG']$, evaluated on the standard Nyquist D-contour, encircle the origin counterclockwise as many times as KG' has unstable open-loop poles. If it is assumed that KG' has the same number of unstable open-loop poles as KG, the encirclement count of the origin must not change as G is warped continuously towards any allowable G'. For the Nyquist Contour to remain fixed as G is warped towards G', it is also necessary to assume that any poles on the $j\omega$-axis be identical for G and G'. Any plant that has an uncertain frequency on the $j\omega$-axis will have an infinite unstructured error in the neighborhood of that frequency, so it is reasonable to assume that the only poles on the $j\omega$-axis are at the origin, or equivalently, that the model have some positive damping. Furthermore, practical plants will be strictly proper, implying that $\lim_{s\to\infty} K(s)G(s)=0$. The Nyquist D-contour can therefore be replaced by the $j\omega$-axis, with the possibility of an indentation about the origin, which will not have any effect on the results for uncertain modal data.

Since $KG(I+\varepsilon\Delta_m)$ is a continuous function of ε, requiring that the encirclement count of $\det[I + KG]$ not change as G is warped towards G' is equivalent to requiring that:

$$\det[I + KG(I+\varepsilon\Delta_m)] \neq 0 \text{ for } 0 \leq \varepsilon \leq 1$$

or in terms of the minimum singular value:

$$\underline{\sigma}[I + K(s)G(s)(I+\varepsilon\Delta_m(s))] > 0, \text{ for } 0\leq\varepsilon\leq1, \quad \overline{\sigma}[\Delta(s)] < 1_m(s), \quad s\varepsilon\Omega_R \qquad (B.1)$$

Dropping the dependence on s, and noting that if $\overline{\sigma}[\Delta(s)]\leq1_m$, then $\overline{\sigma}[\varepsilon\Delta(s)]\leq1_m$, allows us to replace (B.1) by:

$$\underline{\sigma}[I + KG +KG\Delta_m] > 0 \text{ for } \overline{\sigma}[\Delta] \leq 1_m \qquad (B.2)$$

Assume that $\underline{\sigma}[(I + KG)^{-1}]=1/(\overline{\sigma}[I + KG]) > 0$. This is true whenever $\overline{\sigma}[KG] < \infty$, which in turn is true by the definition of the Nyquist D-contour. Multiply (B.2) by $\underline{\sigma}[(I + KG)^{-1}]$:

$$0 < \underline{\sigma}[(I+KG)^{-1}]\underline{\sigma}[I + KG +KG\Delta_m] \leq \underline{\sigma}[I + (I + KG)^{-1}KG\Delta_m] \qquad (B.3)$$

Now let $(I + KG)^{-1}KG$ have the singular value decompostion given by $U\Sigma V^*$ or equivalently the polar decompostion given by $UV^*(V\Sigma V^*)$. Let $\Delta = -\varepsilon 1_m VU^*$ for $0\leq\varepsilon\leq1$. $\underline{\sigma}[\Delta] = \overline{\sigma}[\Delta] = \varepsilon 1_m \leq 1_m$, so this is an uncertainty that falls within the specified bounds. Substitute this in:

$$0 < \underline{\sigma}[I + (I + KG)^{-1}KG\Delta_m] = \underline{\sigma}[I - \varepsilon 1_m V\Sigma V^*] \qquad (B.4)$$

but $(I-\varepsilon 1_m V\Sigma V^*)$ is hermitian, positive semi-definite, so the singular values can be treated as eigenvalues to get:

$$0 < 1 - \varepsilon 1_m \sigma_i(V\Sigma V^*) = 1 - \varepsilon 1_m \sigma_i[(I + KG)^{-1}KG] \qquad (B.5)$$

$$1 - \varepsilon 1_m \overline{\sigma}[(I + KG)^{-1}KG] > 0 \qquad\qquad (B.6)$$

$$\overline{\sigma}[(I + KG)^{-1}KG] > 1/(\varepsilon 1_m) \geq 1/(1_m) \qquad\qquad (B.7)$$

Before continuing to prove sufficiency it is worth noting that the particular uncertainty that will destabilize the system must have a phase characteristic given by $-VU^*$. An uncertaintly with some other phase characteristic might require that $\sigma[\Delta_m(j\omega)] \gg 1_m(\omega)$ before the system would go unstable. This indicates that if there is a some specified relationship between gain uncertainty and phase uncertainty, the unstructured uncertainty representation of Theorem 1 can be arbitrarily conservative. This point is discussed by Lehtomaki [LE1,3,4] in the context of most sensitive directions of the perturbation.

Now prove sufficiency by working backwards:

$$\overline{\sigma}[(I + KG)^{-1}KG] < 1/(1_m) \qquad\qquad (B.8)$$

$$\Longrightarrow 1 > 1_m \overline{\sigma}[(I + KG)^{-1}KG] \geq \overline{\sigma}[\Delta]\overline{\sigma}[(I + KG)^{-1}KG] \qquad\qquad (B.9)$$

$$\Longrightarrow \underline{\sigma}[I + (I + KG)^{-1}KG\Delta_m] \geq 1 - \overline{\sigma}[(I + KG)^{-1}KG\Delta_m] > 0 \qquad\qquad (B.10)$$

Now assume that $\underline{\sigma}[I + KG] > 0$, which is true whenever the nominal feedback system is stable. Multiply by $\underline{\sigma}[I + KG]$:

$$0 < \underline{\sigma}[I + (I + KG)^{-1}KG\Delta_m]\underline{\sigma}[I + KG] \leq \underline{\sigma}[I + KG + KG\Delta_m] \qquad\qquad (B.11)$$

$$\underline{\sigma}[I + KG + KG\Delta_m] > 0 \qquad\qquad (B.12)$$

and Theorem 4.1 is proved[1].

Theorem 4.2:

The major difference in the proof of Theorem 4.2 is in ascertaining the continuity of $L(\epsilon,s)$ as ϵ varies from 0 to 1. In particular $KG(I+\epsilon\Delta_d)^{-1}$ must be a continuous function of ϵ for $0\leq\epsilon\leq1$, or equivalently $L(s)=(I+\Delta_d)^{-1}$ must have no zero or strictly negative real eigenvalues. This is true since if $L(s)$ has no zero or negative eigenvalues, then neither does $(I+\Delta_d)$, and thus Δ_d can have no eigenvalues in the interval $(-\infty,-1]$, so $\epsilon\Delta_d$ never has eigenvalues of -1 and $(I+\epsilon\Delta_d)$ is never singular. If the first requirement is met it is then necessary that:

$$0 < \underline{\sigma}[I + KG(I+\Delta_d)^{-1}] \quad \forall s\epsilon\Omega_R, \ \forall\epsilon\epsilon[0,1] \qquad\qquad (B.13)$$

which in turn is equivalent to:

$$0< \underline{\sigma}[I + KG + \Delta_d] \quad \forall s\epsilon\Omega_R \qquad\qquad (B.14)$$

The proof then continues as with Theorem 4.1.

----

[1] The only difference between our result and the result stated in Ref. [DO1] is that we've replaced $\overline{\sigma}[\Delta(j\omega)]<1_m$ by $\overline{\sigma}[\Delta(j\omega)]\leq1_m$. This is a minor variation, and it was corrected in later papers by Doyle [DO3,4,5]. Furthermore, for practical purposes, the results are identical.

Appendix C: Numerical Considerations in Algebraic LTR

There are essentially five steps in solving for an LTR compensator by the algebraic method. This appendix will describe the numerical considerations important in each step.

1) Calculation of the Plant Numerator Polynomials -

The plant transfer function is as follows:

$$G(s) = C(sI-A)^{-1}B \qquad (C.1)$$

where C is an mxn matrix, A is an nxn matrix, B is an nx1 vector and G(s) is an mx1 vector function of s. To use the algebraic approach the numerator polynomials of G(s) must be found. We have used two methods, the Fadeeva method, which finds the coefficients directly based upon the Cayley Hamilton Theorem [CH1], and a method based on the transfer function zeros. The Fadeeva method works well for small systems but not for large. The first reason for this is that the number of steps is proportional to n^4, which can become computationally very expensive. The second reason is that the algorithm involves raising the matrix A to the (n-1)th power. This works well for discrete time systems, since the eigenvalues of A lie inside the unit circle, but it is very poorly conditioned for continuous time problems, since the eigenvalues of A may be very large.

The second approach is far more reliable. It is based on calculating the zeros in each channel of the plant, calculating a constant that will premultiply the numerator polynomial and then multiplying out the zeros. The zeros of a plant are defined as values of s which result in a zero output for a nonzero input. In terms of the state space representation of the plant for the

ith channel, this can be defined as follows:

$$\begin{bmatrix} (sI-A) & -B \\ C_i & 0 \end{bmatrix} \begin{Bmatrix} x \\ u \end{Bmatrix} = \begin{Bmatrix} 0 \\ y \end{Bmatrix} \qquad (C.2)$$

where C_i is the ith row of C and the plant zeros are the values of s which are a solution to (C.2) for $y = 0$. This can in turn be transformed into the following generalized eigenvalue problem:

$$\begin{bmatrix} A & B \\ -C & 0 \end{bmatrix} \begin{Bmatrix} x \\ u \end{Bmatrix} = s \begin{bmatrix} I & 0 \\ 0 & 0 \end{bmatrix} \begin{Bmatrix} x \\ u \end{Bmatrix} \qquad (C.3)$$

The generalized eigenvalue problem can be solved accurately and efficiently by the QZ-algorithm [ST2], where the computational cost is proportional to n^4. The only tricky step is the separation of finite zeros from infinite zeros. The QZ-algorithm will result in one complex vector α and one real vector β. The eigenvalues are found by dividing the elements of α by the corresponding non-zero elements of β. The first step in separating finite zeros is to eliminate all elements where β is zero. There are two possibilities for eliminating further infinite zeros. The first is to place a threshold on the elements of β, eliminating elements lying below this threshold. This method, however, proves to be very sensitive to the threshold. A more reliable method involves dividing all the remaining elements of α by the corresponding non-zero elements of β and then placing an upper bound on the magnitude of the resulting zeros. The upper bound is easily estimated, with some knowledge of the problem, and this method has proved to work very well. As a final check, the number of zeros for a SISO flexible system will almost always be $n-2$.

The ith numerator polynomial will have the following form:

$$n_i(s) = k_i(s-z_1)(s-z_2)\ldots(s-z_{n-2}) \qquad (C.4)$$

The next step therefore involves computing k_i This is most easily done by noting the following equality:

$$C_i(sI-A)^{-1}B = \frac{k_i(s-z_1)(s-z_2)\ldots(s-z_{n-2})}{(s-p_1)(s-p_2)\ldots(s-p_{n-2})(s-p_{n-1})(s-p_n)} \qquad (C.5)$$

where p_j is the jth pole. (C.5) is valid for any s which is not a pole of the system. k_i can therefore be found by evaluating (C.5) for some $s = s_o$ (eg. $s_o = 1$) and then solving for k_i. Also note that only $(s_oI-A)^{-1}B$ need be evaluated, using a linear equation solver, rather than $(s_oI-A)^{-1}$. The above method was used in Ref. [ED1] to evaluate plant transfer functions for $s = j\omega$.

The final step in solving for the plant numerator polynomials is to multiply out (C.4). The approach based on plant zeros is more complex than the Faddeva method and must be carried out for each channel separately, but it is far more computationally reliable.

2) Solution to the LQR Problem -

The major step in the calculation of full-state feedback control gains is the solution of a Riccati equation for the LQR problem. This is solved by Potter's method [KA1] which involves finding the eigenvalues and eigenvectors of the following Hamiltonian matrix:

$$H = \begin{bmatrix} A & -Q \\ -BR^{-1}B^T & -A^T \end{bmatrix} \qquad (C.6)$$

Finding an accurate solution to the Riccati equation therefore reduces to finding accurate eigenvalues and eigenvectors for (C.6). Inaccuracies can

develop when Q is made very large in comparison with BB^T. This becomes especially important in the solution of the near singular Kalman filter problem for the asymptotic LTR method, since Q may be very large before loop recovery is achieved. This difficulty can be overcome by multiplying both Q and BB^T by the square root of q_c, and then multiplying the final Riccati solution matrix P by the same number, rather than simply multiplying Q by q_c. This procedure keeps H from becoming too "unbalanced" and results in accurate solutions to the Riccati equation, even for very large q_c.

The numerator polynomial for the optimal LQR transfer function $K(sI-A)^{-1}B$ is found by the same methods used to find the plant numerator polynomials.

3) Compensator Order Determination -

The compensator order is found very simply by counting the maximum degree of the plant numerator polynomials and applying equation (4.2.24). If a proper compensator is required the compensator order will be identical to n_N in (4.2.24), while if a strictly proper compensator is required, the compensator order will be $n_N + 1$. The only problem in determining the compensator order is dealing with cases in which the matrix N is (4.2.26) will be singular. This will occur when some plant numerators contain identical zeros. This could be checked, but it essentially corresponds to a poorly posed problem.

4) Solution of Compensator Numerator Polynomials -

Once the plant numerator polynomials, the optimal loop gain polynomial, and the compensator order are found; a set of compensator poles are chosen and the compensator numerator polynomials are found by solving the $m(n_N+1)$ set of linear equations defined by (4.2.26). The solution of these equations depends on the condition of the matrix N, which is discussed in Section 4.4. Assuming that a solution does exist, We use an iterative solution routine. This is performed only once per design, and since the accuracy of the pole/zero cancellations depends heavily on an accurate solution, the extra computational cost and storage required for the iterative solution is considered worthwhile.

5) State-Space Realization of the LTR Compensator -

Since the compensator is found in polynomial form it must be transformed to a state space form. I use a observable-canonical representation [CH1] which is as follows:

$$A = \begin{bmatrix} 0 & \cdots\cdots & 0 & -D_0 \\ 1 & \cdots\cdots & 0 & \cdot \\ 0 & 1 & \cdots & 0 & \cdot \\ \cdot & \cdot & \cdots\cdots & \cdot \\ 0 & 0 & \cdots\cdots & 1 & -D_{n_N} \end{bmatrix}, \qquad B = \begin{bmatrix} n_{1,0} & \cdots & n_{m,0} \\ \cdot & \cdots & \cdot \\ \cdot & \cdots & \cdot \\ \cdot & \cdots & \cdot \\ n_{1,n_N} & \cdots & n_{m,n_N} \end{bmatrix} \qquad (C.7)$$

$$C = \begin{bmatrix} c & 0 & \cdots\cdots & 0 \end{bmatrix}$$

where D_i is the ith coefficient of the compensator denominator polynomial, $n_{i,j}$ is the jth coefficient of the ith compensator numerator polynomial, and c is the product of the compensator poles which are not cancelled.

Since the polynomial coefficients are sometimes very large, and will possibly contribute to later numerical problems, the state-space representation is

134

balanced so as to minimize the 1-norm of the matrix. This is a relatively cheap operation (computational cost proportional to n^2), and does result in better numerical properties for the robustness calculations.